EFFECTS OF PARASITIC INFECTION ON THE PHARMACOKINETICS AND DISPOSITION OF PENTAMIDINE ANALOGS

Claudia Nelly Generaux

A dissertation submitted to the faculty of the University of North Carolina at Chapel Hill in partial fulfillment of the requirements for the degree of Doctor of Philosophy in the School of Pharmacy.

Chapel Hill
2010

Approved by,

Co-advisor: Mary F. Paine, Ph.D.

Co-advisor: Dhiren R. Thakker, Ph.D.

Chairperson: Leaf Huang, Ph.D.

Reader: Kimberly K. Adkison, Ph.D.

Reader: James E. Hall, Ph.D.

Reader: Richard R. Tidwell, Ph.D.

ABSTRACT

Claudia Nelly Generaux: Effects of Parasitic Infection on the Pharmacokinetics and Disposition of Pentamidine Analogs
(Under the direction of Mary F. Paine, Ph.D. and Dhiren R.Thakker, Ph.D.)

Diamidine analogs of pentamidine are under evaluation as new and safer alternatives for treatment of first- and second-stage human African trypanosomiasis (HAT). Bis-*O*-methylamidoxime prodrugs of diamidines depend on hepatic biotransformation for generation of the pharmacologically active diamidines. The goal of this dissertation project was to investigate whether trypanosomal infection attenuates biotransformation of bis-*O*-methylamidoxime prodrugs, with the consequent potential to alter systemic exposure to prodrug and/or active diamidines.

Biotransformation of the prodrug DB868 to the active diamidine, DB829, under investigation for second-stage HAT, mirrored biotransformation of the prodrug for first-stage HAT, pafuramidine, highlighting the central role of biotransformation for bis-*O*-methylamidoxime prodrug activation. In addition to the *O*-demethylation and *N*-dehydroxylation reactions preceding DB829 generation, a previously unrecognized *N*-demethoxylation reaction was observed in human and rat liver microsomes. Formation of DB829 in cultured primary hepatocytes from both species was rapid; however, basolateral export and/or intracellular sequestration limited appearance of DB829 diamidine in culture medium.

In a rat model of first-stage trypanosomiasis, developed and characterized during this investigation, infection altered significantly the pharmacokinetics of both the prodrug, pafuramidine, and active diamidine, furamidine. Compared to uninfected animals, systemic exposure (AUC) of both prodrug and active diamidine was increased significantly in infected animals, by 1.3- and 3-fold, respectively. The increase in pafuramidine AUC during infection was dependent on dose and route of administration, and conformed to expected behavior for a blood-flow limited compound according to the well-stirred model of hepatic clearance. The increase in furamidine AUC during infection was explained, in part, by decreased biliary excretion of furamidine. Simulations of decreased enzyme capacity using different doses and routes of administration provided a framework for considering the impact of infection on pharmacokinetics.

This dissertation project showed that trypanosomal infection is capable of altering the pharmacokinetics of bis-*O*-methylamidoxime prodrugs and corresponding diamidines. Knowledge gained from this work provides a basis for making predictions of pharmacokinetic outcomes during infection and inflammation.

ACKNOWLEDGEMENTS

I want to extend my gratitude to many people who supported me during this dissertation work. First, I would like to thank my co-advisors Dr. Mary Paine and Dr. Dhiren Thakker for their guidance and support. They both challenged me and encouraged me every step of the way. Most importantly they provided me with invaluable feedback that helped me grow scientifically. I also want to express my gratitude to Dr. James Hall for his guidance as my advisor the first years of my graduate studies, and for giving me the opportunity to work in his laboratory in a project that was very fulfilling to me.

I am also grateful to all my committee members, Drs. Kim K. Adkison, Leaf Huang and Richard R. Tidwell for their support, time and insightful discussions. I would especially like to thank Dr. Kim Adkison for providing expertise regarding the bile excretion studies and insightful scientific advice.

I also want to thank a few people who were integral for the studies in this investigation. I want to thank Scott Brantley for his technical assistance in most of the *in vivo* experiments described in this dissertation work. Also, I want to thank Grace Yan for providing her technical expertise in the *in situ* biliary excretion experiments presented in this work, as well as Rachel Goldsmith for assisting in cell culture during my pregnancy. Additionally, I want to thank Matthew Dufek for his assistance and technical expertise in some of the pharmacokinetic studies detailed in this work and Dr. Arlene Bridges for her guidance in mass spectrometric analysis and interpretation.

I want to thank my family for their support and encouragement during my graduate studies. In particular, I want to thank my mother Mery N. Velasco for her unconditional love, support and encouragement. I also want to thank my brother J. Carlos Antequera for his invaluable advice offered through the years, and my father Freddy A. Antequera who from a distance always offered encouragement to continue my studies.

Finally, I want to thank two very special people in my life my husband Grant T. Generaux for his love and support whenever I needed it most, and my little son Aiden N. Generaux who puts a smile on my face no matter how long the day is.

TABLE OF CONTENTS

Page

LIST OF TABLES xi

LIST OF FIGURES xii

LIST OF ABBREVIATIONS xiv

Chapter

1. INTRODUCTION 1

A. DRUG METABOLIZING ENZYMES AND DRUG TRANSPORTERS 2

A.1. Introduction 2

A.2. Modulation of DMEs and DTs 4

B. INFLAMMATION AND THE ACUTE PHASE-RESPONSE 6

B.1. Introduction 6

B.2. Immune Effectors 7

B.3. Mechanisms of DME and DT Modulation by Inflammatory Effectors 8

C. ROLE OF IMMUNE EFFECTORS IN ALTERED PHARMACOKINETICS 10

C.1. Introduction 10

C.2. Modulation of DMEs and DTs by Immune Effectors *In Vitro* 10

C.3. Modulation of DMEs and DTs by Immune Effectors *In Vivo* 13

C.3.1. Effects of DME and DT Modulation in Experimental Animal Models 13

C.3.2. Effects of DME Modulation in Humans 16

D. HUMAN AFRICAN TRYPANOSOMIASIS 18

D.1. Overview 18

D.2. Current Chemotherapy 20

D.2.1. Pentamidine 20

D.2.2. Suramin 21

D.2.3. Melarsoprol 21

D.2.4. Eflornithine 22

D.2.5. Nifurtimox 23

D.3. Development of New Chemotherapy 24

D.3.1. Pentamidine Analogs 24

D.3.2. Diamidine Prodrugs 25

E. OVERVIEW OF PROJECT 27

F. FIGURES 31

G. TABLES 36

H. REFERENCES 38

2. IN VITRO BIOTRANSFORMATION OF THE ANTITRYPANOSOMAL PRODRUG 2, 5-BIS [5-(N-METHOXYAMIDINO)-2-PYRIDYL] FURAN (DB868) BY HUMAN AND RAT ENZYMES: A COMPARTMENTAL MODELING APPROACH TO ELUCIDATE METABOLIC CONVERSION TO THE ACTIVE DRUG 2, 5-BIS (5-AMIDINO-2-PYRIDYL) FURAN (DB829) 49

A. ABSTRACT 50

B. INTRODUCTION 51

C. METHODS 53

D. RESULTS 64

E. DISCUSSION 69

F. FIGURES 75

G. TABLES 84

H. ACKNOWLEDGEMENTS 87

I. FOOTNOTES 87

J. REFERENCES 88

3. TRYPANOSOMAL INFECTION ALTERS THE PHARMACOKINETICS AND DISPOSITION OF THE ANTIPARASITIC AGENT FURAMIDINE AND ITS PRODRUG PAFURAMIDINE IN RATS 91

A. ABSTRACT 92

B. INTRODUCTION 93

C. MATERIALS AND METHODS 96

D. RESULTS 103

E. DISCUSSION 106

F. FIGURES 114

G. TABLES 124

H. ACKNOWLEDGEMENTS 128

I. FOOTNOTES 128

J. REFERENCES 129

4. A SEMI-PHYSIOLOGIC PHARMACOKINETIC MODEL PREDICTS THE EFFECTS OF DECREASED ENZYME CAPACITY ON DRUG EXPOSURE 134

A. INTRODUCTION 135

B. METHODS 135

C. RESULTS 136

D. DISCUSSION 137

E. FIGURES 141

F. TABLES 144

G. REFERENCES 147

5. CONCLUSIONS.....148

A. FUTURE DIRECTIONS 163

B. REFERENCES 167

6. APPENDIX I 172

LIST OF TABLES

Table 1.1 Infectious organisms capable of DME modulation in preclinical species 36

Table 1.2 Effects of DME modulation by infection or inflammatory agents in humans 37

Table 2.1 Protonated molecular ions of the prodrug DB868 and its metabolites, mass shifts and MS^n fragmentations 84

Table 2.2 Apparent first-order rate constants for the metabolism of DB868 (10 μM) in HLM and RLM 85

Table 2.3 Enzyme kinetic parameters for the formation of M1 and M2 in HLM and RLM 86

Table 3.1 Summary of hematological and biochemical marker values of liver and kidney function in control and *T. b. brucei* infected Sprague-Dawley rats (group1) 124

Table 3.2 Summary of hematological and biochemical marker values of liver and kidney function in control and *T. b. brucei* infected Sprague-Dawley rats (group 2) 125

Table 3.3 Pharmacokinetic parameters of pafuramidine and furamidine after intravenous administration of 1.45 μmol/kg pafuramidine to control and infected rats 126

Table 3.4 Pharmacokinetic parameters of pafuramidine, M1 and furamidine after oral administration of 7.5 and 25 μmol/kg pafuramidine to control and infected rats 127

Table 4.1 Physiological parameters used for semi-physiologic pharmacokinetic model 144

Table 4.2 Pharmacokinetic parameters used for simulations of oral and intravenous administration 144

Table 4.3 Results of simulation for intravenous administration 145

Table 4.4 Results of simulation for oral administration 146

LIST OF FIGURES

Figure 1.1 Acute-phase response....31

Figure 1.2 Proposed pathways for modulation of CYPs during inflammation and infection....32

Figure 1.3 Chemical structures of current HAT chemotherapies....33

Figure 1.4 Chemical structures of diamidines and corresponding prodrugs....34

Figure 1.5 Proposed biotransformation of the prodrug pafuramidine leading to the formation of the active diamidine furamidine....35

Figure 2.1 Chemical structures of the prodrug DB868 and active diamidine drug, DB829....75

Figure 2.2 Representative HPLC-UV chromatograms depicting peaks for DB868 and intermediate metabolites....76

Figure 2.3 Proposed biotransformation of the prodrug DB868 leading to the formation of the active diamidine DB829....77

Figure 2.4 Concentration-time profiles of DB868 and intermediate metabolites....78

Figure 2.5 Biotransformation of DB868 by liver microsomal fractions....79

Figure 2.6 Rates of M1 and M2 formation in human and rat liver microsomes....80

Figure 2.7 Time-dependent inhibition of DB868 *N*-demethoxylation in human and rat liver microsomes....81

Figure 2.8 Human and rat CYP enzymes responsible for M1 and M2 formation....82

Figure 2.9 DB868 and phase I metabolites in incubations with human and rat sandwich culture hepatocytes....83

Figure 3.1 Chemical structures of prodrug and active diamidine....114

Figure 3.2 Time course of parasitemia in *T. b. brucei* infected Sprague-Dawley rats....115

Figure 3.3 Representative histology slides of liver and kidney sections of *T. b. brucei* infected Sprague-Dawley rats and un-infected controls....116

Figure 3.4 Relationship between pafuramidine and furamidine exposure ($AUC_{0\text{-}12}$) and dose in control and *T. b. brucei* infected Sprague-Dawley rats....117

Figure 3.5 Pafuramidine and furamidine mean plasma concentration-time profiles in control or *T. b. brucei* infected Sprague-Dawley rats following a 1.45 µmol/kg intravenous infusion (30 min) 118

Figure 3.6 Pafuramidine and furamidine mean plasma concentration-time profiles in control or *T .b. brucei* infected Sprague-Dawley rats following oral administration of a 7.5 µmol/kg dose 119

Figure 3.7 Pafuramidine and furamidine mean plasma concentration-time profiles in control or *T. b. brucei* infected Sprague-Dawley rats following oral administration of a 25 µmol/kg dose 120

Figure 3.8 Mean M1 plasma concentration-time profiles in control or *T. b. brucei* infected Sprague-Dawley rats following oral administration of a 7.5 and 25 µmol/kg pafuramidine dose 121

Figure 3.9 Biliary excretion rates of furamidine in control and infected Sprague-Dawley rats following intraduodenal administration of 7.5 µmol/kg pafuramidine 122

Figure 3.10 Bile flow in control and infected Sprague-Dawley rats 123

Figure 4.1 Model used for simulations of intravenous administration of drug 141

Figure 4.2 Model used for simulations of oral administration of drug 142

Figure 4.3 Scheme depicting the effects of decreased enzyme capacity (25%) on the AUC of drugs 143

LIST OF ABBREVIATIONS

ABC	ATP-binding cassette
ABT	1-Aminobenzotriazole
AhR	Aryl hydrocarbon receptor
AKR	Aldo-keto reductase
ALDH	Aldehyde dehydrogenase
ALT	Alanine aminotrasterase
ANOVA	Analysis of variance
ATP	Adenosine tri-phosphate
AUC	Area under the curve
BBB	Blood-brain barrier
BCG	*Corynebacterium parvum*, and *Bordetella pertussis*
BCRP	Breast cancer resistance protein
BIL	Bilirubin
BSEP	Bile salt export pump
BUN	Blood urea nitrogen
BW	Body weight
CAR	Constitutive androstane receptor
CES	Carboxylesterase
CHF	Congestive heart failure
CHO	Chinese hamster ovary
Cl	Clearance
Cl_{app}	Apparent clearance

Cl/F	Oral clearance
Cl_{int}	Intrinsic clearance
Cl_{max}	Maximal clearance
Cl_{po}	Oral clearance
C_{max}	Maximum concentration
CNS	Central nervous system
CNT	Concentrative nucleoside transporter
CSF	Cerebrospinal fluid
Css	Steady-state concentration
CYP	Cytochrome P450
DAPI	4',6-diamidino-2-phenylindole
DME	Drug-metabolizing enzyme
DMEM	Dulbecco's modified eagle medium
DMSO	Dimethyl sulfoxide
DNA	Deoxyribonucleic acid
DT	Drug transporter
E	Extraction ratio
EDTA	Ethylenediaminetetraacetic acid
EM	Extensive metabolizer
ENT	Equilibrative nucleoside transporter
f_a	Fraction absorbed
f_u	Unbound fraction
FCA	Freund's complete adjuvant

FLD	Fluorescence detector
FMO	Flavin monooxygenase
FXR	Farnesoid X receptor
GST	Glutathione S-transferase
H&E	Hematoxylin and eosin
HAPT	High-affinity pentamidine transporter
HAT	Human African trypanosomiasis
HCT	Hematocrit
HE	High extraction
HLM	Human liver microsomes
HMI	Modified Iscove's medium
HPLC	High pressure liquid chromatography
HSCH	Human sandwich cultured hepatocytes
IC_{50}	Concentration resulting in half maximal inhibition
IL	Interleukin
i.p.	Intraperitoneal
INF	Interferon
k	First order rate constant
k_a	First order rate constant for absorption
K_m	Half maximum velocity
K_p	Partition coefficient
LAPT	Low affinity pentamidine transporter
LDL	Low density lipoprotein

LE	Low extraction
LPS	Lipopolysaccharide
LXR	Liver X receptor
MATE	Multidrug and toxin extrusion transporter
MDR	Multidrug resistance
mRNA	Messenger ribonucleic acid
MRP	Multidrug reistance protein
MRT	Mean residence time
MS	Mass spectrometry
NADH	Nicotinamide adenine dinucleotide
NADPH	Nicotinamide adenine dinucleotide phosphate
NAPQI	*N*-acetyl-benzoquinone imine
NECT	Nifurtimox-Eflornithine Combination Therapy
NF-κB	Nuclear factor kappa B
NO	Nitric oxide
NOS	Nitric oxide synthase
NTCP	Sodium/taurocholate co-peptide transporter
OATP	Organic anion transporting polypeptide
OCT	Organic cation transporter
ODC	Ornithine decarboxylase
P2	Aminopurine transporter 2
P_{app}	Apparent permeability
PEPT	Peptide transporter

P-gp	P-glycoprotein
PM	Poor metabolizer
PPAR	Peroxisome proliferator activated receptor
PXR	Pregnane X receptor
Q	Liver blood flow
RBC	Red blood cell
RES	Reticuloendothelial system
RLM	Rat liver microsomes
RNA	Ribonucleic acid
RSCH	Rat sandwich cultured hepatocytes
RXR	Retinoid X receptor
S	Substrate concentration
S_{50}	Half maximal velocity for allosteric kinetics
SCH	Sandwich cultured hepatocytes
SCR	Serum creatinine
SLC	Solute carrier
SP-A	Surfactant protein A
SP-D	Surfactant protein D
STAT3	Signal transducer and activator of transcription 3
SULT	Sulfotransferase
$t_{1/2}$	Half-life
TBuMa	Tributylmethylammonium
TFA	Trifluoroacetic acid

TGF	Transforming growth factor
T_{max}	Time of maximum concentration
TNF	Tumor necrosis factor
UGT	UDP-glucuronosyltransferase
UV	Ultraviolet
V	Volume
V_{max}	Maximum velocity
VSG	Variant surface glycoprotein
V_{ss}	Volume of distribution at steady state
WBC	White blood cell
WHO	World Health Organization
X_0	Dose

CHAPTER 1

INTRODUCTION

A. DRUG METABOLIZING ENZYMES AND DRUG TRANSPORTERS

A.1. Introduction

Drug metabolizing enzymes (DMEs) and drug transporters (DTs), together, play an essential role in the absorption and disposition of xenobiotics. Upon entry into the body, xenobiotics encounter various DME systems to transform compounds into more water soluble and polar compounds that are more easily eliminated from the body (Beale et al., 2004). These biotransformations often render the parent compounds pharmacologically inactive, preventing their accumulation and potential for toxicity. In some cases, however, metabolic biotransformations are a necessary step to activate a pharmacologically active species (i.e., prodrugs) or result in the formation of toxic species (Beale et al., 2004). As with DMEs, DTs are essential in the disposition of xenobiotics. They are involved in facilitating xenobiotic absorption, tissue distribution, and elimination.

Drug metabolizing enzymes are categorized into two groups depending on whether they carry functionalization reactions or conjugation reactions. Functionalization, or phase I, reactions introduce functional groups to xenobiotics to increase their polarity and make them more conducive to conjugation reactions. Conjugation, or phase II, reactions also increase the polarity and water solubility of xenobiotics by attaching polar functionalities to compounds (Beale et al., 2004). Phase I reactions include oxidative, reductive and hydrolytic reactions and are carried out by several enzyme families including, but not limited to, aldehyde dehydrogenase (ALDH) cytochrome P450 (CYP), flavin monooxygenase (FMO), aldo-ketoreductase (AKR) and carboxylesterase (CES). Enzyme families involved in conjugation reactions include UDP-glucuronosyltransferase (UGT), sulfotransferase (SULT), and glutathione S-transferase (GST) (Casarett et al., 2008).

Drug transporters are categorized according to their energetics of transport and are divided into active and facilitative transporters (Martin and Sinko, 2006). Active transporters use ATP as the energy source to translocate substrates across membranes (i.e., primary active transporters). In addition to being ATP-dependent, some active transporters utilize a co-substrate (e.g., Na^+, K^+, H^+) to move substrates across membranes (i.e., secondary active transporters). Facilitative transporters do not require energy to move substrates; rather, they use a concentration gradient as a driving force to move substrates across membranes. Two superfamilies of transporters comprising both the active and facilitative proteins are most often associated with the disposition of most xenobiotics. These families include the ATP-binding cassette (ABC) superfamily and the solute carrier (SLC) superfamily.

The ABC superfamily is composed of only three families of transporters, including the multidrug resistance proteins (MDR), breast cancer resistance proteins (BCRP) and multidrug resistance associated proteins (MRP). Among the SLC transporters families include the sodium taurocholate cotransporting polypeptide (NTCP), organic anion transporters polypeptide (OATP), organic cation transporters (OCT), peptide transporters (PEPT), concentrative nucleoside transporters (CNT), equilibrative nucleoside transporters (ENT), and multidrug and extrusion transportes (MATE) (Klaassen and Aleksunes, 2010).

In the liver the NTCP, OATP, OCT and CNT transporters are localized in the basolateral membrane of hepatocytes and function to take up substrates from blood into hepatocytes. The ABC transporters MDR, BSEP and MRP are efflux transporters that function to export substrates from within hepatocytes to systemic circulation (e.g., MRP3, MRP4) or to excrete substrates into the bile (MDR, MRP2 and BSEP) (Klaassen and Aleksunes, 2010).

Because of their central role in drug absorption and disposition, modulation of DMEs and DTs could have profound implications on the pharmacokinetics and pharmacodynamics of therapeutic agents. Some of the ways in which DMEs and DTs could be modulated and regulated are presented in the next section.

A.2. Modulation of DMEs and DTs

Various factors could influence the expression and function of DMEs and DTs. These proteins can be directly acted on, such in the case of chemical enzyme inhibition or their gene expression could be modulated via intermediates (e.g. nuclear receptors), as in cases of chemical enzyme induction. DME inhibition has been extensively studied due to its known potential to have large negative impact on safety, as exemplified by potentially deadly drug interactions (Davies et al., 1989). Inhibition primarily affects substrate binding, for which various modes of inhibition have been described: competitive, non-competitive, uncompetitive and mixed inhibition. Chemical inhibition could be transient (reversible inhibition) or have lasting effects (irreversible inhibition), where covalent binding of the inhibitor to the enzymes has deleterious effects by removing the inhibitor-bound enzyme from the enzyme pool. Because of the extensive knowledge and good understanding of the interaction between inhibitors and DMEs, today is possible to make predictions of pharmacokinetic outcomes *in vivo* (humans) using data generated *in vitro* (Obach et al., 1997).

In contrast to the effect of inhibition on DME and DT function, regulation of gene expression of DME and DT is most often manifested as protein induction. It is mediated by direct binding of xenobiotics to nuclear receptors. Specifically, transcriptional activation of target DME and DT genes occurs by binding of nuclear receptors to promoter regions

(response elements) of target genes triggering induction of mRNA expression (Xu et al., 2005; Muntane, 2009). Among the nuclear receptors known to be involved in protein induction are the aryl hydrocarbon receptor (AhR), the constitutive androstane receptor (CAR), the pregnane X receptor (PXR), the peroxisome proliferator activated receptors (PPAR), the liver X receptor (LXR), the retinoid X receptor (RXR), and the farnesoid X receptor (FXR). Nuclear receptors often form heterodimers with other nuclear receptors in order to induce mRNA transcription. For example, upon binding to the ligand phenobarbital, PXR dimerizes with RXR resulting in induced expression of CYP3A. Nuclear receptors are known to activate gene transcription in a coordinated fashion through overlapping target specificity (Xu et al., 2005). For example, both the PXR and CAR nuclear transcription factors are known to induce phase I enzymes (i.e., CYP) and drug transporters (e.g., P-gp, MRP, OATP). A common consequence of DME induction is loss of efficacy due to decreased drug levels at the site of pharmacological action. However, beneficial side effects of induction of DMEs are sometimes seen, as is the case with phenobarbital induction of UGT1A1 in Crigler-Najar patients, where hyperbilirubenimia is reduced *via* an increase in UGT1A1 metabolism (Sugatani et al., 2001).

For more than three decades it has been recognized that infection and inflammation are also capable of modulating the expression and activity of DMEs and DTs (Morgan, 1997). A number of examples in various experimental systems have provided insight about the agents and conditions that evoke these changes. As such, this chapter will present the knowledge gained in the past several years about the role of infection and inflammation in the modulation of DMEs and DTs and the impact of this phenomenon in the clinic.

B. INFLAMMATION AND THE ACUTE-PHASE RESPONSE

B.1. Introduction

The inflammatory response is a mechanism of innate immunity, initiated in response to a stimulus such as an infectious or noxious agent, tissue or cell damage (Vassileva and Piquette-Miller, 2010). It involves a complex cascade of events in which effector molecules and cells are activated with the goal of containing and removing the harmful agent. The mediators of the inflammatory response include effector molecules such as cytokines and nitric oxide, and immune cells, which work in concert to eliminate invading pathogens. The effector molecules are generated by the reticuloendothelial system (RES) (i.e., phagocytic cells) at the infection site to signal immune cells (i.e., neutrophils, and monocytes) to move to the affected tissue to combat the infection (Janeway, 2005). Together, effector molecules and immune cells initiate the classical clinical signs of inflammation: redness, heat, pain and swelling.

The inflammatory response, along with other mechanisms of innate immunity (i.e., complement activation), successfully remove the pathogen from the body, or contain it at the site of infection while adaptive immunity develops. The adaptive immune response also utilizes effector molecules and immune cells to fight infection; however, in contrast to innate immunity, which is a more general response, both effectors and immune cells (i.e., T cells and B cells) of the adaptive immune response have greater specificity to kill the pathogen (Janeway, 2005). For example, T cells recognize and activate pathogen-containing macrophages, triggering their apoptotic mechanisms to induce cell death, or they release growth factors for B cell proliferation (T_H1 cells and T_H2 cells, respectively). B cells produce specific antibodies that neutralize pathogens, activate complement, and opsonize

pathogens for phagocytosis and stimulate natural killer cells to kill infected cells. Although some of the same cytokines present during innate immunity are still present during adaptive immunity, the main role of cytokines in the adaptive immune response is to regulate lymphocyte growth, behavior and functional differentiation (Janeway, 2005).

B.2. Immune Effectors

Immune effectors, including cytokines, are low molecular weight soluble proteins produced by various cells including macrophages, dendritic cells, lymphocytes (e.g, natural killer cells, and T cells), as well as endothelial and epithelial cells (Bogdan et al., 1992). They can act as autocrine, paracrine and endocrine modulators depending on whether the target is the cells that produce them, nearby cells or distant cells (Janeway, 2005). Among the various downstream effects produced by cytokines released during innate immunity is initiation of the acute-phase response (Ceciliani et al., 2002). During the acute-phase response, the cytokines TNF-α, IL1-β and IL-6, produced by phagocytic cells, act on hepatocytes to up-regulate synthesis of acute-phase proteins inducing their levels in serum (Figure 1.1). Concurrent with the up-regulation of liver acute-phase proteins, other proteins referred as negative "acute-phase reactants" are down-regulated thereby decreasing their concentration in serum. Acute-phase proteins up-regulated in the liver include C-reactive protein, haptoglobin, fibrinogen, serum amyloid protein, mannose binding lectin, lung surfactant proteins A (SP-A) and (SP-D), complement C_3 and α-1 acid glycoprotein (Sheth and Bankey, 2001). The general function of these proteins is to opsonize pathogens, activate the complement pathway or to act as coagulation factors. Negative acute-phase proteins include albumin, antithrombin, transferrin, transthyretin, transcortin and retinol-binding protein (Ritchie et al., 1999). A general function of the negative acute-phase proteins is to

aid in the restoration of homeostasis by either increasing cortisol levels (e.g.,transcortin suppression) or by increasing coagulation rate (e.g.,suppression of thrombin)(Pugeat et al., 1989).

Another inflammatory mediator of immunity is nitric oxide (NO), which is secreted by activated macrophages and other mammalian cells to fight infection (Saad et al., 1995). NO is synthesized from L-arginine by nitric oxide synthase (NOS). NO is normally present at low levels in the cytosol of macrophages, but upon immunologic stimulus, substantial increases of this cytotoxic product has been observed (Nathan and Hibbs, 1991). NO cytotoxic effects have been shown with a variety of pathogens including yeast, bacteria, helminthes and parasites. The microbicidal action of NO is by targeting key iron-containing enzymes, such as ribonucleotide reductase (involved in DNA synthesis), and mitochondrial enzymes that function within the electron transport chain (Nathan and Hibbs, 1991).

B.3. Mechanisms of DME and DT Modulation by Inflammatory Effectors

As discussed above, immune response mechanisms involve the activation of immune cells and mediators that help the host contain the antigen or eradicate it. Among the immune mediators, cytokines and NO have been implicated in the down-regulation of DMEs DTs (Abdel-Razzak et al., 1993; Chen et al., 1995; Yaghi et al., 2004; Geier et al., 2005). The primary mechanisms shown to contribute to CYP suppression include loss of gene expression and enzyme inactivation.

DME and DT modulation by cytokines was shown to occur through induction of signaling cascade events that ultimately modulate the constitutive expression of the gene (Renton, 2004). This cascade is initiated upon binding of a particular cytokine to their respective receptors on the surface of target cells (e.g, hepatocytes), followed by activation of

cytosolic transcription factors (e.g., NFK-β, STAT3) or nuclear receptors (e.g., PXR, CAR) that are translocated to the nucleus. In the nucleus, these transcription factors or nuclear receptors bind to DNA response elements on target genes to either suppress or induce their transcription (Ho and Piquette-Miller, 2006). A general scheme showing this mechanism of DME and DT modulation was proposed by Renton (2004) as depicted in Figure 1.2. This mechanism of down-regulation shares similarities with the ligand-dependent regulation of gene expression observed for induction of DMEs and DTs.

The most commonly studied cytokines capable of mediating DME or DT suppression include the pro-inflammatory cytokines TNF-α, IL-1 and IL-6 (Morgan, 1997). These cytokines are the main cytokines in the activation of the acute-phase response (Figure 1.1). Interferons, a type of cytokine common to viral infections, also have been studied extensively as mediators of CYP modulation, particularly because they are administered therapeutically for treatment of hepatitis C and some cancers (e.g, INFα-2β for melanoma) (Israel et al., 1993; Okuno et al., 1993; Pageaux et al., 1998; Islam et al., 2002). Additionally, interferons are highly induced after vaccine administration, which has often been shown to result in CYP suppression and impaired drug metabolism (Kramer and McClain, 1981; Gray et al., 1983; Hayney and Buck, 2002).

Much evidence also has implicated NO as an immune mediator capable of provoking CYP loss in inflammation and infection (Khatsenko et al., 1993; Muller et al., 1996; Yaghi et al., 2004). The proposed mechanism by which NO elicits CYP suppression is by direct inactivation of the enzyme through binding to the heme iron (Khatsenko et al., 1993). This mechanism has been shown to occur both *in vitro* using LPS as an inflammatory stimulus and *in vivo* in an animal model of acute pneumonia (Ferrari et al., 2001; Yaghi et al., 2004).

C. ROLE OF IMMUNE EFFECTORS IN ALTERED PHARMACOKINETICS

C.1. Introduction

Numerous studies have established that inflammatory mediators such as cytokines and nitric oxide (Peterson and Renton, 1984; Abdel-Razzak et al., 1993; Abdel-Razzak et al., 1994; Khatsenko et al., 1998; Lee and Piquette-Miller, 2001; Sukhai et al., 2001; Gharavi and El-Kadi, 2007) are capable of modulating the expression and activity of DMEs and DTs. One of the earliest reports showing the consequences of impaired metabolic activity was demonstrated in a pediatric population where theophylline clearance was significantly reduced during an influenza outbreak, causing toxic elevations of the drug (Kraemer et al., 1982). Since then, a handful of clinical reports associating decreased drug clearance and toxicity during episodes of inflammation or infection have emerged in the literature. At the same time, significant efforts to understand the mechanisms and agents that produce these changes were launched. Using a variety of *in vitro* and *in vivo* systems, significant progress has been made toward increasing the understanding of the mechanisms behind inflammatory modulation on DMEs and DTs and its pharmacological consequences. The next few sections highlight specific examples of DME and DT modulation using these systems.

C.2. Modulation of DMEs and DTs by Immune Effectors *In Vitro*

In vitro studies have been essential to confirm that inflammatory mediators were involved in the suppression of DMEs and DTs and to dissect the mechanisms by which inflammatory agents and mediators alter the expression and function of these enzymes. For example, using primary human hepatocytes, it was demonstrated that the mRNA of the major CYP enzymes (i.e., CYP1A2, CYP2C, CYP2E1, and CYP3A) was down-regulated up to 40% upon stimulation with the cytokines IL-1β, IL-4, IL-6, TNF-α, and INF- γ, with the

exception of CYP2E1, which was induced upon treatment with IL-4 (Abdel-Razzak et al., 1993). Similarly, using primary rat hepatocytes, it was shown that the mRNA of Cyp2c11 was down-regulated by the pro-inflammatory cytokines IL-1, IL-6, and TNF-α. Additionally, this study showed that protein suppression followed mRNA suppression and that stimulation by two cytokines (i.e., IL1 and IL-6) produced additive effects.

The contrasting effects of pro-inflammatory cytokines versus anti-inflammatory cytokines (i.e., IL-10) were demonstrated in studies with rat hepatocytes, where modulation of the expression of enzymes of the CYP4F family was investigated. CYP4F enzymes were up-regulated upon stimulation by pro-inflammatory cytokines, whereas the anti-inflammatory IL-10 induced suppression of CYP4F expression (Kalsotra et al., 2007).

Studies by Abdel-Razzak et al, demonstrated that aside from constitutive protein levels, induced CYPs also were altered by inflammatory mediators. For example, it was shown that induced CYP1A1 and CYP1A2 from human hepatocyte cultures were down-regulated by TGFβ-1 (Abdel-Razzak et al., 1994). Similarly, phenobarbital induced CYPs were down-regulated upon stimulation with IL-1β in primary cultures of rat hepatocytes (Abdel-Razzak et al., 1995). Experiments with mouse hepatocytes showed that inflammatory agents such as dextran sulfate were not capable of eliciting effects on DME levels alone but needed to be co-cultured with Kupffer cells to elicit suppression of CYP levels, indicating that factors released by Kupffer cells were the mediators of protein down-regulation (Peterson and Renton, 1984). Supporting Kupffer cell-mediated effects, another study showed down-regulation of CYP3A4 activity by IL-2 generated from Kupffer cells in co-cultures with human hepatocytes (Sunman et al., 2004).

Although the studies described above demonstrate convincingly that specific cytokines have the ability to down-regulate CYPs, there was no direct evidence showing that these inflammatory mediators secreted *in vivo* diminished activity of CYP enzymes. To address this question, Bleau et al., used serum of humans afflicted with an acute viral respiratory infection and serum of rabbits exposed to the inflammatory agent turpentine to show that the inflammatory mediators contained in these sera (i.e., IL1β, IL-6 and IFN- γ), lowered the total CYP content of human hepatocytes by 40% (Bleau et al., 2000).

Limited and contrasting results *in vitro* were reported regarding suppression of phase II enzymes. For instance, in one report it was shown that the conjugating enzyme GST-α was up- regulated when IL-4 was incubated with primary cultures of human hepatocytes (Langouet et al., 1995). However, another report using primary pig hepatocytes demonstrated the suppression of CYP enzymes and UGT activities by pro-inflammatory cytokines (Monshouwer et al., 1996). Down-regulation of drug transporters mediated by pro-inflammatory cytokines was also shown *in vitro*; however, fewer examples have been reported. In human hepatoma cells (HuH7), IL-6 suppressed the expression and activity of MDR1. However, IL-6 induction of expression and activity of MRP transporters was observed with hepatoma cell lines HuH7 and HepG2 (Lee and Piquette-Miller, 2001). Studies using human hepatocytes and HepaRG cells showed that the mRNA expression, protein levels and activity of the transporter NTCP were down-regulated by IL-1β. Additionally, the mRNA expression of the transporters OATP2B1, OATP1B1, OATP1B3, MRP2, MRP3, MRP4, BCRP and BSEP was also shown to be down-regulated by IL-1β after 24h treatment with this cytokine (Le Vee et al., 2008).

C.3. Modulation of DMEs and DTs by Immune Effectors *In Vivo*

C.3.1. Effects of DME and DT Modulation in Experimental Animal Models

In vivo experimental models are a valuable tool to study the overall effects of inflammation and infection on the modulation of DMEs and DTs, as they provide a more realistic representation of how the entire system responds to infectious or inflammatory insult. Specifically, experimental models overcome the limitations of static *in vitro* systems, where the administration of single cytokines fails to capture the complexity of the inflammatory response. For example, activation of different cytokine cascades and the kinetics of cytokine production cannot be duplicated *in vitro*. However, these dynamic changes can be captured by experimental models, allowing for investigation into the role of intensity and duration of cytokine exposure (Kato et al., 2008).

Several models of inflammation and infection were used to examine DME and DT modulation *in vivo*. Among the inflammatory agents used to study these effects are LPS, turpentine, dextran sulfate and particulate irritants. All these agents induce the acute-phase response, albeit via different cytokine responses depending on the agent involved. The LPS model of inflammation has been the most common model used for examining both DMEs and DTs. Using data compiled from various studies, Yang et. al. (2008) showed that the general effect of *Escherichia coli* LPS challenge on rat hepatic CYP proteins was suppression of the majority of CYP enzymes (i.e., Cyp1a1, Cyp1a2, Cyp2c11, Cyp2e1, Cyp3a1, Cyp3a2 and Cyp4a1/2). However, as shown in studies *in vitro*, some CYPs were not affected (i.e., Cyp2c12) and some were up-regulated (i.e., Cyp4a3). The magnitude of suppression was reported to range from 21% to 80% (Yang and Lee, 2008). Consistent with up-regulation of Cyp4a3 reported by Yang, other members of the Cyp4 family (i.e., Cyp4f4

and Cyp4f5) have exhibited up-regulation in rats challenged with *E. coli* LPS (Cui et al., 2003).

Effects on drug transporters were also demonstrated in a CNS rat model of inflammation, where intracranial LPS administration suppressed the expression of P-glycoprotein (*mdr1a*) at the blood brain barrier (BBB) by 50%. Interestingly, the effects were not limited to the BBB but were also observed in distant tissues such as the liver, where P-gp also was suppressed (Goralski et al., 2003). Other studies with LPS challenge to rats had suppressive effects in other organs such as the intestine and placenta (Kalitsky-Szirtes et al., 2004; Wang et al., 2005).

In addition to what has been observed following LPS administration, differential effects on CYPs were observed using a collagen-induced model of arthritis in rat. While activities for Cyp1a1 and Cyp2b1/2 decreased by 85% and 50%, respectively, Cyp3a protein and activity increased 100% (Ferrari et al., 1993). In contrast, a detailed study using the Freund's complete adjuvant (FCA) model of arthritis showed that mRNA levels, protein levels and catalytic activity of CYPs (i.e., Cyp2b, Cyp2c11 and Cyp2e1) were consistently down-regulated, with maximal effects between 24 and 48 h post FCA stimulation. However, no changes were seen for Cyp3a2 mRNA levels or activity (Projean et al., 2005).

As with inflammatory agents, different infectious organisms, including bacteria, viruses and parasites, were used to study the effects of infection on CYP modulation (Table 1.1). Concurrent with results of experimental models using inflammatory stimuli, mixed effects on CYP modulation were observed. For example, up-regulation of hepatic Cyp1a1 and Cyp2b1 was observed in an infection of rats with the parasite *Taenia taeniformis*, whereas no change was observed for Cyp2e1 (Montero et al., 2003). In contrast,

parasitic infection with *Fasciola hepatica* in sheep showed a significant decrease in Cyp3a protein expression (Calleja et al., 2000).

A recent study investigating the effects of infection on acetaminophen toxicity demonstrated that the consequences of suppression of CYP enzymes may not always be negative. This study showed that in a murine model of acute viral hepatitis, suppression of Cyp1a2 and Cyp2e1 had hepatoprotective effects from acetaminophen induced injury (Getachew et al., 2010). Cyp2e1 is involved in the metabolism of the toxic *N*-acetyl-benzoquinone imine (NAPQI), which reacts with proteins and other molecules to initiate cell damage and oxidative stress (Wolf et al., 2007).

Modulation of CYPs was shown to occur with inflammation triggered by cancer (Charles et al., 2006; Kacevska et al., 2008; Robertson et al., 2008; Sharma et al., 2008). Moreover, it has been shown recently that activation of the immune response by novel cancer drug delivery methods has untoward effects on DMEs. For example, some recombinant adenoviruses used for gene delivery have tropisms for the liver that are likely to elicit immune responses and thus affect CYP enzymes. The hypothesis that recombinant adenovirus may modulate CYP enzymes was tested by Callahan et al. (2005). Results from this study showed that rats infected with recombinant adenovirus 5 suppressed Cyp3a1/2 mRNA expression, protein expression, and activity while Cyp2c11 protein levels were significantly increased above control (Callahan et al., 2005). A follow up study by the same group examined the effects of gene therapy on the pharmacokinetics of anti-cancer agent, docetaxel, which is eliminated by Cyp3a. Rats given the combination therapy of recombinant adenovirus (AdlacZ or Adp53) and docetaxel showed significantly slower

docetaxel elimination compared to rats that were given docetaxel alone (Wonganan et al., 2009).

Despite the numerous studies examining the changes elicited by inflammation on DMEs at the molecular level, limited data are available on studies investigating the overall effects of CYP or transporter down-regulation on the pharmacokinetics of drugs in pre-clinical species. From the few studies that have examined the effects of LPS inflammation on the pharmacokinetics of drugs (i.e., antipyrine, chlorzoxazone, ipriflavone, midazolam and telithromycin), it appears that in general, this inflammatory agent reduces the systemic clearance of these drugs compared to control (Rockich and Blouin, 1999; Ueyama et al., 2005; Chung et al., 2008; Kato et al., 2008; Lee et al., 2008).

The data presented from *in vivo* experimental studies show that while the general trend for the effect of inflammation and infection on CYP enzymes is down-regulation, differential effects may be observed on different subsets of CYPs depending on the experimental model used, and the inflammatory agent stimulating the immune response.

C.3.2. Effects of DME Modulation in Humans

Recognition that infection and inflammation can elicit changes in drug disposition has important implications in human medicine, as it could impact the way drugs are developed and monitored. Some of the clinical outcomes resulting from these changes include reduced drug clearance, potentially resulting in exaggerated pharmacological response or toxicity; reduced concentrations of therapeutically active compounds, in cases where metabolic activation is necessary for the generation of the pharmacologically active agent (e.g., active metabolite generated from a prodrug) (Renton, 2005).

Controlled studies implicating suppression of CYPs as a mechanism for altered pharmacokinetics in humans are limited; however, several examples with circumstantial evidence exist (Table 1.2). The only two controlled clinical studies available, using LPS as the inflammatory stimulus, showed that clearance of the drugs antipyrine, hexobarbital and theophylline was significantly reduced in male subjects given LPS compared to those given saline. A subsequent study by the same group showed that these changes were not gender specific (Shedlofsky et al., 1994; Shedlofsky et al., 1997). These seminal studies demonstrated that the effects imposed by inflammation on metabolism were not particular to animal models and were duplicated in humans. In addition, some examples of bacterial, viral and parasitic infection were reported to decrease drug clearance in humans (Chang et al., 1978; Sonne et al., 1985; Pukrittayakamee et al., 1997).

For enzymes with clinically significant polymorphisms (i.e., CYP2D6, CYP2C19), inflammation was shown to diminish CYP levels to such a degree that discordant phenotypes were reported in patients afflicted with conditions such as lupus, cancer and active HIV. In one report, a higher frequency of CYP2D6 poor metabolizer (PM) phenotype was observed in the patient population suffering from lupus compared to normal subjects. Similarly, cancer patients with the CYP2C19 extensive metabolizer genotype showed a PM phenotype (Baer et al., 1986; O'Neil et al., 2000; Williams et al., 2000).

The above examples are supporting evidence that infection can elicit altered pharmacokinetics without resulting in untoward effects of pharmacology and toxicity. In contrast, toxic events were reported in three separate case studies where transient elevations of the steady state concentration of clozapine (2- to 3-fold) were observed in patients

afflicted by acute respiratory or urinary tract infections (Raaska et al., 2002; de Leon and Diaz, 2003; Jecel et al., 2005).

As demonstrated by the *in vitro* and *in vivo* examples given above, significant progress has been made to further our understanding about the mediators and underlying mechanisms involved in the modulation of DMEs and DTs during inflammation and infection. However, while the consequences of these changes are recognized to have an impact in human medicine, at present it is still unclear how to predict the manner in which a particular infectious agent or inflammatory episode may alter the pharmacokinetics and disposition of a particular drug. The challenge arises from the inability to predict the degree of the modulation, the differential responses of specific CYPs and drug transporters (e.g., suppression vs. induction) to the particular infectious or inflammatory stimulus, coupled with the complexity of the inflammatory response and its dynamic nature.

D. HUMAN AFRICAN TRYPANOSOMIASIS

D.1. Overview

Human African trypanosomiasis (HAT), also known as sleeping sickness, is caused by *Trypanosoma brucei* subspecies (WHO, 2010). The disease is transmitted to humans by the bite of the tsetse fly and distributes in regions of sub-Saharan Africa inhabited by this vector. Infections by the *T. b. rhodesiense* subspecies are prevalent in the southeastern region of sub-Saharan Africa whereas infections with *T. b. gambiense* occur at a higher incidence in western regions of sub-Saharan Africa. HAT has two defined stages during disease progression. In the first-stage, trypanosomes are confined to the hemolymphatic system while in second-stage parasites invade the CNS. Symptoms of first-stage infection

are flu-like and include headache, malaise, fever and lymphoadenopathy (Sternberg, 2004). Symptoms of second-stage are more serious and include motor and sensory disorders accompanied by neurological degeneration leading to sleep abnormalities, seizure and comma. Although both first- and second-stage symptoms are present in patients afflicted by both Rhodesian and Gambian forms of the disease, the rate of disease progression from first- to second-stage is markedly different depending on the subspecies involved. Second-stage symptoms of *T. b. rhodesiense* are characterized by rapid onset and are detectable within weeks to months, whereas the development of second-stage *T. b. gambiense* symptoms may take months to years. Without treatment, HAT is fatal (Barrett et al., 2007).

African trypanosomes elicit a rapid innate immune response upon entry into the host, which is characterized by macrophage activation and release of the immune effectors such as NO and pro-inflammatory cytokines TNF-α and IL-1 (Sternberg, 2004). Adaptive immunity is initiated by activation of the humoral response and clearance of opsonized parasites by the reticuloendothelial system (Sternberg, 2004). Unfortunately, the adaptive immune response is not sufficient to clear the parasite completely from the host, as the parasite employs the process of antigenic variation to evade the immune response (Janeway, 2005). African trypanosomes are coated with a variant surface glycoprotein (VSG) attached to their cell membrane (Sternberg, 2004). This protein is highly antigenic and easily recognized by the immune system. Upon initial infection, antibodies are raised against the VSG of the first population of parasites. During antigenic variation, a small number of trypanosomes switch their VSG gene and express a new antigenic coat, enabling the parasites to stay ahead of the host defenses. While the host eliminates the first variant, the new population of parasites displaying new VSG is unaffected (Donelson et al., 1998).

D.2. Current Chemotherapy

The process of antigenic variation presents a challenge for the development of vaccines against HAT, limiting the treatment for this disease to chemotherapy. A handful of drugs are currently available for the treatment of HAT (Figure 1.3). However, these drugs are associated with toxicities or impractical dosing regimens (Fairlamb, 2003). For the first-stage disease, the drugs pentamidine and suramin are available. For second-stage disease, melarsoprol and eflornithine are used as monotherapy, and nifurtimox is used in combination with eflornithine when melarsoprol is ineffective.

D.2.1. Pentamidine

Pentamidine is a highly soluble aromatic diamidine used for the treatment of first-stage *T. b. gambiense* infection. Pentamidine is administered parenterally *via* intramuscular injection at a dose between 4 mg/kg daily for 7-10 days (Nok, 2003). Pentamidine is taken up into trypanosomes *via* three different transport systems, including the aminopurine transporter (P2), the high-affinity pentamidine transporter (HAPT1) and the low affinity pentamidine transporter (LAPT1) (Barrett et al., 2007). Accumulation of pentamidine in trypanosomes is rapid and extensive, reaching up to millimolar concentrations (Mathis et al., 2006). It has been shown that the drug targets organelles containing negative charged moieties, including membrane phospholipids, polyphosphates in acidocalcisomes, RNA, DNA, and DNA containing organelles such as the kinetoplast (Mathis et al., 2006); however, the exact mechanism of action is unknown (Barrett et al., 2007). Pentamidine is metabolized in the liver, with only 12% cleared by the kidney unchanged. Plasma protein binding for pentamidine is approximately 70% (Brunton et al., 2006). The drug distributes extensively to tissues, with large amounts accumulating in the liver, kidney, adrenals and spleen. The

terminal half-life of pentamidine was shown to range between 2-4 weeks (Bronner et al., 1991). Intramuscular administration has shown to be associated with the development of an abscess at the site of injection. Side effects of pentamidine include hypoglycemia, hypotension, tachycardia and nephrotoxicity (Barrett et al., 2007).

D.2.2. Suramin

Suramin is a large polysulfonated naphthylamine closely related to the naphthalene dyes trypan blue and trypan red. It is used primarily against first-stage *T. b. rhodesiense* infections and is sometimes given in combination with pentamidine to treat early-stage *T. b. gambiense* infections (Fairlamb, 2003). Suramin is administered as a slow intravenous infusion as a regimen of five individual doses, with each dose given every 3-7 days for a period of 3 weeks (Brunton et al., 2006). The uptake of suramin into the trypanosomes is unknown, but it has been hypothesized that it is taken up by endocytosis bound to low density lipoprotein (LDL) *via* the LDL receptor. The trypanocidal action of suramin remains unknown, but it has been proposed that glycolytic enzyme inhibition could account, at least in part, for its mode of action (Fairlamb, 2003). Suramin is eliminated from the body primarily by renal clearance (80%), with little hepatic metabolism. As a polyanionic compound, suramin is highly bound to albumin (99.7%) and has low tissue distribution. It has a long terminal elimination half-life of approximately 90 days. As with pentamidine, suramin is associated with adverse effects, including headache, skin hypersensitivity, nephrotoxicity and neurological complications (Brunton et al., 2006).

D.2.3. Melarsoprol

The arsenic-containing melarsoprol was used, until recently (see NECT combination therapy below), as first line therapy for the treatment of second-stage *T. b. rhodesiense* and

T. b. gambiense infections. It must be administered intravenously, three times daily or four times daily for a period of three to four weeks (Fairlamb, 2003). Following intravenous administration, melarsoprol is bioconverted to the active melarsen oxide. Melarsen oxide is taken up into the trypanosome by the same aminopurine transporter (P2) that takes up pentamidine, although involvement of the HAPT1 transporter has also been suggested. Once in the trypanosome, melarsen oxide conjugates with the thiol containing trypanothione, forming the complex Mel T. Mel T inhibits the trypanothione reductase enzyme, disrupting the essential thiol-redox balance within the trypanosome, ultimately killing the parasite (Fairlamb, 2003). Melarsoprol is converted to melarsen oxide in the plasma, and the metabolite is cleared rapidly, with an elimination half-life of 3.5 h (Brunton et al., 2006). Despite being distributed to the brain minimally (2% of plasma maximal levels), melarsen oxide effectively kills CNS parasites. Severe adverse effects are reported for melarsoprol, which can lead ultimately to coma and death. These events occur in melarsoprol treated patients that develop severe post-treatment reactive encephalopathy, with an incidence of 5-10% of cases, of which 50% die (Legros et al., 2002).

D.2.4. Eflornithine

Eflornithine is an analogue of the amino acid ornithine. It is used for the treatment of second-stage *T. b. gambiense* infections. As with other HAT drugs, the dose regimen for eflornithine is impractical. The drug must be given as 2-h intravenous infusions QID over a period of 7 to 14 days (Barrett et al., 2007). Eflornithine kills the parasite by binding irreversibly to ornithine decarboxylase (ODC), which is essential in polyamine biosynthesis. Although not selective to the parasite, the consequences of irreversible ODC binding by eflornithine in host cells is thought to be ameliorated by induction of other polyamine

biosynthesis pathways and uptake of extracellular polyamines (Fairlamb, 2003). The major pathway of eflornithine elimination is by renal clearance, with 80% of the drug excreted unchanged. The elimination half-life is approximately 3 h. Eflornithine does not bind to proteins in the plasma (Brunton et al., 2006). Cerebrospinal fluid (CSF) to plasma ratio was reported to be in excess of 90%, affording the drug's excellent characteristics to kill central-nervous system (CNS) trypanosomes (Burri and Brun, 2003). Although eflornithine therapy is not life-threatening, several untoward effects have been reported, including seizures, anemia, diarrhea and leucopenia (Barrett et al., 2007).

D.2.5. Nifurtimox

Nifurtimox is a small nitrofuran, registered for the treatment of Chagas' disease, or American trypanosomiasis. This drug has been used against second-stage *T. b. gambiense* infections as compassionate treatment in relapsed cases after melarsoprol therapy (Fairlamb, 2003). Nifurtimox is administered orally, as 8-20 mg/kg daily for up to 120 days. Nitro partial reduction, coupled with generation of reactive oxygen species and superoxide anions, are thought to be the mechanism by which nifurtimox exerts its trypanocidal action (Fairlamb, 2003). Following oral administration, the time to maximum nifurtimox concentration was reported to be 3.5 h and the elimination half life ~3h. Nifurtimox is thought to undergo extensive first-pass metabolism, with less than 0.5% of the dose excreted unchanged in urine (Brunton et al., 2006). Toxicities associated with nifurtimox include neurological and gastrointestinal disorders (Priotto et al., 2006).

The use of combination therapy for the treatment of second-stage HAT has recently proven successful. A clinical trial with Nifurtimox-Eflornithine Combination Therapy (NECT) conducted in Congo showed that this combination was a much safer alternative

compared to melarsoprol monotherapy and had an improved dosing regimen compared to eflornithine monotherapy (Priotto et al., 2006). NECT therapy was recently approved in 2009 for use against second-stage HAT. Despite achievement of this milestone in HAT medicines, choices for chemotherapy are still far from satisfactory. Moreover, recent reports of resistance against eflornithine (Balasegaram et al., 2009) raise concerns about the lasting advantages of NECT. Hence, there is great urgency to devote efforts to the discovery and development of new HAT therapies.

D.3. Development of New Chemotherapy

D.3.1. Pentamidine Analogs

Some progress has been made over the last few years in finding new chemical entities that are potent against African trypanosomes. One such agent, the pentamidine analog furamidine, and its prodrug pafuramidine (Figure. 1.4), successfully entered clinical development for the treatment of first-stage HAT. Unfortunately, the development of pafuramidine and furamidine was discontinued due to renal toxicity associated with the drug (Wenzler et al., 2009). Despite this drawback, other diamidines have shown outstanding *in vitro* activity against both sub-species of trypanosomes, *T. b. rhodesiense* and *T. b. gambiense*. *In vitro* IC_{50} values for the diamidines DB820 and DB829 were <10 ng/mL against the STIB900wt strain of *T. b. rhodesiense*. The IC_{50} values against the *T. b. gambiense* isolates, STIB930, ITMAP141267 and K03048 were <40 ng/mL, comparable to melarsoprol (IC_{50} <10 ng/mL) against the same strains. The physicochemical properties of diamidines render these molecules impermeant to biological membranes. Calculated pK_a values range from 9 – 11 (MarvinSketch 5.1.3-2, 2008, ChemAxon http://www.chemaxon.com). Accordingly, diamidines exist as charged species at

physiological pH, and when given orally, have low oral bioavailability due to poor absorption, resulting in a lack of efficacy (Boykin et al., 1995). As a consequence, a prodrug strategy was utilized to make these compounds more suitable for oral delivery, the preferred and most practical route of administration, especially in rural areas of endemic countries.

D.3.2. Diamidine Prodrugs

Prodrugs are defined as inactive therapeutic agents that are transformed into one or more active metabolites (Ettmayer et al., 2004). Pafuramidine and the bis-*O*-methylamidoxime aza analogs DB844 and DB868 were designed as prodrugs of the diamidines furamidine, DB820, and DB829, respectively (Ismail et al., 2006) (Figure 1.4). These prodrugs were created by masking the positive charge of the amidine functional groups with *O*-alkyl moeities, resulting in increased lipophilicity and intestinal permeability, and in turn, improved absorption and oral bioavailability (Zhou et al., 2002; Saulter, 2005).

Biotransformation of the bis-*O*-methylamidoxime prodrugs to the active diamidines requires a series of oxidative and reductive enzymatic reactions. The biotransformation of the prodrug pafuramidine to furamidine (Figure 1.5) involves oxidative catalysis by CYP enzymes and reductive catalysis by the cytochrome b_5/NADH-cytochrome b_5 reductase system (Saulter et al., 2005; Wang et al., 2006). Some of the intermediate metabolites of the three prodrugs also are prodrugs, since the desirable physicochemical properties are retained. For example, upon oral administration, the M1 metabolite of pafuramidine is efficacious in the first-stage mouse model of trypanosomiasis, and the M1 metabolites of DB844 and DB868 were efficacious in both the first-stage and second-stage mouse model of trypanosomiasis (Wenzler et al., 2009).

The biotransformation of the bis-*O*-methylamidoxime prodrugs of pentamidine analogs occurs primarily in the liver, where the metabolites are eliminated via biliary excretion and/or transported back into systemic circulation (Midgley et al., 2007). Tissue distribution data from rats given a single oral dose (10 mg/kg or 27 μmol/kg) of the prodrug pafuramidine indicated that the diamidine (furamidine) was retained extensively in the liver, as illustrated by a liver to plasma ratio of 1300:1. In the liver furamidine was found to be associated with the mitochondrial, nuclear and microsomal fractions (Midgley et al., 2007). Extensive accumulation of diamidines in organs like the liver and kidney raise concerns regarding the potential for toxicity, particularly if accumulation occurs over extended periods of time. However, retention/accumulation of diamidines in organs such as the brain might be desirable for second-stage HAT, as the primary obstacle for drug delivery to the CNS is the BBB. It is possible that efficacy of the prodrugs DB844 and DB868 in the second-stage mouse model of trypanosomiasis reflects passive entry of prodrugs into the brain, followed by *in situ* conversion to the active diamidines and retention of the cationic drugs within the CNS. Alternatively, the liver-generated diamidine enters the brain *via* an unidentified carrier mediated mechanism. Furamidine and pentamidine were recently shown to be substrates of the human facilitative organic cation transporter 1 (hOCT1) in Chinese hamster ovary (CHO) cells stably transfected hOCT1 (Ming et al., 2009). The expression of this transporter in the blood brain barrier of humans are reported to be low (Zhang et al., 1997), which could explain in part the lack of efficacy of pafuramidine toward late-stage infection. Considering the potency of diamidines against African trypanosomes and the optimal properties of some molecules to penetrate the brain, this class of drugs represents a promising alternative for the treatment of second-stage HAT.

E. OVERVIEW OF PROJECT

DMEs and DTs are known to be modulated by pro-inflammatory cytokines in various tissues, including organs that are central to drug elimination such as the liver and kidney (Renton, 2005). The extent of modulation has been shown to vary depending on the degree of inflammation, source of insult, and experimental model used to study these changes (Montero et al., 2003; De-Oliveira et al., 2010; Getachew et al., 2010). The current understanding is that infectious or inflammatory episodes will down-regulate DMEs and DTs (Morgan et al., 2008). However, mixed effects (e.g., up-regulation and down-regulation) were observed for different subsets of CYP enzymes and drug transporters. In spite of the recognition of the occurrence of these modulatory effects on DMEs and DTs during infection, limited data are available on studies investigating the overall effects of CYP and transporter down-regulation on the pharmacokinetics of drugs. At present it is not possible to predict prospectively the overall effects that infection or inflammation will have on the pharmacokinetics of a compound.

Diamidines are among the few chemical entities currently in development for the treatment of the deadly disease human African trypanosomiasis (Figure 1.4) (Barrett et al., 2007). Bis-*O*-methylamidoxime prodrugs of diamidines require enzymatic biotransformation to generate the pharmacologically active compound (Zhou et al., 2004). Moreover, because diamidines are charged molecules at physiological pH and are not able to passively diffuse across membranes, they rely on transporters for elimination and to reach their pharmacological site of action (Ming et al., 2009). As such, modulation of the metabolizing enzymes and/or drug transporters involved in the disposition of diamidines and their prodrugs may have profound implications on the pharmacokinetics and pharmacological

effects of these agents. Accordingly, the goal of this dissertation project was to: 1) ascertain, in a rat model of first-stage trypanosomiasis, whether trypanosomal infection would diminish the conversion of the prodrug pafuramidine into the active diamidine furamidine and 2) determine, in this model, the effect of trypanosomal infection on the pharmacokinetics of the orally and intravenously administered bis-*O*-methylamidoxime prodrug pafuramidine and its active diamidine metabolite furamidine. The results of this investigation helped clarify questions regarding the impact of trypanosomal infection on the development of this class of compounds and furthered our understanding on the role of infection on drug disposition by providing a framework for recognizing compounds which may be sensitive to the impact of infection based on their pharmacokinetics and route of administration.

Central hypothesis: Trypanosomal infection will alter the pharmacokinetics of bis-*O*-methylamidoxime prodrugs and the corresponding diamidine active metabolites due to down-regulation of drug metabolizing enzymes. To test this hypothesis, *in vitro* experiments using rat and human hepatic enzymes and *in vivo* experiments in a rat model of first-stage HAT were conducted as outlined in the following specific aims:

Specific Aim 1: Characterize the hepatic biotransformation pathway of the bis-*O*-methylamidoxime prodrug DB868 to the diamidine active metabolite DB829 in humans and rats using *in vitro* systems

Hypothesis: Metabolic activation of the prodrug DB868 to the active drug DB829 involves sequential oxidation and reductive reactions prior the generation of DB829.

To test this hypothesis, multiple *in vitro* tools (i.e., purified/recombinant CYP enzymes, liver microsomes and sandwich-cultured hepatocytes) and analytical systems (i.e., HPLC/UV and HPLC/MS/MS) were used to characterize and identify the intermediate metabolites in the DB868 to DB829 conversion by both humans and rat hepatic enzymes. The *in vitro* tools used for this specific aim are well characterized and routinely used to examine drug metabolism and hepatic disposition. Additionally, kinetic modeling was used to determine the rate of formation of intermediate metabolite. It was postulated that the DB868 biotransformation would mirror the biotransformation of the analog prodrug pafuramidine in which oxidative and reductive steps preceded the generation of the active diamidine furamidine.

Specific Aim 2: Determine the effect of trypanosomal infection on the pharmacokinetic behavior of orally and intravenously administered pafuramidine and metabolically formed furamidine in a rat experimental model of first-stage trypanosomiasis

Hypothesis: Trypanosomal infection is expected to decrease the clearance and increase the exposure of the prodrug pafuramidine, resulting in diminished exposure of the active drug furamidine.

The effects of trypanosomal infection *in vivo* were addressed with the following two sub-aims:

2.1 Develop and characterize a rat model of first-stage trypanosomiasis

To mimic first-stage HAT, Sprague-Dawley rats were infected with the S427 strain of *T. b. brucei* (non-human infective strain). After determining the virulence and course of parasitemia in this experimental model, the changes elicited by the infection on the liver and kidney were evaluated. Specifically, histopathologic and molecular changes (i.e., measured by liver and kidney biochemical markers) were examined.

2.2 Evaluate the pharmacokinetics of orally and intravenously administered pafuramidine and metabolically formed furamidine in the rat experimental model of first-stage trypanosomiasis

Plasma concentrations of pafuramidine and furamidine were determined following intravenous and oral administration of pafuramidine. Non-compartmental analysis was used to obtain relevant pharmacokinetic parameters. It was postulated that trypanosomal infection will down-regulate drug metabolizing enzymes such that measurable changes in the pharmacokinetic parameters of the prodrug pafuramidine and furamidine would be observed in infected animals compared to controls. An increase in pafuramidine systemic exposure of at least 1.2-fold was expected, in infected animals, with a commensurate decrease in furamidine exposure.

F. FIGURES

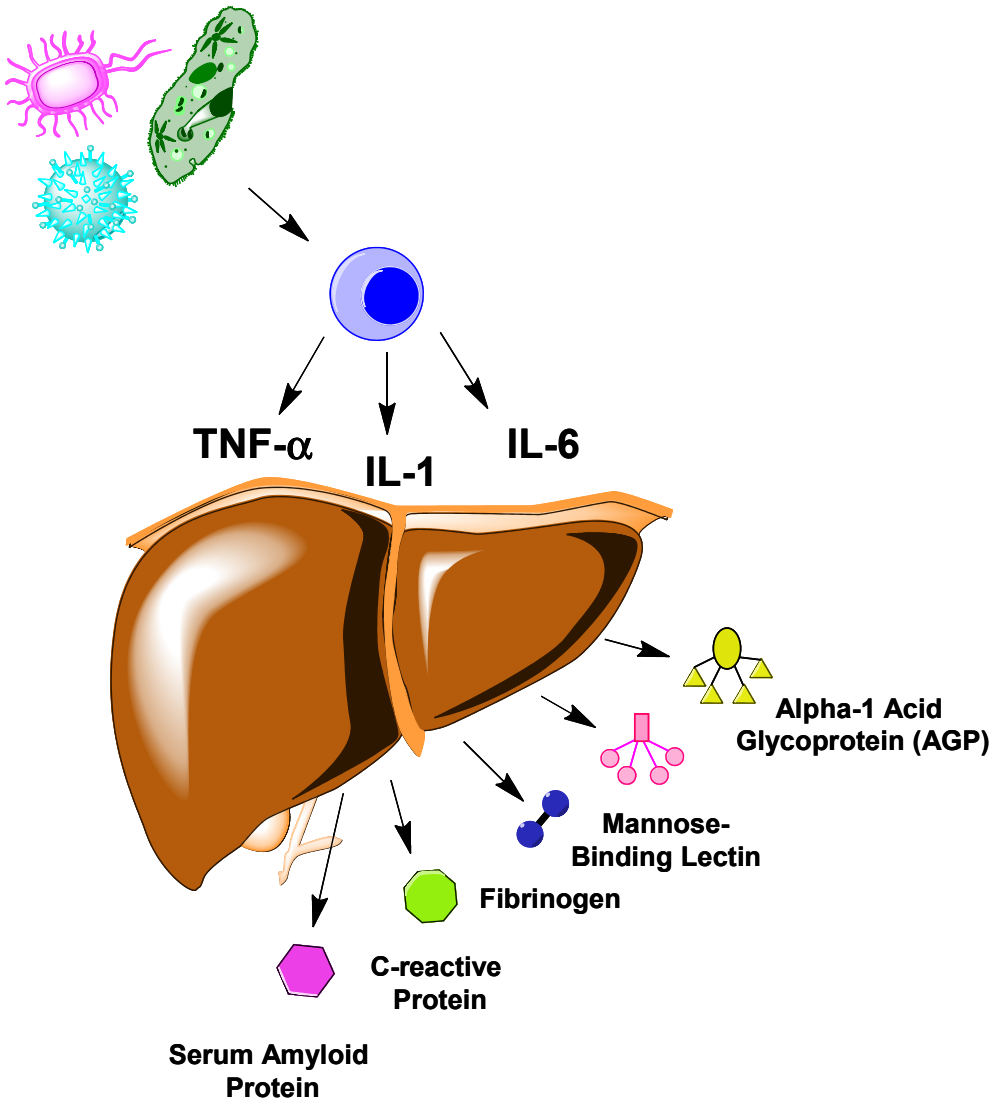

Figure 1.1 Acute-phase response. Pathogens induce macrophage activation and production of the pro-inflammatory cytokines TNF-α, IL-1 and IL-6, which in turn induce the synthesis of acute-phase proteins by the liver.

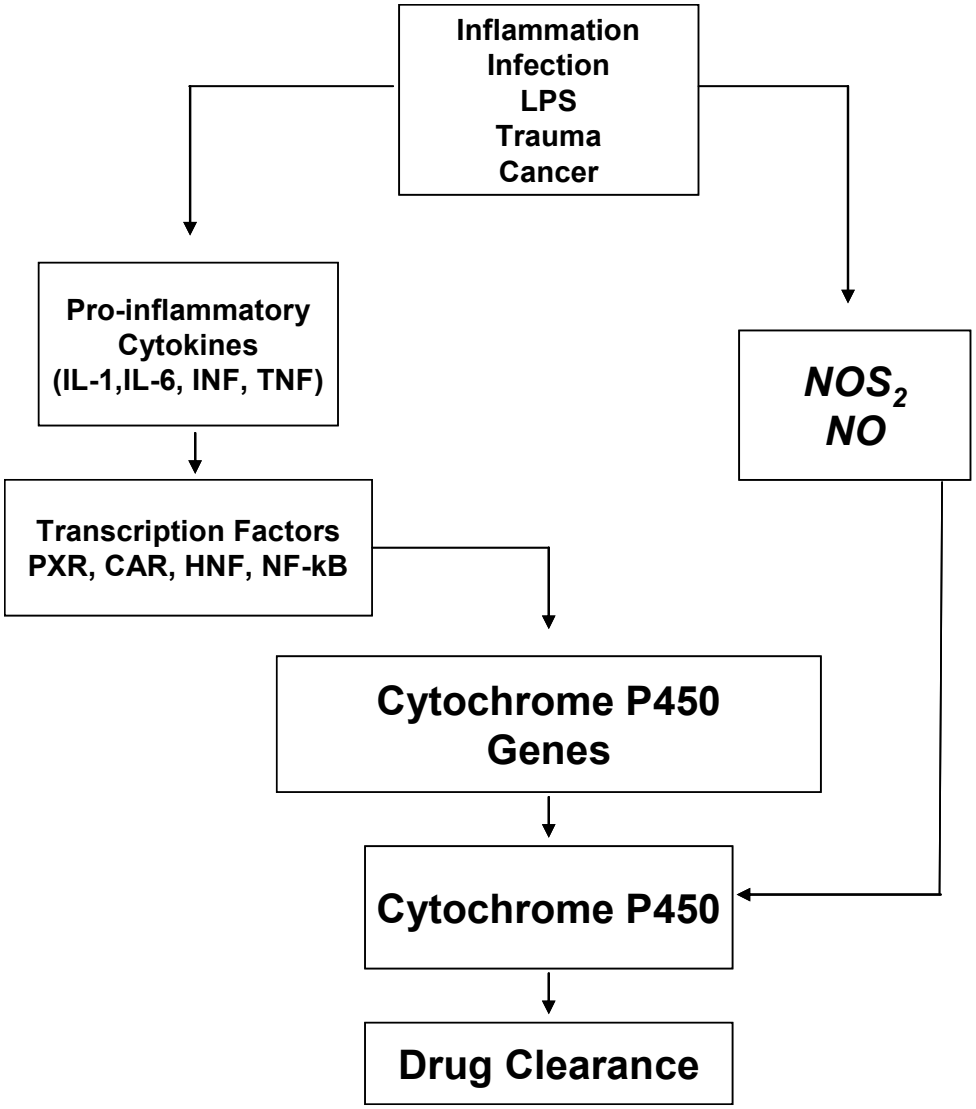

Figure 1.2. Proposed pathways for modulation of CYPs during inflammation and infection. Inflammatory stimuli trigger the synthesis of the immune response effectors, cytokines and nitric oxide (NO). Cytokines down-regulate CYP gene and protein expression through the involvement of transcription and nuclear factors (e.g., PXR, CAR, HNF, NF-κB). NO, generated by nitric oxide synthase (NOS_2), down-regulates CYPs by directly inactivating protein function. Figure was reproduced from Renton, 2004 with permission (Renton, 2004).

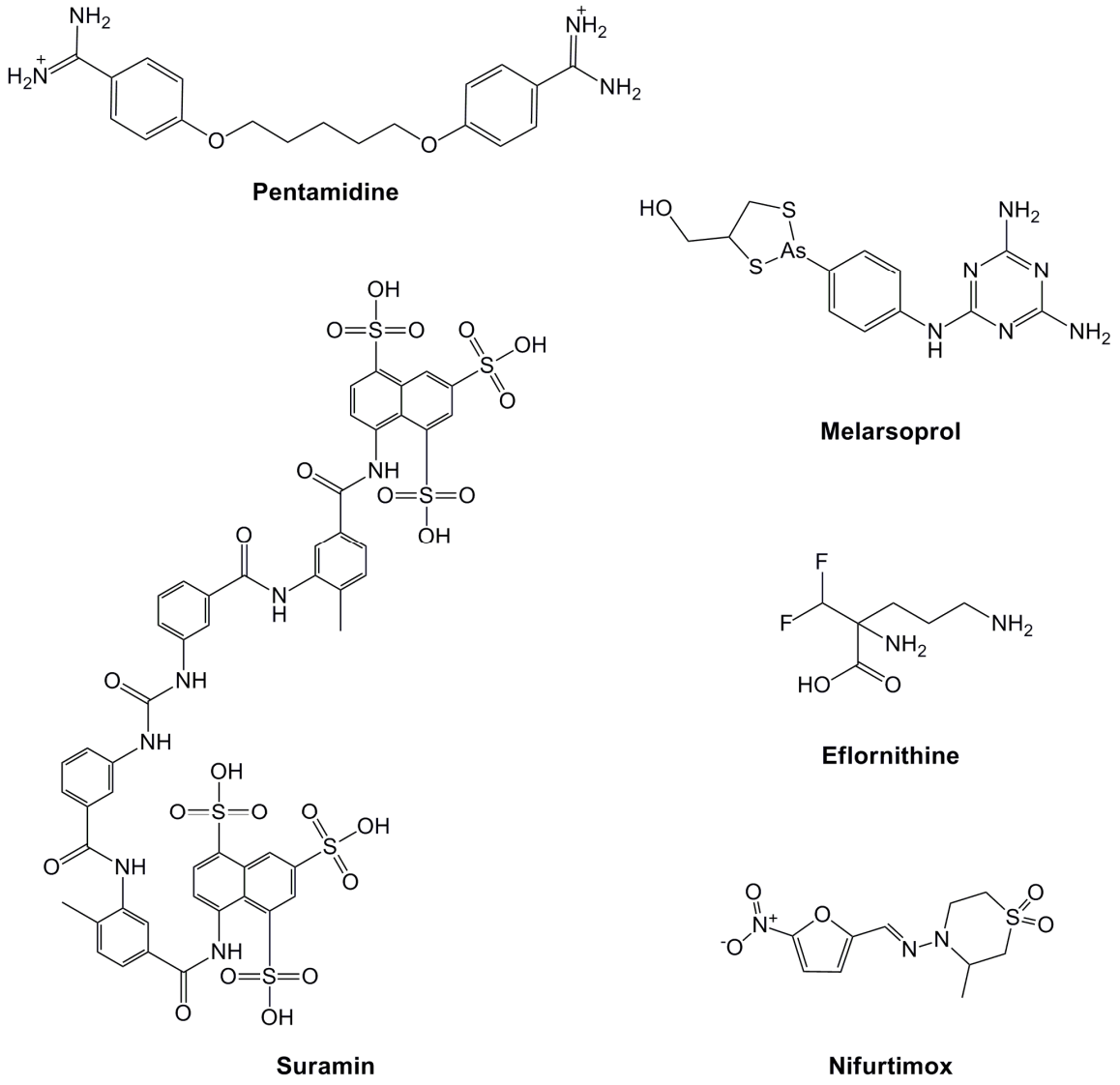

Figure 1.3. Chemical structures of current human African trypanosomiasis (HAT) chemotherapies. Treatments for first- and second-stage HAT are shown on left- and right-hand side, respectively.

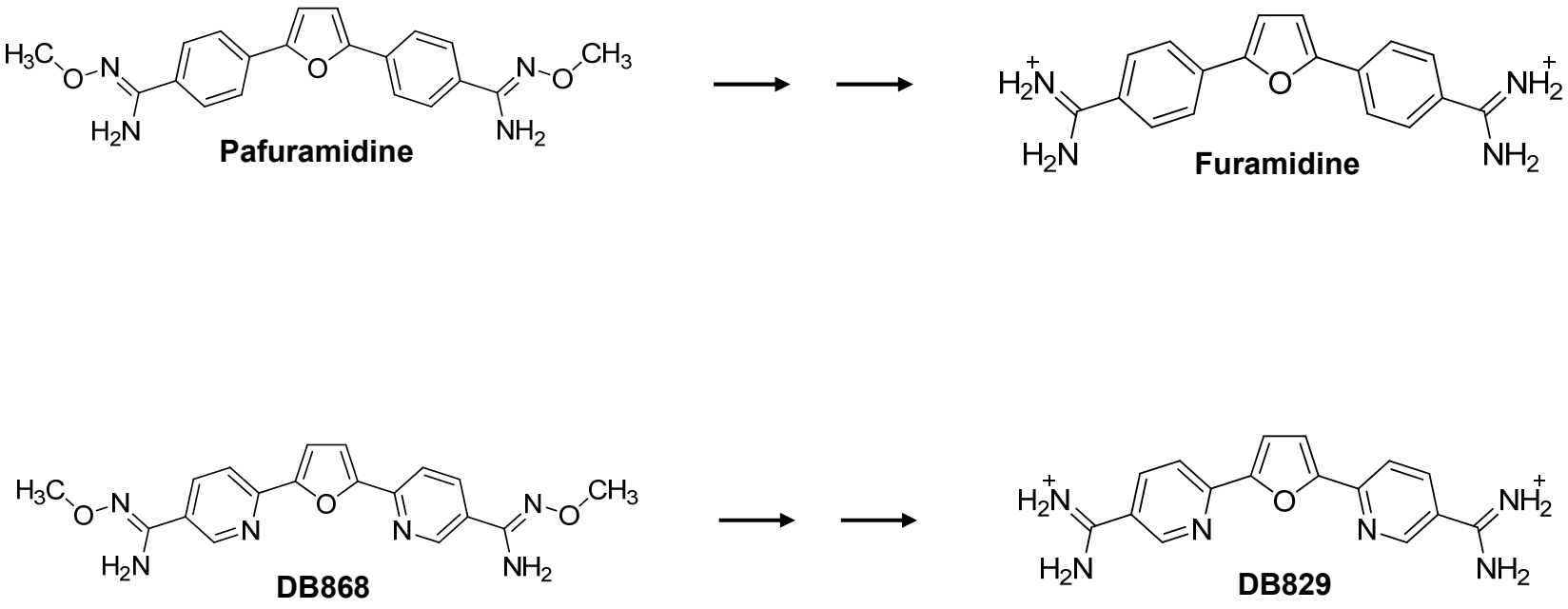

Figure 1.4. Chemical structures of diamidines and their corresponding bis-*O*-methylamidoxime prodrugs.

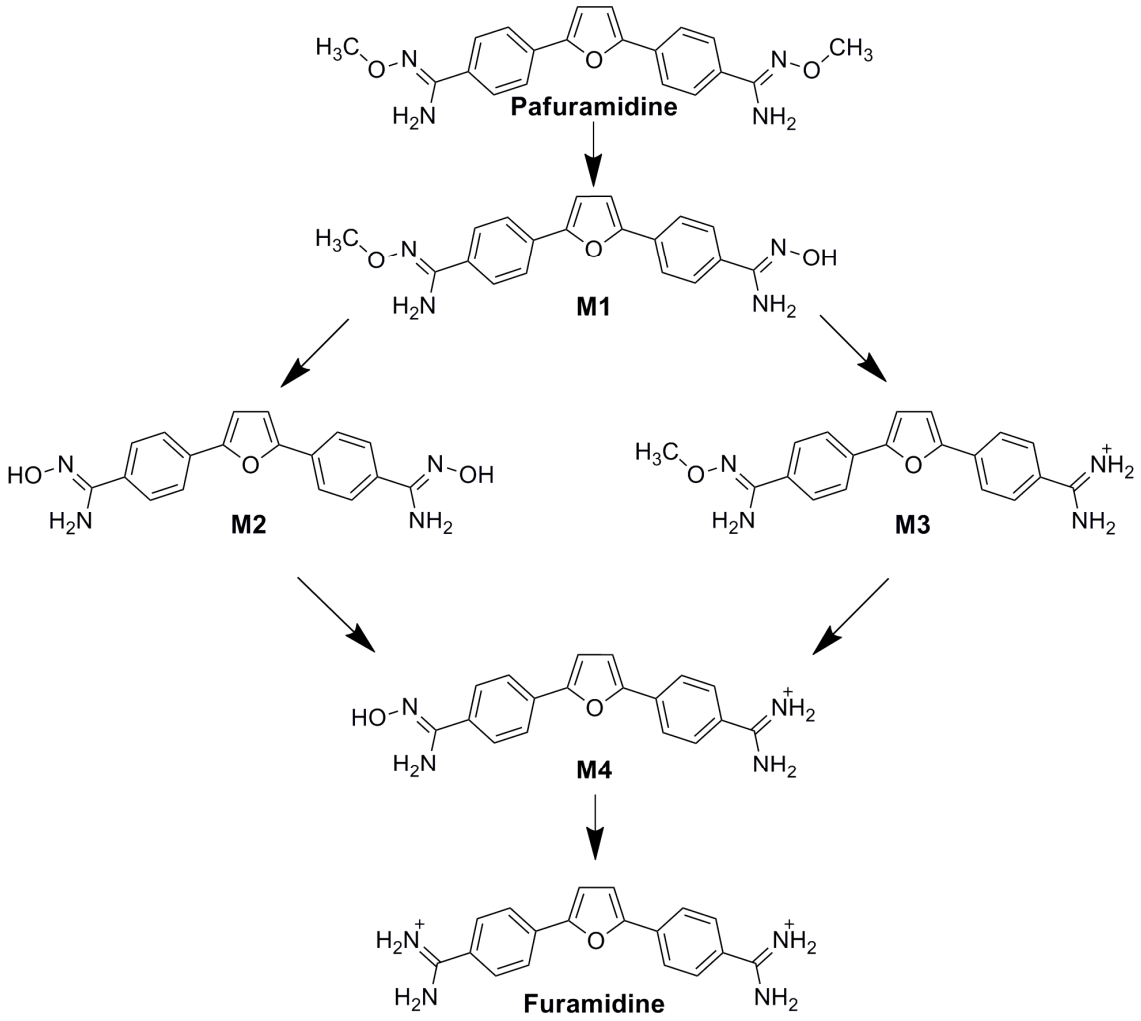

Figure 1.5. Proposed biotransformation of the prodrug pafuramidine leading to the formation of the active diamidine furamidine.

G. TABLES

Table 1.1 Infectious organisms capable of DME modulation in preclinical species

Infectious Organism	Species	Effect[1]	Reference
Bacteria			
Chlamydia trachomatis	Mice	CYP1A ↓, CYP2B ↓ (49%)[c]	(Khatsenko et al., 1998)
Pseudomonas aeruginosa	Rats	CYP2J4 ↓(42%) [c]	(Yaghi et al., 2004)
Corynobacterium parvum	Mice	CYP2C↓(50%) [b], CYP3A ↓(60%) [b] CYP4A↓(90%) [b], CYP2E↔ [b]	(Richardson et al., 2006)
Parasites			
Trypanosoma brucei gambiense	Mice	CYP ↓ (14%) [a] (40%) [c]	(Shertzer et al., 1981)
Trypanosoma brucei gambiense	Vole	CYP ↓ (60%) [a]	(Shertzer et al., 1982)
Fasciola hepatica	Sheep	CYP3A↓(23%)[b] GST↔[c]	(Calleja et al., 2000)
Plasmodium berghei	Mice	CYP1A↓ (40%)[c], CYP2B↓(50%)[c] CYP2A5↑ (100%)[c]	(De-Oliveira et al., 2010)
Viruses			
Encephalomyocarditis virus	Rats	CYP3A↓ (50%) [b c] Cytochrome b_5↓ (40%) [b]	(Renton, 1981)
Adenovirus	Rats	CYP3A2 ↓ (47%)[c]	(Wonganan et al., 2009)
Adenovirus (viral hepatitis)	Mice	CYP1A2↔[b], CYP2E1↓ (90%) [b]	(Getachew et al., 2010)

1. Effect on protein (magnitude of modulation).
a. Total protein
b. Protein expression
c. Enzyme activity

Table 1.2 Effects of DME modulation by infection or inflammatory agents in humans

Infection or Inflammatory Agent	Drug	Outcome	Reference
Adenoviral Infection	Theophylline	↑ $t_{½}$ (1.6-fold)	(Chang et al., 1978)
Asthma	Theophylline	↓ Cl (2-fold)	(Kraemer et al., 1982)
BCG Vaccine	Theophylline	↓Cl (1.4-fold) ↑ $t_{½}$ (1.2-fold)	(Gray et al., 1983)
Pneumonia	Antipyrine	↓Cl (1.5-fold)	(Sonne et al., 1985)
Systemic Lupus Erythematosus	Debrisoquine	↑ CYP2D6 PM phenotype frequency (21% patients *vs* 8% healthy)	(Baer et al., 1986)
IL-6	Cyclosporin	↑ C_{ss} (3.3-fold)	(Chen et al., 1994)
Influenza Vaccine	Chlorzoxazone	↔Cl	(Kim and Wilkinson, 1996)
Endotoxin	Antipyrine, Hexobarbitone, Theophylline	↓Cl (1.3-fold) ↓Cl (1.2-fold) ↓Cl (1.2-fold)	(Shedlofsky et al., 1994; Shedlofsky et al., 1997)
Malaria	Quinine	↓Cl (2.4-fold)	(Pukrittayakamee et al., 1997)
Advanced Cancer	Omeprazole	↑ CYP2D6 PM phenotype frequency (25% patients *vs* 3% healthy)	(Williams et al., 2000)
HIV (active illness)	Dextromethorphan	Shift from CYP2D6 EM to PM phenotype (3% PM to 7%)	(O'Neil et al., 2000)
Rheumatoid Arthritis	S-Verapamil R-Verapamil	↓Cl/F (2.2-fold) ↓Cl/F (1.5-fold)	(Mayo et al., 2000)
CHF	Caffeine Mephenytoin	↓CYP1A2 activity ↓CYP2C19 activity	(Frye et al., 2002)
Pneumonia	Clozapine	↑ C_{ss} (3.3-fold)	(Raaska et al., 2002)
Respiratory Infection	Clozapine	↑ C_{ss} (2-fold)	(de Leon and Diaz, 2003)
Urinary Tract Infection	Clozapine	↑ C_{ss} (2.2-fold)	(Jecel et al., 2005)

BCG. *Corynebacterium parvum*, and *Bordetella pertussis*
IL-6. Interleukin 6
HIV. Human Immunodeficiency Virus
CHF. Congestive Heart Failure
$t_{½}$. Half life
Cl. Systemic Clearance
CL/F. Oral Clearance
Css. Steady-State concentration

H. REFERENCES

Abdel-Razzak Z, Corcos L, Fautrel A, Campion JP and Guillouzo A (1994) Transforming growth factor-beta 1 down-regulates basal and polycyclic aromatic hydrocarbon-induced cytochromes P-450 1A1 and 1A2 in adult human hepatocytes in primary culture. *Mol Pharmacol* **46:**1100-1110.

Abdel-Razzak Z, Corcos L, Fautrel A and Guillouzo A (1995) Interleukin-1 beta antagonizes phenobarbital induction of several major cytochromes P450 in adult rat hepatocytes in primary culture. *FEBS Lett* **366:**159-164.

Abdel-Razzak Z, Loyer P, Fautrel A, Gautier JC, Corcos L, Turlin B, Beaune P and Guillouzo A (1993) Cytokines down-regulate expression of major cytochrome P-450 enzymes in adult human hepatocytes in primary culture. *Mol Pharmacol* **44:**707-715.

Baer AN, McAllister CB, Wilkinson GR, Woosley RL and Pincus T (1986) Altered distribution of debrisoquine oxidation phenotypes in patients with systemic lupus erythematosus. *Arthritis Rheum* **29:**843-850.

Balasegaram M, Young H, Chappuis F, Priotto G, Raguenaud ME and Checchi F (2009) Effectiveness of melarsoprol and eflornithine as first-line regimens for gambiense sleeping sickness in nine Medecins Sans Frontieres programmes. *Trans R Soc Trop Med Hyg* **103:**280-290.

Barrett MP, Boykin DW, Brun R and Tidwell RR (2007) Human African trypanosomiasis: pharmacological re-engagement with a neglected disease. *Br J Pharmacol* **152:**1155-1171.

Beale JM, Block JH, Gisvold O and Wilson CO (2004) *Wilson and Gisvold's textbook of organic medicinal and pharmaceutical chemistry / edited by John H. Block, John M. Beale Jr*. Lippincott Williams & Wilkins, Philadelphia.

Bleau AM, Levitchi MC, Maurice H and du Souich P (2000) Cytochrome P450 inactivation by serum from humans with a viral infection and serum from rabbits with a turpentine-induced inflammation: the role of cytokines. *Br J Pharmacol* **130:**1777-1784.

Bogdan C, Paik J, Vodovotz Y and Nathan C (1992) Contrasting mechanisms for suppression of macrophage cytokine release by transforming growth factor-beta and interleukin-10. *J Biol Chem* **267:**23301-23308.

Boykin DW, Kumar A, Spychala J, Zhou M, Lombardy RJ, Wilson WD, Dykstra CC, Jones SK, Hall JE, Tidwell RR and et al. (1995) Dicationic diarylfurans as anti-Pneumocystis carinii agents. *J Med Chem* **38:**912-916.

Bronner U, Doua F, Ericsson O, Gustafsson LL, Miezan TW, Rais M and Rombo L (1991) Pentamidine concentrations in plasma, whole blood and cerebrospinal fluid during treatment of Trypanosoma gambiense infection in Cote d'Ivoire. *Trans R Soc Trop Med Hyg* **85:**608-611.

Brunton LL, Gilman A, Goodman LS, Lazo JS and Parker KL (2006) *Goodman & Gilman's the pharmacological basis of therapeutics*. McGraw-Hill, New York.

Burri C and Brun R (2003) Eflornithine for the treatment of human African trypanosomiasis. *Parasitol Res* **90 Supp 1:**S49-52.

Callahan SM, Ming X, Lu SK, Brunner LJ and Croyle MA (2005) Considerations for use of recombinant adenoviral vectors: dose effect on hepatic cytochromes P450. *J Pharmacol Exp Ther* **312:**492-501.

Calleja C, Bigot K, Eeckhoutte C, Sibille P, Boulard C and Galtier P (2000) Comparison of hepatic and renal drug-metabolising enzyme activities in sheep given single or two-fold challenge infections with Fasciola hepatica. *Int J Parasitol* **30:**953-958.

Casarett LJ, Doull J and Klaassen CD (2008) *Casarett and Doull's toxicology : the basic science of poisons*. McGraw-Hill Medical, New York.

Ceciliani F, Giordano A and Spagnolo V (2002) The systemic reaction during inflammation: the acute-phase proteins. *Protein Pept Lett* **9:**211-223.

Chang KC, Bell TD, Lauer BA and Chai H (1978) Altered theophylline pharmacokinetics during acute respiratory viral illness. *Lancet* **1:**1132-1133.

Charles KA, Rivory LP, Brown SL, Liddle C, Clarke SJ and Robertson GR (2006) Transcriptional repression of hepatic cytochrome P450 3A4 gene in the presence of cancer. *Clin Cancer Res* **12:**7492-7497.

Chen JQ, Strom A, Gustafsson JA and Morgan ET (1995) Suppression of the constitutive expression of cytochrome P-450 2C11 by cytokines and interferons in primary cultures of rat hepatocytes: comparison with induction of acute-phase genes and demonstration that CYP2C11 promoter sequences are involved in the suppressive response to interleukins 1 and 6. *Mol Pharmacol* **47:**940-947.

Chen YL, Le Vraux V, Leneveu A, Dreyfus F, Stheneur A, Florentin I, De Sousa M, Giroud JP, Flouvat B and Chauvelot-Moachon L (1994) Acute-phase response, interleukin-6, and alteration of cyclosporine pharmacokinetics. *Clin Pharmacol Ther* **55:**649-660.

Chung HJ, Kang HE, Bae EJ, Lee I, Kim SG and Lee MG (2008) Effects of E. Coli lipopolysaccharide on the pharmacokinetics of ipriflavone and its metabolites, M1 and M5, after intravenous and oral administration of ipriflavone to rats: decreased metabolism of ipriflavone due to decreased expression of hepatic CYP1A2 and 2C11. *J Pharm Sci* **97:**5024-5036.

Cui X, Kalsotra A, Robida AM, Matzilevich D, Moore AN, Boehme CL, Morgan ET, Dash PK and Strobel HW (2003) Expression of cytochromes P450 4F4 and 4F5 in infection and injury models of inflammation. *Biochim Biophys Acta* **1619:**325-331.

Davies AJ, Harindra V, McEwan A and Ghose RR (1989) Cardiotoxic effect with convulsions in terfenadine overdose. *BMJ* **298:**325.

De-Oliveira AC, Carvalho RS, Paixao FH, Tavares HS, Gueiros LS, Siqueira CM and Paumgartten FJ (2010) Up- and down-modulation of liver cytochrome P450 activities and associated events in two murine malaria models. *Malar J* **9:**81.

de Leon J and Diaz FJ (2003) Serious respiratory infections can increase clozapine levels and contribute to side effects: a case report. *Prog Neuropsychopharmacol Biol Psychiatry* **27:**1059-1063.

Donelson JE, Hill KL and El-Sayed NM (1998) Multiple mechanisms of immune evasion by African trypanosomes. *Mol Biochem Parasitol* **91:**51-66.

Ettmayer P, Amidon GL, Clement B and Testa B (2004) Lessons learned from marketed and investigational prodrugs. *J Med Chem* **47:**2393-2404.

Fairlamb AH (2003) Chemotherapy of human African trypanosomiasis: current and future prospects. *Trends Parasitol* **19:**488-494.

Ferrari L, Jouzeau JY, Gillet P, Herber R, Fener P, Batt AM and Netter P (1993) Interleukin-1 beta differentially represses drug-metabolizing enzymes in arthritic female rats. *J Pharmacol Exp Ther* **264:**1012-1020.

Ferrari L, Peng N, Halpert JR and Morgan ET (2001) Role of nitric oxide in down-regulation of CYP2B1 protein, but not RNA, in primary cultures of rat hepatocytes. *Mol Pharmacol* **60:**209-216.

Frye RF, Schneider VM, Frye CS and Feldman AM (2002) Plasma levels of TNF-alpha and IL-6 are inversely related to cytochrome P450-dependent drug metabolism in patients with congestive heart failure. *J Card Fail* **8:**315-319.

Geier A, Dietrich CG, Voigt S, Ananthanarayanan M, Lammert F, Schmitz A, Trauner M, Wasmuth HE, Boraschi D, Balasubramaniyan N, Suchy FJ, Matern S and Gartung C (2005) Cytokine-dependent regulation of hepatic organic anion transporter gene transactivators in mouse liver. *Am J Physiol Gastrointest Liver Physiol* **289:**G831-841.

Getachew Y, James L, Lee WM, Thiele DL and Miller BC (2010) Susceptibility to acetaminophen (APAP) toxicity unexpectedly is decreased during acute viral hepatitis in mice. *Biochem Pharmacol* **79:**1363-1371.

Gharavi N and El-Kadi AO (2007) Role of nitric oxide in downregulation of cytochrome P450 1a1 and NADPH: Quinone oxidoreductase 1 by tumor necrosis factor-alpha and lipopolysaccharide. *J Pharm Sci* **96:**2795-2807.

Goralski KB, Hartmann G, Piquette-Miller M and Renton KW (2003) Downregulation of mdr1a expression in the brain and liver during CNS inflammation alters the in vivo disposition of digoxin. *Br J Pharmacol* **139:**35-48.

Gray JD, Renton KW and Hung OR (1983) Depression of theophylline elimination following BCG vaccination. *Br J Clin Pharmacol* **16:**735-737.

Hayney MS and Buck JM (2002) Effect of age and degree of immune activation on cytochrome P450 3A4 activity after influenza immunization. *Pharmacotherapy* **22:**1235-1238.

Ho EA and Piquette-Miller M (2006) Regulation of multidrug resistance by pro-inflammatory cytokines. *Curr Cancer Drug Targets* **6:**295-311.

Islam M, Frye RF, Richards TJ, Sbeitan I, Donnelly SS, Glue P, Agarwala SS and Kirkwood JM (2002) Differential effect of IFNalpha-2b on the cytochrome P450 enzyme system: a potential basis of IFN toxicity and its modulation by other drugs. *Clin Cancer Res* **8:**2480-2487.

Ismail MA, Arafa RK, Brun R, Wenzler T, Miao Y, Wilson WD, Generaux C, Bridges A, Hall JE and Boykin DW (2006) Synthesis, DNA affinity, and antiprotozoal activity of linear dications: Terphenyl diamidines and analogues. *J Med Chem* **49:**5324-5332.

Israel BC, Blouin RA, McIntyre W and Shedlofsky SI (1993) Effects of interferon-alpha monotherapy on hepatic drug metabolism in cancer patients. *Br J Clin Pharmacol* **36:**229-235.

Janeway C (2005) *Immunobiology : the immune system in health and disease*. Garland Science, New York.

Jecel J, Michel TM, Gutknecht L, Schmidt D, Pfuhlmann B and Jabs BE (2005) Toxic clozapine serum levels during acute urinary tract infection: a case report. *Eur J Clin Pharmacol* **60:**909-910.

Kacevska M, Robertson GR, Clarke SJ and Liddle C (2008) Inflammation and CYP3A4-mediated drug metabolism in advanced cancer: impact and implications for chemotherapeutic drug dosing. *Expert Opin Drug Metab Toxicol* **4:**137-149.

Kalitsky-Szirtes J, Shayeganpour A, Brocks DR and Piquette-Miller M (2004) Suppression of drug-metabolizing enzymes and efflux transporters in the intestine of endotoxin-treated rats. *Drug Metab Dispos* **32:**20-27.

Kalsotra A, Anakk S, Brommer CL, Kikuta Y, Morgan ET and Strobel HW (2007) Catalytic characterization and cytokine mediated regulation of cytochrome P450 4Fs in rat hepatocytes. *Arch Biochem Biophys* **461:**104-112.

Kato R, Yamashita S, Moriguchi J, Nakagawa M, Tsukura Y, Uchida K, Amano F, Hirotani Y, Ijiri Y and Tanaka K (2008) Changes of midazolam pharmacokinetics in Wistar rats treated with lipopolysaccharide: relationship between total CYP and CYP3A2. *Innate Immun* **14:**291-297.

Khatsenko OG, Barteneva NS, de la Maza LM and Kikkawa Y (1998) Role of nitric oxide in the inhibition of cytochrome P450 in the liver of mice infected with Chlamydia trachomatis. *Biochem Pharmacol* **55:**1835-1842.

Khatsenko OG, Gross SS, Rifkind AB and Vane JR (1993) Nitric oxide is a mediator of the decrease in cytochrome P450-dependent metabolism caused by immunostimulants. *Proc Natl Acad Sci U S A* **90:**11147-11151.

Kim RB and Wilkinson GR (1996) CYP2E1 activity is not altered by influenza vaccination. *Br J Clin Pharmacol* **42:**529-530.

Klaassen CD and Aleksunes LM (2010) Xenobiotic, bile acid, and cholesterol transporters: function and regulation. *Pharmacol Rev* **62:**1-96.

Kraemer MJ, Furukawa CT, Koup JR, Shapiro GG, Pierson WE and Bierman CW (1982) Altered theophylline clearance during an influenza B outbreak. *Pediatrics* **69:**476-480.

Kramer P and McClain CJ (1981) Depression of aminopyrine metabolism by influenza vaccination. *N Engl J Med* **305:**1262-1264.

Langouet S, Corcos L, Abdel-Razzak Z, Loyer P, Ketterer B and Guillouzo A (1995) Up-regulation of glutathione S-transferases alpha by interleukin 4 in human hepatocytes in primary culture. *Biochem Biophys Res Commun* **216:**793-800.

Le Vee M, Gripon P, Stieger B and Fardel O (2008) Down-regulation of organic anion transporter expression in human hepatocytes exposed to the proinflammatory cytokine interleukin 1beta. *Drug Metab Dispos* **36:**217-222.

Lee G and Piquette-Miller M (2001) Influence of IL-6 on MDR and MRP-mediated multidrug resistance in human hepatoma cells. *Can J Physiol Pharmacol* **79:**876-884.

Lee JH, Cho YK, Jung YS, Kim YC and Lee MG (2008) Effects of Escherichia coli lipopolysaccharide on telithromycin pharmacokinetics in rats: inhibition of metabolism via CYP3A. *Antimicrob Agents Chemother* **52:**1046-1051.

Legros D, Ollivier G, Gastellu-Etchegorry M, Paquet C, Burri C, Jannin J and Buscher P (2002) Treatment of human African trypanosomiasis--present situation and needs for research and development. *Lancet Infect Dis* **2:**437-440.

Martin AN and Sinko PJ (2006) *Martin's physical pharmacy and pharmaceutical sciences : physical chemical and biopharmaceutical principles in the pharmaceutical sciences*. Lippincott Williams & Wilkins, Philadelphia.

Mathis AM, Holman JL, Sturk LM, Ismail MA, Boykin DW, Tidwell RR and Hall JE (2006) Accumulation and intracellular distribution of antitrypanosomal diamidine compounds DB75 and DB820 in African trypanosomes. *Antimicrob Agents Chemother* **50:**2185-2191.

Mayo PR, Skeith K, Russell AS and Jamali F (2000) Decreased dromotropic response to verapamil despite pronounced increased drug concentration in rheumatoid arthritis. *Br J Clin Pharmacol* **50:**605-613.

Midgley I, Fitzpatrick K, Taylor LM, Houchen TL, Henderson SJ, Wright SJ, Cybulski ZR, John BA, McBurney A, Boykin DW and Trendler KL (2007) Pharmacokinetics and metabolism of the prodrug DB289 (2,5-bis[4-(N-methoxyamidino)phenyl]furan monomaleate) in rat and monkey and its conversion to the antiprotozoal/antifungal drug DB75 (2,5-bis(4-guanylphenyl)furan dihydrochloride). *Drug Metab Dispos* **35:**955-967.

Ming X, Ju W, Wu H, Tidwell RR, Hall JE and Thakker DR (2009) Transport of dicationic drugs pentamidine and furamidine by human organic cation transporters. *Drug Metab Dispos* **37:**424-430.

Monshouwer M, Witkamp RF, Nujmeijer SM, Van Amsterdam JG and Van Miert AS (1996) Suppression of cytochrome P450- and UDP glucuronosyl transferase-dependent enzyme activities by proinflammatory cytokines and possible role of nitric oxide in primary cultures of pig hepatocytes. *Toxicol Appl Pharmacol* **137:**237-244.

Montero R, Serrano L, Davila VM, Ito A and Plancarte A (2003) Infection of rats with Taenia taeniformis metacestodes increases hepatic CYP450, induces the activity of CYP1A1, CYP2B1 and COH isoforms and increases the genotoxicity of the procarcinogens benzo[a]pyrene, cyclophosphamide and aflatoxin B(1). *Mutagenesis* **18:**211-216.

Morgan ET (1997) Regulation of cytochromes P450 during inflammation and infection. *Drug Metab Rev* **29:**1129-1188.

Morgan ET, Goralski KB, Piquette-Miller M, Renton KW, Robertson GR, Chaluvadi MR, Charles KA, Clarke SJ, Kacevska M, Liddle C, Richardson TA, Sharma R and Sinal CJ (2008) Regulation of drug-metabolizing enzymes and transporters in infection, inflammation, and cancer. *Drug Metab Dispos* **36:**205-216.

Muller CM, Scierka A, Stiller RL, Kim YM, Cook DR, Lancaster JR, Jr., Buffington CW and Watkins WD (1996) Nitric oxide mediates hepatic cytochrome P450 dysfunction induced by endotoxin. *Anesthesiology* **84:**1435-1442.

Muntane J (2009) Regulation of drug metabolism and transporters. *Curr Drug Metab* **10:**932-945.

Nathan CF and Hibbs JB, Jr. (1991) Role of nitric oxide synthesis in macrophage antimicrobial activity. *Curr Opin Immunol* **3:**65-70.

Nok AJ (2003) Arsenicals (melarsoprol), pentamidine and suramin in the treatment of human African trypanosomiasis. *Parasitol Res* **90:**71-79.

O'Neil WM, Gilfix BM, Markoglou N, Di Girolamo A, Tsoukas CM and Wainer IW (2000) Genotype and phenotype of cytochrome P450 2D6 in human immunodeficiency virus-positive patients and patients with acquired immunodeficiency syndrome. *Eur J Clin Pharmacol* **56:**231-240.

Obach RS, Baxter JG, Liston TE, Silber BM, Jones BC, MacIntyre F, Rance DJ and Wastall P (1997) The prediction of human pharmacokinetic parameters from preclinical and in vitro metabolism data. *J Pharmacol Exp Ther* **283:**46-58.

Okuno H, Takasu M, Kano H, Seki T, Shiozaki Y and Inoue K (1993) Depression of drug-metabolizing activity in the human liver by interferon-beta. *Hepatology* **17:**65-69.

Pageaux GP, le Bricquir Y, Berthou F, Bressot N, Picot MC, Blanc F, Michel H and Larrey D (1998) Effects of interferon-alpha on cytochrome P-450 isoforms 1A2 and 3A activities in patients with chronic hepatitis C. *Eur J Gastroenterol Hepatol* **10:**491-495.

Peterson TC and Renton KW (1984) Depression of cytochrome P-450-dependent drug biotransformation in hepatocytes after the activation of the reticuloendothelial system by dextran sulfate. *J Pharmacol Exp Ther* **229:**299-304.

Priotto G, Fogg C, Balasegaram M, Erphas O, Louga A, Checchi F, Ghabri S and Piola P (2006) Three Drug Combinations for Late-Stage *Trypanosoma brucei gambiense* Sleeping Sickness: A Randomized Clinical Trial in Uganda. *PLOS Clin Trial* **1:**e39.

Projean D, Dautrey S, Vu HK, Groblewski T, Brazier JL and Ducharme J (2005) Selective downregulation of hepatic cytochrome P450 expression and activity in a rat model of inflammatory pain. *Pharm Res* **22:**62-70.

Pugeat M, Bonneton A, Perrot D, Rocle-Nicolas B, Lejeune H, Grenot C, Dechaud H, Brebant C, Motin J and Cuilleron CY (1989) Decreased immunoreactivity and binding activity of corticosteroid-binding globulin in serum in septic shock. *Clin Chem* **35:**1675-1679.

Pukrittayakamee S, Looareesuwan S, Keeratithakul D, Davis TM, Teja-Isavadharm P, Nagachinta B, Weber A, Smith AL, Kyle D and White NJ (1997) A study of the factors affecting the metabolic clearance of quinine in malaria. *Eur J Clin Pharmacol* **52:**487-493.

Raaska K, Raitasuo V, Arstila M and Neuvonen PJ (2002) Bacterial pneumonia can increase serum concentration of clozapine. *Eur J Clin Pharmacol* **58:**321-322.

Renton KW (1981) Depression of hepatic cytochrome P-450-dependent mixed function oxidases during infection with encephalomyocarditis virus. *Biochem Pharmacol* **30:**2333-2336.

Renton KW (2004) Cytochrome P450 regulation and drug biotransformation during inflammation and infection. *Curr Drug Metab* **5:**235-243.

Renton KW (2005) Regulation of drug metabolism and disposition during inflammation and infection. *Expert Opin Drug Metab Toxicol* **1:**629-640.

Richardson TA, Sherman M, Antonovic L, Kardar SS, Strobel HW, Kalman D and Morgan ET (2006) Hepatic and renal cytochrome p450 gene regulation during citrobacter rodentium infection in wild-type and toll-like receptor 4 mutant mice. *Drug Metab Dispos* **34:**354-360.

Ritchie RF, Palomaki GE, Neveux LM, Navolotskaia O, Ledue TB and Craig WY (1999) Reference distributions for the negative acute-phase serum proteins, albumin, transferrin and transthyretin: a practical, simple and clinically relevant approach in a large cohort. *J Clin Lab Anal* **13:**273-279.

Robertson GR, Liddle C and Clarke SJ (2008) Inflammation and altered drug clearance in cancer: transcriptional repression of a human CYP3A4 transgene in tumor-bearing mice. *Clin Pharmacol Ther* **83:**894-897.

Rockich K and Blouin R (1999) Effect of the acute-phase response on the pharmacokinetics of chlorzoxazone and cytochrome P-450 2E1 in vitro activity in rats. *Drug Metab Dispos* **27:**1074-1077.

Saad B, Frei K, Scholl FA, Fontana A and Maier P (1995) Hepatocyte-derived interleukin-6 and tumor-necrosis factor alpha mediate the lipopolysaccharide-induced acute-phase response and nitric oxide release by cultured rat hepatocytes. *Eur J Biochem* **229:**349-355.

Saulter J, Kurian J, Trepanier L, Tidwell R, Bridges A, Boykin D, Stephens C, Anbazhagan M and Hall JE (2005) Unusual Dehydroxylation of Antimicrobial Amidoxime Prodrugs by Cytochrome b_5 and NADH Cytochrome b_5 Reductase. *Drug Metab Dispos* **33:**1886-1893.

Saulter JY (2005) *Permeability and metabolism of potential prodrugs for the antimicrobial agent 2,5 bis(4-amidinophenyl)furan (DB75)*. University of North Carolina School of Pharmacy, Chapel Hill, NC.

Sharma R, Kacevska M, London R, Clarke SJ, Liddle C and Robertson G (2008) Downregulation of drug transport and metabolism in mice bearing extra-hepatic malignancies. *Br J Cancer* **98:**91-97.

Shedlofsky SI, Israel BC, McClain CJ, Hill DB and Blouin RA (1994) Endotoxin administration to humans inhibits hepatic cytochrome P450-mediated drug metabolism. *J Clin Invest* **94:**2209-2214.

Shedlofsky SI, Israel BC, Tosheva R and Blouin RA (1997) Endotoxin depresses hepatic cytochrome P450-mediated drug metabolism in women. *Br J Clin Pharmacol* **43:**627-632.

Shertzer HG, Hall JE and Seed JR (1981) Hepatic mixed-function oxidase activity in mice infected with Trypanosoma brucei gambiense or treated with trypanocides. *Mol Biochem Parasitol* **3:**199-204.

Shertzer HG, Hall JE and Seed JR (1982) Hepatic microsomal alterations during chronic trypanosomiasis in the field vole, Microtus montanus. *Mol Biochem Parasitol* **6:**25-32.

Sheth K and Bankey P (2001) The liver as an immune organ. *Curr Opin Crit Care* **7:**99-104.

Sonne J, Dossing M, Loft S and Andreasen PB (1985) Antipyrine clearance in pneumonia. *Clin Pharmacol Ther* **37:**701-704.

Sternberg JM (2004) Human African trypanosomiasis: clinical presentation and immune response. *Parasite Immunology* **26:**476.

Sugatani J, Kojima H, Ueda A, Kakizaki S, Yoshinari K, Gong QH, Owens IS, Negishi M and Sueyoshi T (2001) The phenobarbital response enhancer module in the human bilirubin UDP-glucuronosyltransferase UGT1A1 gene and regulation by the nuclear receptor CAR. *Hepatology* **33:**1232-1238.

Sukhai M, Yong A, Pak A and Piquette-Miller M (2001) Decreased expression of P-glycoprotein in interleukin-1beta and interleukin-6 treated rat hepatocytes. *Inflamm Res* **50:**362-370.

Sunman JA, Hawke RL, LeCluyse EL and Kashuba AD (2004) Kupffer cell-mediated IL-2 suppression of CYP3A activity in human hepatocytes. *Drug Metab Dispos* **32:**359-363.

Ueyama J, Nadai M, Kanazawa H, Iwase M, Nakayama H, Hashimoto K, Yokoi T, Baba K, Takagi K and Hasegawa T (2005) Endotoxin from various gram-negative bacteria has differential effects on function of hepatic cytochrome P450 and drug transporters. *Eur J Pharmacol* **510:**127-134.

Vassileva V and Piquette-Miller M (2010) Inflammation: extinguishing the fires within. *Clin Pharmacol Ther* **87:**375-379.

Wang JH, Scollard DA, Teng S, Reilly RM and Piquette-Miller M (2005) Detection of P-glycoprotein activity in endotoxemic rats by 99mTc-sestamibi imaging. *J Nucl Med* **46:**1537-1545.

Wang MZ, Saulter JY, Usuki E, Cheung YL, Hall M, Bridges AS, Loewen G, Parkinson OT, Stephens CE, Allen JL, Zeldin DC, Boykin DW, Tidwell RR, Parkinson A, Paine MF and Hall JE (2006) CYP4F enzymes are the major enzymes in human liver microsomes that catalyze the O-demethylation of the antiparasitic prodrug DB289 [2,5-bis(4-amidinophenyl)furan-bis-O-methylamidoxime]. *Drug Metab Dispos* **34:**1985-1994.

Wenzler T, Boykin DW, Ismail MA, Hall JE, Tidwell RR and Brun R (2009) New treatment option for second-stage African sleeping sickness: in vitro and in vivo efficacy of aza analogs of DB289. *Antimicrob Agents Chemother* **53:**4185-4192.

WHO. 2010. Http://www.who.int/mediacentre/factsheets/fs259/en/

Williams ML, Bhargava P, Cherrouk I, Marshall JL, Flockhart DA and Wainer IW (2000) A discordance of the cytochrome P450 2C19 genotype and phenotype in patients with advanced cancer. *Br J Clin Pharmacol* **49:**485-488.

Wolf KK, Wood SG, Allard JL, Hunt JA, Gorman N, Walton-Strong BW, Szakacs JG, Duan SX, Hao Q, Court MH, von Moltke LL, Greenblatt DJ, Kostrubsky V, Jeffery EH, Wrighton SA, Gonzalez FJ, Sinclair PR and Sinclair JF (2007) Role of CYP3A and CYP2E1 in alcohol-mediated increases in acetaminophen hepatotoxicity: comparison of wild-type and Cyp2e1(-/-) mice. *Drug Metab Dispos* **35:**1223-1231.

Wonganan P, Zamboni WC, Strychor S, Dekker JD and Croyle MA (2009) Drug-virus interaction: effect of administration of recombinant adenoviruses on the pharmacokinetics of docetaxel in a rat model. *Cancer Gene Ther* **16:**405-414.

Xu C, Li CY and Kong AN (2005) Induction of phase I, II and III drug metabolism/transport by xenobiotics. *Arch Pharm Res* **28:**249-268.

Yaghi A, Bend JR, Webb CD, Zeldin DC, Weicker S, Mehta S and McCormack DG (2004) Excess nitric oxide decreases cytochrome P-450 2J4 content and P-450-dependent arachidonic acid metabolism in lungs of rats with acute pneumonia. *Am J Physiol Lung Cell Mol Physiol* **286:**L1260-1267.

Yang KH and Lee MG (2008) Effects of endotoxin derived from Escherichia coli lipopolysaccharide on the pharmacokinetics of drugs. *Arch Pharm Res* **31:**1073-1086.

Zhang L, Dresser MJ, Gray AT, Yost SC, Terashita S and Giacomini KM (1997) Cloning and functional expression of a human liver organic cation transporter. *Mol Pharmacol* **51:**913-921.

Zhou L, Lee K, Thakker DR, Boykin DW, Tidwell RR and Hall JE (2002) Enhanced permeability of the antimicrobial agent 2,5-bis(4-amidinophenyl)furan across Caco-2 cell monolayers via its methylamidoidme prodrug. *Pharm Res* **19:**1689-1695.

Zhou L, Thakker DR, Voyksner RD, Anbazhagan M, Boykin DW, Hall JE and Tidwell RR (2004) Metabolites of an orally active antimicrobial prodrug, 2,5-bis(4-amidinophenyl)furan-bis-O-methylamidoxime, identified by liquid chromatography/tandem mass spectrometry. *J Mass Spectrom* **39:**351-360.

CHAPTER 2

IN VITRO BIOTRANSFORMATION OF THE ANTITRYPANOSOMAL PRODRUG 2, 5-BIS [5-(*N*-METHOXYAMIDINO)-2-PYRIDYL] FURAN (DB868) BY HUMAN AND RAT ENZYMES: A COMPARTMENTAL MODELING APPROACH TO ELUCIDATE METABOLIC CONVERSION TO THE ACTIVE DRUG 2, 5-BIS (5-AMIDINO-2-PYRIDYL) FURAN (DB829)

This chapter will be submitted to the *Journal of Pharmacology and Experimental Therapeutics* and is formatted in the style of this journal.

A. ABSTRACT

DB868 is the prodrug of the antitrypanosomal diamidine DB829 and a potential candidate drug for treatment of second-stage human African trypanosomiasis (HAT). Oral administration of DB868 in a murine model of second-stage HAT was 100% effective, indicating in vivo metabolic activation. To date, the biotransformation of DB868 is unknown; accordingly, this study characterized the phase-I biotransformation of DB868 in liver microsomes and sandwich-cultured hepatocytes from humans and rats (HLMs, RLMs and HSCHs, RSCHs, respectively). DB868 generated four NADPH-dependent metabolites (M1-M4) which corresponded to *O*-demethylated, and *N*-dehydroxylated products based on mass spectrometry analysis. M1 formation in HLMs followed Michaelis-Menten kinetics (K_m = 11 μM), whereas a two-enzyme model described the kinetics of M1 in RLMs (K_m = 0.5 μM, high affinity component). M1 formation was catalyzed by CYP1A2, CYP3A and CYP4F2 in humans, and CYP1A2, CYP2D2 and CYP4F1 in rats. M2 formation in HLMs exhibited allosteric kinetics via CYP1A2 ($CL_{max} \approx 2$ μL/min/mg protein); whereas M2 formation in RLMs was negligible. Kinetic analysis of the DB868 metabolic pathway gave an insight into an unusual *N*-demethoxylation reaction which was confirmed experimentally. In HLMs, DB829 was negligible after 180 min incubations but formed readily in hepatocytes of both species, with the majority of the compound sequestered intracellularly. Collectively this study shows extensive hepatic metabolism of DB868 in humans and rats with four phase-I metabolites generated before DB829; however, despite the importance of metabolism activating the prodrug hepatocyte data suggests that systemic availability of DB829 is limited by intracellular binding and efflux rather than metabolism.

B. INTRODUCTION

Human African trypanosomiasis (HAT) is a neglected parasitic disease that afflicts exclusively the world's poorest populations (Barrett, 2007). According to the latest reports by the World Health Organization, 36 countries in sub-Saharan Africa are considered endemic for the disease (WHO, 2010). HAT is caused by the parasite *Trypanosoma brucei*, which is transmitted to the host by the bite of the Tsetse fly. The disease is characterized by two defined stages. During the first stage of the infection, the trypanosomes are confined to the hemolymphatic system; symptoms include headache, malaise, fever, joint pain (Sternberg, 2004). The second stage of the infection begins once the trypanosomes have migrated to the central nervous system (CNS), initiating deterioration of neurological function, which includes disruptions in the sleep/wake cycle, hence the name "sleeping sickness" (Sternberg, 2004). Without treatment, progressive CNS damage leads to coma and eventually, death.

Current therapeutic agents for the treatment of HAT are scarce and are associated with moderate to severe side effects, as well as impractical dosing regimens (Fairlamb, 2003). The two drugs that are approved for the first-stage infection are pentamidine and suramin. Both must be given parenterally, over a course of at least seven days (pentamidine) to four weeks (suramin) (Barrett, 2007). Moreover, due to an inability to enter the CNS, neither agent is effective against the second-stage infection. As with the first-stage infection, only two drugs are approved for the second-stage infection: melarsoprol and eflornithine. The arsenic-containing melarsoprol must be administered intravenously, three to four times daily, for a period of three to four weeks. Moreover, 5-10% of the melarsoprol treated patients suffer severe post-treatment reactive encephalopathy, of which 50% die (Legros et

al., 2002). Although eflornithine therapy is not life-threatening, the drug must be administered intravenously as multiple infusions daily, usually every six hours for two weeks (Barrett et al., 2007). Studies with eflornithine in combination with nifurtimox (a drug for the treatment for Chagas disease) as an alternative first-line therapy for the treatment for second stage HAT showed promise (Priotto et al., 2006) and in 2008 the Nifurtimox-Eflornithine Combination Therapy (NECT) was approved; however, emergence of resistance against this eflornitine has recently been reported (Balasegaram et al., 2009). Currently, no drugs are in development for the second stage HAT, hence the discovery and development of new treatments especially with orally administered medication, is of high urgency.

An analog of pentamidine, 2,5-bis(5-amidino-2-pyridyl) furan (DB829), is an aromatic diamidine that has shown excellent in vitro activity against different sub-species of trypanosomes, including *Trypanosoma brucei gambiense*, the subspecies causative of second stage HAT. The in vitro potency of DB829 against three *T. b. gambiense* isolates, including STIB930, ITMAP141267 and K03048, was comparable to that of melarsoprol, as measured by IC_{50} values of <40 ng/mL (Fairlamb, 2003; Wenzler et al., 2009). Moreover, intraperitoneal administration of DB829 in the GVR35 CNS murine model (20 mg/kg for 10 days), which mimics the second-stage HAT, showed a 100% cure rate (Fairlamb, 2003; Wenzler et al., 2009).

The two positive charges on diamidines (calculated pK_as range from 9-11) render these compounds impermeant to biological membranes via passive diffusion; thus when given orally these dications have low bioavailability due to poor absorption, resulting in a lack of efficacy (Boykin et al., 1995). To improve the oral bioavailability of DB829, the prodrug DB868 was prepared by masking each amidino group of the DB829 molecule with

O-methoxy functional groups (Figure 2.1) (Ismail et al., 2003). In vivo studies showed that DB868 had a 100% cure rate in the GVR35 CNS murine model of HAT at an oral daily dose of 100 mg/kg for 5 days (Wenzler, 2009) indicating that the prodrug was orally bioavailable and that it was activated to DB829 in vivo sufficiently to achieve therapeutic efficacy. However, despite these positive results in mice, it is unknown whether the activation of the prodrug to DB829 will be sufficient in other preclinical species or in humans to achieve therapeutic efficacy.

Accordingly, the goal of this investigation was to characterize the in vitro biotransformation of the prodrug DB868 to the active drug DB829 with microsomes and hepatocytes prepared from humans and rats. The results of these studies will help guide the preclinical and clinical evaluation of DB868 for the treatment of second stage HAT.

C. METHODS

Chemicals and Reagents. DB829, d_6-DB829, DB840 (M2), DB868 lot D, d_6-DB868, DB1217 (M3), and DB1679 (M1), were synthesized in the laboratory of D.W. Boykin (Ismail et al., 2003; Mohamed and David, 2006). Pooled male rat and mixed gender human liver microsomes (RLMs and HLMs, respectively) were obtained from XenoTech, LLC (Lenexa, KS). All human and rat recombinant enzymes were derived from insect cells (SUPERSOMES™) and were obtained from BD Gentest (Woburn, MA). The human recombinant enzymes CYP1A2, CYP2D6, CYP3A4 as well as the rat recombinant enzymes CYP1A2, CYP2D1 and CYP2D2 were co-expressed with NADPH-cytochrome P450 reductase. The human recombinant enzyme CYP4F2, and the rat recombinant enzymes CYP2A1, CYP2A2, CYP2B1, CYP2C6, CYP2C11, CYP2C13, CYP2E1, CYP3A1 were co-

expressed with NADPH cytochrome P450 reductase and cytochrome b_5. Purified rat CYP4F1, CYP4F4, CYP4F5 and CYP4F6 were a gift from Dr. Deanna Kroetz (University of California San Francisco). Dubelcco's modified Eagle's Medium (DMEM, without phenol red), and purified recombinant human NADPH-cytochrome P450 reductase were obtained from Invitrogen (Carlsbad, CA). Human and rat sandwich culture hepatocytes (HSCHs and RSCHs, respectively) were obtained from Cellz Direct (Durham, NC). Acetonitrile and HPLC-grade water were purchased from Fisher Scientific (Pittsburgh, PA). 1-Aminobenzotriazole (ABT), ammonium formate, catalase, dilauroylphosphatidylcholine, dimethyl sulfoxide (DMSO), formic acid, glucose 6-phosphate, glucose 6-phosphate dehydrogenase, methanol, β-NADPH, sodium cholate and trifluoroacetic acid (TFA) were obtained from Sigma-Aldrich (St. Louis, MO).

Metabolite Profiling and Structure Identification Experiments. Incubation mixtures contained HLMs or RLMs (0.5 mg/mL), potassium phosphate buffer (100 mM, pH 7.4), $MgCl_2$ (10 mM), and the prodrug DB868 (15 μM). The total incubation volume was 500 μL. The mixtures were warmed to 37°C, and the reactions were initiated by the addition of β-NADPH (2 mM). Incubations were performed in duplicate. Reactions were terminated at 0, 5, 15, 30, 60, 90, 120 and 180 min by removing 50-μL aliquots from the incubation mixture and adding to an equal volume of ice-cold acetonitrile. Proteins were precipitated by centrifugation (3000 rpm for 5 min), and the supernatant was analyzed for prodrug, active metabolite, and intermediate metabolites by HPLC/MS/MS.

Metabolite Quantification Experiments. Incubation mixtures contained HLM or RLM (0.5 mg/mL), potassium phosphate buffer (100 mM, pH 7.4), $MgCl_2$ (10 mM), $NADP^+$ (1 mM), glucose 6-phosphate (5 mM), glucose 6-phosphate dehydrogenase (1 unit/ml), and

the prodrug DB868 (10 μM). The NADPH-generating system was used in this case to ensure that cofactor was not depleted by 180 min. However, similar results were obtained using NADPH (2 mM) in a repeat experiment. DB868 was dissolved in DMSO such that the final solvent concentration was 0.5% (v/v). Incubations were performed in triplicate. The total incubation volume was 250 μL. The reactions were initiated at 10-sec intervals by the addition of the NADPH-generating system. Reactions were terminated at 0, 2.5, 5, 10, 15, 30, 45, 60, 90, 120 and 180 min by the addition of ice-cold acetonitrile (125 μL). Proteins were precipitated by centrifugation (3000 rpm for 10 min), and the supernatant was analyzed for prodrug, active metabolite, and intermediate metabolites by HPLC-UV.

Enzyme Kinetic Experiments Incubation mixtures contained HLMs or RLMs (0.5 mg/mL), potassium phosphate buffer (100 mM, pH 7.4), $MgCl_2$ (10 mM), NADPH (2 mM), and either DB868 (0.1 - 100 μM) or M1 (0.1 - 25 μM). DB868 and M1 were dissolved in DMSO such that the final solvent concentration was 0.5% (v/v). Incubations were performed in triplicate. The total incubation volume was 250 μL for incubations with DB868 or M1. The reactions were initiated by the addition of the NADPH (2 mM). The reactions were terminated at 5 min for incubations containing HLMs or at 10 min for incubations containing RLMs. The reactions were stopped with acetonitrile (125 μL) containing d_6-DB868 which was the internal standard. Proteins were precipitated by centrifugation (3000 rpm for 10 min), and the supernatant was analyzed by HPLC/MS/MS. The metabolites M1 and M3 were quantified when DB868 was the substrate and M2 and M3 were quantified when M1 was the substrate. All primary metabolites were evaluated under initial rate conditions such that the substrate consumption was < 20%.

Time-Dependent Inhibition Experiments. To test whether M3 was an *N*-demethoxylation product of DB868, the suicide CYP inhibitor ABT (Ortiz de Montellano and Mathews, 1981) was used to abolish M1 formation which was known to be a precursor of M3. Incubations were carried out according to the methods described by (Linder et al., 2009) with minor modifications. Briefly, primary incubations mixtures contained HLMs or RLMs (1 mg/mL primary incubation or 0.5 mg/mL secondary incubation), ABT (1 mM, primary incubation) or DB868 (10 μM secondary incubation), potassium phosphate buffer (100 mM, pH 7.4), $MgCl_2$ (10 mM) and NADPH (2 mM). All incubations were carried out at 37°C. Control primary incubations contained water in place of β-NADPH. At 0 or 30 min, aliquots were removed from primary incubation and placed in secondary incubations (10-fold dilution). Secondary incubations were carried out for 5 min with HLMs or 10 min with RLMs, and were stopped with ice-cold acetonitrile (100 μL). Proteins were precipitated by centrifugation (3000 rpm for 10 min), and the supernatant was analyzed for M1 and M3 quantification by HPLC-UV.

Recombinant Enzyme Experiments. The incubation mixtures contained select human or rat recombinant enzymes (final concentration 0.1 pmol/μL), potassium phosphate buffer (100 mM, pH 7.4), $MgCl_2$ (10 mM), β-NADPH (2 mM), and either DB868 or M1 (final concentration 5 μM). Human recombinant CYP1A2, CYP2D6, CYP3A4, and CYP4F2 were examined based on preliminary data excluding the involvement of CYP2C9, CYP2C19 and CYP2E1, whereas in rat, recombinant enzymes CYP1A2, CYP2A1, CYP2A2, CYP2B1, CYP2C6, CYP2C11, CYP2C13, CYP2D1, CYP2D2, CYP2E1 and CYP3A1 were examined. DB868 and M1 were dissolved in DMSO such that the final solvent concentration was 0.5% (v/v). The total incubation volume was 200 μL. The reactions were initiated by

the addition of NADPH (2 mM) and were terminated at 15 min by the addition of ice-cold acetonitrile (100 μL). Proteins were precipitated by centrifugation (3000 rpm for 10 min), and the supernatant was analyzed by HPLC/UV for M1 when DB868 was the substrate or M2 when M1 was the substrate.

Purified Rat CYP4F Experiments. Incubations with purified rat CYP4F proteins were carried out using the methods of Xu et.al. (2004) with minor modifications (Xu et al., 2004). Briefly, incubation mixtures containing CYP4F (5 pmol), cytochrome *b*5 (5 pmol), NADPH-cytochrome P450 reductase (50 pmol), catalase (10 μg/ml), dilauroylphosphatidylcholine (20 μg/ml), and sodium cholate (0.2 mg/mL) were incubated for 10 min at 37°C prior the addition of potassium phosphate buffer (100 mM, pH 7.4), $MgCl_2$ (10 mM), NADPH (2 mM), and DB868 (final concentration 5 μM). The total incubation volume was 100 μL. The reactions were initiated by the addition of the NADPH (2 mM) and were terminated at 30 min by the addition of ice-cold acetonitrile (50 μL). Proteins were precipitated by centrifugation (3000 rpm for 10 min), and the supernatant was analyzed for M1 by HPLC-UV.

Metabolism of DB868 in Sandwich-Cultured Rat Hepatocytes. To assess whether the negligible levels of DB829 formation in HLMs and RLMs was a limitation of this in vitro system, DB868 was incubated with sandwich-culture hepatocytes prepared from humans and rats. The metabolic activities of the major CYP enzymes as well as phase II enzymes are maintained in sandwich cultured hepatocytes (Kern et al., 1997). Additionally, unlike suspended hepatocytes (Bow et al., 2008), hepatocytes cultured in a sandwich configuration have the advantage of expressing exteriorized efflux transporters on both the basolateral and apical membranes (Chandra and Brouwer, 2004) allowing to discern the extent of

intracellular, and extracellular concentrations of intermediate and active metabolites. Human (HSCHs) and rat (RSCHs) hepatocytes were cultured in 24-well plates or 12-well plates, respectively, and the experiments were carried out on either the fifth (HSCHs) or fourth day post seeding (RSCHs). On the day of the experiment, the culture medium was removed from wells and the hepatocytes were rinsed three times with warm DMEM. Incubations were started by the addition of DB868 in DMEM to the wells (10 μM final concentration). At each time point (i.e., 0.5, 2, 4 and 24 h), medium was collected from wells and stored in microcentrifuge tubes at -80°C until further processing. The remaining medium was aspirated from the wells, and the wells were rinsed three times with ice-cold DMEM to stop the reaction. A chilled methanol 0.1% TFA solution containing d_6-DB868 and d_6-DB829 as internal standards, was added to the wells, and the contents were scraped off into microcentrifuge tubes. The tubes were vortexed briefly (10 min) and were stored at -80°C until further processing. Intracellular and extracellular samples were analyzed for DB868 and phase I metabolites by HPLC/MS/MS. Total protein content was determined by the Bradford method (Bio-Rad Laboratories, Hercules, CA).

HPLC-UV Chromatography. Chromatographic analysis of DB868 and its phase I metabolites was performed on an Agilent 1100 Series HPLC system (Palo Alto, CA) using methods described by (Wang et al., 2006) with minor modifications. Briefly, DB868 and metabolites were separated using a Zorbax SB-CN (5 μm, 2.1 x 150 mm) column equipped with a Zorbax SB-CN guard column (5 μm, 4.6 x 12.5 mm) obtained from Agilent (Palo Alto, CA). Quantification of DB868 and metabolites was achieved using an external calibration curve and comparison of peak areas to those of authentic standards (with the exception of M4, for which no authentic standard was available).

Analysis of DB868 Metabolites by HPLC-ion Trap Mass Spectrometry. DB868 was incubated with HLMs and RLMs for 180 min, as described above. The quenched reaction mixtures were analyzed by HPLC-UV-FLD-MS, and HPLC-UV-FLD-auto MS^n. The HPLC-MS was, in all cases, an Agilent 1100 system comprised of an autosampler, binary pumps, column heater, diode array detector, fluorescence detector, and ion trap mass spectrometer. The HPLC was controlled by Chemstations software (Agilent, version A.9), while the ion trap was controlled by Trap Software (Bruker, version 4.1). Analytes were eluted by reverse phase chromatography using a Zorbax SB-CN (5 µm, 2.1 x 150 mm) column equipped with a Zorbax SB-CN guard column (5 µm, 4.6 x 12.5 mm) obtained from Agilent, (Palo Alto, CA) at a flow rate of 0.35 mL/min. The mobile phases were prepared with 35 mM formic acid and 15 mM ammonium formate in 100% water (mobile phase A), or 80:20 acetonitrile:water (mobile phase B). The mobile phase gradient started with 5% mobile phase B and increased linearly to 60% over 22 min. A sharp increase to 100% occurred over 30 sec and was maintained for the next 2.5 min. The column was equilibrated at 5% organic for the next 4 min. The injection volume was 40 µL. The column temperature was 25°C. The UV absorbance was monitored at 359 nm, and fluorescence was monitored using an excitation of 359 nm and an emission of 462 nm. When the mass spectrometer was used, the eluent passed from the FLD directly to the ion trap equipped with an electrospray source. Data from the ion trap was collected in positive ion mode as either MS-only or as auto MS^n total ion chromatograms. MS-only detection was used to determine the m/z to be included in MS^n analysis in subsequent injections. Based upon MS data and known metabolism of analogous compounds, proposed intermediate metabolites were synthesized. Confirmation of the proposed metabolites involved matching both the retention times and the

fragmentation patterns of analytes found in metabolism samples and of purified analytical standards.

Quantification of DB868 and Metabolites by HPLC-mass Spectrometry. Quantification of DB868, and metabolites was perfomed on an Applied Biosystems ABI4000 mass spectrometer with TurboIonspray® source (Applied Biosystems, Foster City, CA). The typical sample injection volume was 4 µL (Leap CTC thermostatted autosampler, Carrboro, NC). Wash solvents for the syringe and injection loop were 50:50 (wash A) and 80:20 (wash B) methanol:water with 0.1% formic acid. The analytes were eluted from an Aquasil C18 column (d_p = 5 µm, 2.1 x 50 mm; Thermo Electron Corporation, San Jose, CA) by a Shimadzu solvent delivery system (Columbia, MD) using a mobile phase gradient. Mobile phase A consisted of 0.1% formic acid in 100% water while mobile phase B consisted of 0.1% formic acid in 100 % methanol. The mobile phase gradient began with a 0 - 0.5 min hold at 10% B; 0.5 - 4.0 min linear gradient to 90% B; 4.0 - 5.0 min hold at 90% B, 5.0 - 5.5 min linear gradient to 10% B, 5.5 - 6.0 min hold at 10% B. The flow rate was 0.5 mL/min with the exception of the 90% B wash, when the flow was increased to 1.2 mL/min. Eluent from 0 -0.8 min was diverted to waste while eluent from 0.8 - 4.2 min was directed to the mass spectrometer. The total runtime, including equilibration, was 6 min per injection. The mass spectrometer was operated in positive ion mode using multiple reaction monitoring: DB868, 367.1→320.2 *m*/*z*; M1, 353.2→306.2 *m*/*z*; M2, 339.2→306.2 *m*/*z;* M3, 336.8→290.2 *m*/*z*; M4, 323.2→290.2 *m*/*z*; DB829, 307.3→290.2 *m*/*z*; d_6-DB868, 373.1→323.2 *m*/*z*; and d_6-DB829, 313.3→396.2 *m*/*z*;. With the exception of M4, operator controlled parameters were optimized by direct infusion of analytical standards. Calibration curves for DB868, M1, M2, and M3 were constructed as peak area ratios of analyte d_6-DB868. Calibration curves for

DB829 were constructed as peak area ratios of DB829: d_6-DB829. Tuning, operation, integration and data analysis were performed using Analyst® software v.1.4.1 (Applied Biosystems). The wide dynamic range (0.1-100 μM) of DB868 used in the enzyme kinetic experiments made the quantification of M1 difficult by HPLC/MS-MS, due to ion-suppression of the d_6-DB868 internal standard at high concentrations of DB868. This difficulty was overcome by cross-validating the M1 calibration curve between the HPLC-UV and HPLC/MS/MS platforms (range of overlapping concentrations 50 to 10000 nM).

Kinetic Modeling. A kinetic modeling approach was used to assess the consequences of both parallel and sequential reactions on the rates of metabolic activation of DB868, which provided a more representative picture of intermediate metabolite formation in vivo. This approach gave insight into a rare metabolic pathway which was not discerned using traditional approaches (e.g., mass spectrometry structural identification and knowledge of common metabolic steps). The model was structured according to the proposed pathway described for the analog prodrug DB289 (Zhou et al., 2004) and included the substrate DB868, and the metabolites M1, M2 and M3 (Figure 2.5A). M4 was omitted from the model as this metabolite was not quantified due to lack of an authentic standard. The rate constants k_1, k_2 and k_3 were used to represent degradation of the prodrug or generation of the metabolites M3 and M2, respectively. It was assumed that all processes were unidirectional and that there was no inhibition in the metabolic steps. The DB868, M1, M2 and M3 RLM data were fit simultaneously using initial estimates obtained from pilot depletion experiments with DB868 and M1 (data not shown). The final model selection was based on standard criteria including visual inspection, residual analysis, and parameter precision. The software

WinNonlin 5.0.1 (Pharsight, Mountain View, CA) was used for model development and data analysis.

Data Analysis. Unless otherwise indicated all data are presented as mean ± SD. First-order rate constants and enzyme kinetic experiments parameters are shown as mean estimates and percents of coefficient of variance (%CVs).

Kinetics of metabolite formation: The kinetic parameters for the M1 formation by HLMs were estimated using the Michaelis-Menten equation, where V_{max}, is the maximal velocity, K_m is half the maximal velocity and S is the substrate concentration.

Equation 1: $$\upsilon = \frac{V_{max} \bullet S}{K_m + S}$$

M1 formation by RLMs was best described by a two-enzyme kinetic system; where V_{max1} and K_{m1} are the maximal and half the maximal velocities for the first enzyme; V_{max2} and K_{m2} are the maximal and half the maximal velocities for the second enzyme; and S is the substrate concentration.

Equation 2: $$\upsilon = \frac{V_{max1} \bullet S}{K_{m1} + S} + \frac{V_{max2} \bullet S}{K_{m2} + S}$$

M2 formation by HLMs exhibited allosteric kinetics and was estimated using the Hill equation

Equation 3: $$\upsilon = \frac{V_{max} \bullet S^n}{S_{50}{}^n + S^n}$$

Where V_{max}, is the maximal velocity, S_{50} represents half the maximal velocity, n is the Hill coefficient and S is the substrate concentration. Cl_{max} was determined from these parameters as follows:

Equation 4: $$CL_{max} = \frac{V_{max}}{S_{50}} \bullet \frac{(n-1)}{n\,(n-1)^{1/n}}$$

A mechanistic description of the allosteric effect was also assessed by estimating two distinct affinities of the ligand for two binding sites (i.e., V_{max1}, K_{m1} and V_{max2}, K_{m2}) (Korzekwa et al., 1998).

Equation 5: $$\upsilon = \frac{\frac{V_{max1} \bullet [S]}{K_{m1}} + \frac{V_{max2} \bullet [S]^2}{K_{m1} \bullet K_{m2}}}{1 + \frac{[S]}{K_{m1}} + \frac{[S]^2}{K_{m1} \bullet K_{m2}}}$$

All data fits were performed with the software WinNonlin 5.0.1 (Pharsight, Mountain View, CA).

Statistical analysis for the time-dependent inhibition experiments was done using one-way ANOVA with the Bonferroni test for multiple comparisons. Differences were deemed significant if $p < 0.05$.

D. RESULTS

Identification of the Metabolites of 2, 5-Bis [5-(*N*-methoxyamidino)-2-pyridyl] furan (DB868). The biotransformation of the prodrug DB868 (Figure 2.1) was NADPH-dependent in both humans and rats (Figure 2.2). After a 180-min incubation, four intermediate metabolites, designated M1, M2, M3, and M4, were produced in addition to the formation of the active diamidine, DB829. In both the UV (Figure 2.2) and the total ion (not shown) chromatograms, the prodrug and intermediate metabolites eluted at 18.5 (DB868), 14.5 (M1), 12.3 (M3), 10.5 (M2), and 8.3 (M4) min. DB829 was formed in trace amounts by HLMs, with a retention time of 5.8 min, whereas none was detected in reaction mixtures involving RLMs.

Identification of metabolites from microsomal incubations was accomplished using HPLC separation coupled with ion trap MS/MS analysis in positive ionization mode. Full scan analysis of incubations of DB868 with HLMs or RLMs gave molecular ions $[M+H]^+$ at *m/z* 367 (DB868), 353 (M1), 337 (M3), 339 (M2) and 323 (M4). The ion at *m/z* 307 (DB829) was only detected in full scans with HLMs (Table 2.1). Fragmentation of the prodrug gave one major product at *m/z* 320 and two minor products at *m/z* 336 and 290. The MS^3 of *m/z* 320 yielded a major ion at *m/z* 273 and a minor ion at *m/z* 289. The most abundant products of MS^2 and MS^3 corresponded to a loss of 47 Da, presumably derived from the loss of the neutral molecules NH_3 and $O{=}CH_2$ by a rearrangement of a six-membered transition state (Zhou et al., 2002). The fragmentation patterns observed for DB868 in the microsomal incubations were similar to those obtained from the DB868 authentic standard.

M1 was the most abundant metabolite detected in incubations with HLMs and RLMs (Figure 2.2). The M1 molecular ion at *m/z* 353 was 14 Da less than the parent, indicating metabolic loss of a methyl group. Fragmentation of the M1 molecular ion at *m/z* 353 produced one major ion at *m/z* 306 and two minor products at *m/z* 336 and 289. Similar to the prodrug, the ion at *m/z* 306 was formed by a loss of 47 Da. The product ion at *m/z* 306 fragmented further into an ion at *m/z* 289, corresponding to the loss of an –OH radical. The molecular ion for M2 at *m/z* 339 was 28 Da less than the molecular ion of DB868 and was 14 Da less than the molecular ion of M1, indicating a de-methylation of M1. The major MS^2 product of *m/z* 339 was at *m/z* 322, a loss of 17 Da, which was most likely the loss an –OH radical. The MS^3 for this fragment ion produced a major fragment at *m/z* 306. The molecular ion of M3 at *m/z* 337 was 16 Da less than the molecular ion of M1, possibly due to a loss of an -OH group and protonation of the amidino group. The MS^2 of *m/z* 337 yielded a major fragment at *m/z* 290, and the MS^3 of this fragment led to the product ion at *m/z* 273. Like the prodrug and M1, the ion at *m/z* 290 was 47 Da less than the molecular ion at m/z 337. Further fragmentation to *m/z* 273 was presumably from loss of the $-NH_2$ radical. The molecular ion of M4 at *m/z* 323 was 16 Da less than the molecular ion of M2 and 14 Da less than the molecular ion of M3, potentially by loss of an -OH group from M2 or loss of a CH_3 group from M3. The molecular ion at *m/z* 323 was fragmented only once due to its low intensity. This fragmentation produced a major product at *m/z* 306 and two small products at *m/z* 290 and 278. Fragmentation of the active metabolite DB289 was not possible due to low levels at the 180 min incubation time point (HLM samples) that did not lie within the threshold for MS^n analysis; however, the retention time matched that of the authentic standard in UV chromatograms. The structural determination of the metabolites in the

DB868 biotransformation pathway was confirmed by comparison of HPLC retention times and fragmentation patterns with those of authentic standards, with the exception of M4 for which no authentic metabolite was available.

Biotransformation of DB868 to the active drug by human and rat liver microsomes. Incubations of DB868 (10 μM) with HLMs and RLMs showed differential extents and rates of metabolite formation. The concentration-time profiles of microsomal incubation mixtures showed that HLMs metabolized DB868 nearly completely in 180 min compared to only 43% depletion of the substrate by RLMs (Figure 2.4). In both species, the *O*-demethylation product of DB868 (M1) was the major metabolite formed, accounting for approximately 43% (HLM) and 30% (RLM) at 180 min of the initial concentration of prodrug. The *O*-demethylation product of M1, (M2) was detected readily in incubations with HLM but was formed in negligible amounts in incubations with RLM over the 180-min incubation period, accounting for ~40% and 0.1% respectively, of initial DB868 concentrations. After 180 min incubation, the monomethoxy-monoamidine metabolite (M3) accounted for 15% and 6.4% of the initial concentration of the prodrug, in incubations with HLMs and RLMs, respectively. Trace amounts of the monooxime-monoamidine metabolite (M4) were detected in incubations with both species; however, quantification of this metabolite was not possible due to the lack of an authentic standard. The near complete mass balance achieved by quantifying metabolites M1-M3 at 180 min indicate that M4 accounted for a very small percentage of the initial prodrug concentration in both species. Only trace amounts of the diamidine, DB829, were detected in UV chromatograms of 180 min incubations with HLMs, suggesting a very slow conversion of intermediate metabolites into DB829 (Figure 2.2) in liver microsomal samples.

The rates of conversion of the prodrug to the intermediate metabolites were determined by kinetic modeling and enzyme kinetic experiments. Kinetic modeling of the RLM data described the data for DB868, M1 and M2 data adequately; however, the early time points for M3 were largely underestimated. The addition of a process representing direct formation of M3 from DB868 significantly improved the model fit to the M3 data (Figure 2.5B) suggesting the possibility of an additional metabolic process involved in the generation of M3. The relative rates of formation of M1 in RLMs were several fold faster compared to M2 and M3 as reflected by the magnitude in apparent clearances (Cl_{app}) (Table 2.2). A similar approach was used to determine the relative rates of metabolite formation in HLMs. The rat model described the DB868, M1 and M3 human data well; however, large discrepancies were observed between the predicted fit and the M2 data (fit not shown). As such enzyme kinetic experiments were conducted to understand the enzyme kinetic of intermediate metabolite formation.

Michaelis-Menten kinetics best described the formation of M1 by HLMs (Figure 2.6A). In RLMs, M1 formation was best described by two-enzyme Michaelis-Menten kinetics. The Eadie-Hofstee plot of these data depicted the characteristic concave curve of a two enzyme system (Figure 2.6B). Formation of M2 in HLMs was best described by sigmoidal kinetics (Figure 2.6C). Additional analysis of the HLM M2 data using the Korzekwa equation (Equation 6) yielded kinetic parameters for both the low and high affinity ligands of the allosteric process (Table 2.3). The kinetic parameters K_m and V_{max} for the formation of M2 in RLMs were not recoverable because saturation was not achieved during the experiment (Figure 2.6D). Similarly, saturation was not achieved for M3 formation by either HLMs or RLMs when M1 was the substrate.

Time-dependent Inhibition Experiments Demonstrate Direct *N*-demethoxylation of DB868 for the Generation of M3. Kinetic modeling with HLMs and RLMs suggested a direct reduction from DB868 to M3. This would imply that the CYP-mediated oxidative demethylation of DB868 to M1 is not required for the formation of M3 from DB868. To test this hypothesis, formation of M3 in the presence of mechanism-based CYP inhibitor, ABT (Ortiz de Montellano and Mathews, 1981), was examined. For both HLMs (Figure 2.7A) and RLMs (Figure 2.7B), formation of M1 was reduced when CYP enzymes were inhibited by ABT, however, the formation of M3 increased under these experimental conditions, clearly establishing that formation of M1 was not obligatory for the formation of M3.

Human and Rat Enzymes Involved in the *O*-demethylation Steps of the DB868 Metabolic Pathway. Studies with human recombinant enzymes showed that the DB868 *O*-demethylation was not catalyzed by CYP2C9, CYP2C19 and CYP2E1 (data not shown), but was catalyzed by CYP1A2, CYP3A4 and CYP4F2; whereas, the M1 *O*-demethylation was catalyzed by CYP1A2, (Figure 2.8A). Experiments with rat recombinant enzymes and purified rat CYP4F showed that DB868 *O*-demethylation was catalyzed by CYP1A2, CYP2D2, and CYP4F1 (Figure 2.8B). Since the M1 *O*-demethylation (M2) in RLMs was negligible the enzymes responsible for this reaction were not examined.

Metabolic Activation of DB868 in Human and Rat Hepatocytes Yields Measurable DB829 Levels. To assess whether the incomplete metabolic activation of DB868 in liver microsomes was a limitation of the in vitro system, metabolic activation of DB868 by sandwich-cultured hepatocytes from humans (HSCHs) and rats (RSCHs) was evaluated. Incubations of DB868 (10 μM) with HSCHs showed nearly complete depletion of the prodrug from the medium after 4h; whereas approximately half of the dose remained in

the medium at 4 h when DB868 was incubated with RSCHs (Figure 2.9). As with HLMs and RLMs, M1 was detected readily in the medium of HSCHs and RSCHs with amounts peaking at 4 h. As expected, M2 formation in HSCHs was extensive, as evidenced by amounts accumulated in the medium; whereas negligible amounts were detected in experiments with RSCHs at 24 h. Appreciable amounts of M3 were detected in both the medium and lysate of HSCHs and RSCHs during the course of the incubation, with the highest amounts detected in the medium at 24h. Time dependent intracellular formation of DB829 was observed in both HSCHs and RSCHs with little amounts detected in the medium for up to 24 h (Figure 2.9).

E. DISCUSSION

Second stage HAT, also known as sleeping sickness, begins once the trypanosomes penetrate the CNS. The disease represents approximately 90% of all HAT cases reported (WHO 2010) and is fatal if left untreated. Until recently, melarsoprol and eflornithine were the only drugs approved as first line treatment for second stage HAT. Although effective, both drugs have a number of safety and practical concerns. For example, melarsoprol causes death in 5% of patients (Chappuis et al., 2005) and eflornithine, although not life-threatening, has an impractical administration regimen with 14 day around the clock infusions. In 2008, the nifurtimox-efllornithine combination therapy (NECT) was approved as a much safer and practical alternative to melarsoprol or eflornithine mono-therapy, however, emergence of resistance to eflornithine has been reported (Balasegaram et al., 2009) and remains a concern. Based on these complications, the development of new alternatives to treat second-stage HAT is of high urgency.

The pentamidine analog, DB829, has demonstrated efficacy in a mouse model of second stage HAT (Fairlamb, 2003; Wenzler et al., 2009). However, due to the dicationic nature of the amidine moieties at physiologic pH, DB829 is absorbed poorly into the systemic circulation when administered orally. To improve the extent of absorption, a prodrug strategy was utilized, in which the *O*-methyl moieties were used to mask the amidine functional groups, creating DB868. This prodrug was 100% effective when administered orally to the murine model of second stage infection suggesting effective biotransformation in vivo.

To understand how the prodrug is metabolically converted to the active drug, DB829, the in vitro biotransformation pathway of this compound was characterized using liver microsomes and sandwich-cultured hepatocytes (SCH) prepared from humans and rats. In both HLMs and RLMs, four NADPH-dependent intermediate metabolites were detected (M1-M4). M1, M2, and M4 were produced via *O*-demethylation of DB868, M1, and M3, respectively; whereas M3, M4, and DB829 were produced *via* dehydroxylation of M1, M2, and M4, respectively (Table 2.1). These assignments were based on extensive LC/MS^n data, and are consistent with the knowledge of common metabolic reactions and assignments of the metabolites of an analogous prodrug, DB289 (Zhou et al., 2004), which was in development for the treatment of first stage HAT (Fairlamb, 2003; Wenzler et al., 2009).

DB868 was metabolized extensively by both liver microsomes and hepatocytes of humans and rats, indicating that hepatic metabolism will contribute to its conversion to the active drug, DB829, and to its systemic clearance. As assessed by the formation of M1, which is the primary metabolite of DB868, the disappearance of the prodrug caused by HLMs and RLMs was comparable, with Cl_{int} values (calculated as the ratio of V_{max} to K_m) of

31 and 24 μL/min/mg protein, respectively. However, based on K_m values of 11 and 0.5 μM for human and rat, respectively, saturation of metabolism in rats is expected to occur at much lower concentrations compared to humans. This conclusion is supported by the change in magnitude of Cl_{app}, when DB868 was incubated at a concentration of 10 μM. At this concentration, the Cl_{app} in HLMs and RLMs was 15 and 2.3 μL/min/mg protein, respectively, representing enzymes operating at approximately one-half and one-tenth of the respective Cl_{int} values (Table 2.2). These observations suggest that, in vivo, the hepatic metabolism of DB868 in rats will be more easily saturable compared to that in humans. However, because DB868 binds extensively to plasma proteins in both species (Yan, unpublished observations), saturation of metabolism is unlikely to occur in vivo.

The *O*-demethylation of DB868 (M1 formation) was catalyzed most efficiently by human recombinant CYP4F2, followed by CYP1A2 and CYP3A4 (Figure 2.8A). These results are consistent with those reported by Wang and colleagues (2006), who showed that the *O*-demethylation of the analog prodrug, DB289, also is catalyzed most efficiently by CYP4F2. In contrast to observations with human enzymes, the *O*-demethylation of DB868 was catalyzed by rat CYP2D2, CYP1A2 and CYP4F1. Whether CYP2D2 or CYP4F1 is the primary enzyme catalyzing this reaction in unclear because the velocities of M1 formation were obtained from two different systems (e.g., rat recombinant enzymes versus purified enzymes), in which the ratio of cytochrome b5, P450 reductase and CYP content vary.

A noticeable species difference in the biotransformation of DB868 was the extent of M2 formation at the end of the 180-minute incubation period, where the amount of M2 formed by HLMs was 25-fold greater than that formed by RLMs (Figure 2.4). This difference could be explained by the distinct differences in the kinetic processes driving M2

formation in both species, where allosteric kinetics governs M2 formation by HLMs (CL_{max} = 3.2 μL/min/mg protein) in contrast to linear unsaturable kinetics observed when RLMs are used (Cl_{int}= 0.3 μL/min/mg protein) (Figure 2.7). CL_{max} is a surrogate for Cl_{int} for enzymes that exhibit allosteric kinetics (Witherow and Houston, 1999), representing the maximal activity of an enzyme before reaching saturation. Based on graphical analysis of the CL_{app} versus substrate (M1) plot (not shown) the value of Cl_{max} for M2 (3.2 μL/min/mg protein) would correspond to a concentration of substrate (M1) of ~15 μM which is unlikely to occur in vivo. A less conservative value of CL_{int} (1.8 μL/min/mg protein) for the allosteric formation of M2, derived from the Korzekwa equation, correspond to concentrations of M1 of approximately 2 μM (from CL_{app} versus substrate plot) that would be more likely to occur in vivo (Table 2.3) (Korzekwa et al., 1998; Tracy, 2006). CYP enzymes that have been shown to have substrates whose metabolism exhibit allosteric kinetics include CYP1A2 and CYP3A4 (Hutzler et al., 2001; Atkins, 2004; Cameron et al., 2007; Isin et al., 2008). In HLMs, M2 formation was catalyzed most efficiently by CYP1A2, consistent with the allosteric behavior of this enzyme with other substrates, such as α-napthoflavone, pyrene, and 1-hydroxypyrene (Sohl et al., 2008).

An unexpected finding derived from kinetic modeling of DB868 and intermediate metabolites was that M3 generation not only occurred from M1 *N*-dehydroxylation but also *via N*-demethoxylation of DB868. Time-dependent inhibition studies with the non-specific CYP inhibitor ABT showed that inhibition of CYP-mediated formation of M1 did not reduce M3 formation, suggesting that M3 could be formed independently from M1 formation (Figure 2.6). The significant increase in M3 observed after 30 min pre-incubations with ABT in the presence or absence of NADPH needs to be further investigated but points to possible

enzyme activation by ABT. To the authors' knowledge, *N*-demethoxylation reactions are rare with mammalian enzymes, although such reactions have been described in environmental research, where soil bacteria and fungi were demonstrated to be efficient in degrading *N*-methoxy containing phenylurea herbicides (e.g., linuron and metobromuron) (Berger, 1998; Badawi et al., 2009). It is hypothesized that in microsomes the reductase system cytochrome b_5 and NADPH P450 reductase could carry out *N*-demethoxylation reactions, since incubations of DB868 with recombinant CYP4F2 enzymes that were co-expressed with NADPH P450 reductase and cytochrome b5 formed M3 in the presence of NADPH (data not shown).

The phase I metabolism of DB868 in sandwich-cultured hepatocytes from humans and rats was similar to that by microsomes with the exception that DB829 was formed readily in cells. Extensive depletion of DB868 from the medium was observed with hepatocytes of either species (half-life 1h and 3.6 h in HSCH and RSCHs, respectively). M1, M2 and M3 were detected in the medium of HSCHs; whereas only M1 and M3 were present in the medium of RSCHs during the incubation time. The absence of M2 in the medium of RSCHs suggests that the rat may not be an adequate toxicological model for the development of DB868. Higher extent of M3 formation was observed in hepatocytes of both species when compared to M3 formation by microsomes, perhaps due to precursors of M3 having access to mitochondrial reductases not present in microsomes. For example, it has been shown that mitochondrial cytochrome b_5 and b_5 reductase efficiently reduce amidoximes to amidines (Saulter et al., 2005). Similarly, it has been shown that a benzamidoxime reductase in the outer membrane of mitochondria is capable of efficiently activating *N*-hydroxylated prodrugs to amidines (Clement et al., 2005; Havemeyer et al., 2006). The higher amounts of M3 in

hepatocytes could correlate to the observed higher extent of DB829 formation in hepatocytes compared to microsomes, given that M3 is an upstream precursor of DB829 in both species. Similarly, differences in the extent of M2 formation between species contributed to the approximately 10-fold difference in intracellular DB829.

Collectively, this study shows that DB868 is efficiently biotransformed by both human and rat hepatic enzymes to the active diamidine, DB829. In particular, larger amounts of DB829 formed in human hepatocytes, suggest that in vivo generation of DB829 will unlikely be limited by metabolism. However, extensive intracellular accumulation of DB829 points to the importance of intracellular binding and hepatic efflux transporters on the basolateral membrane in influencing the availability of DB829 in systemic circulation. Additionally, this study highlights the value of kinetic analysis in giving insight into novel metabolic pathways or processes maybe not recognized using traditional techniques.

F. FIGURES

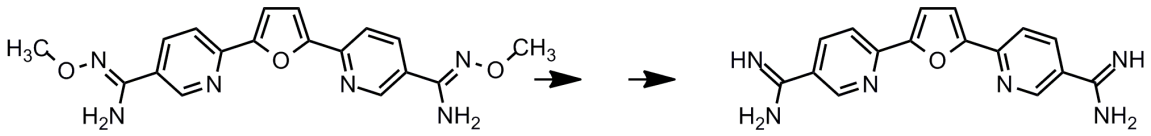

Figure 2.1 Chemical structures of the prodrug DB868 and active diamidine drug, DB829.

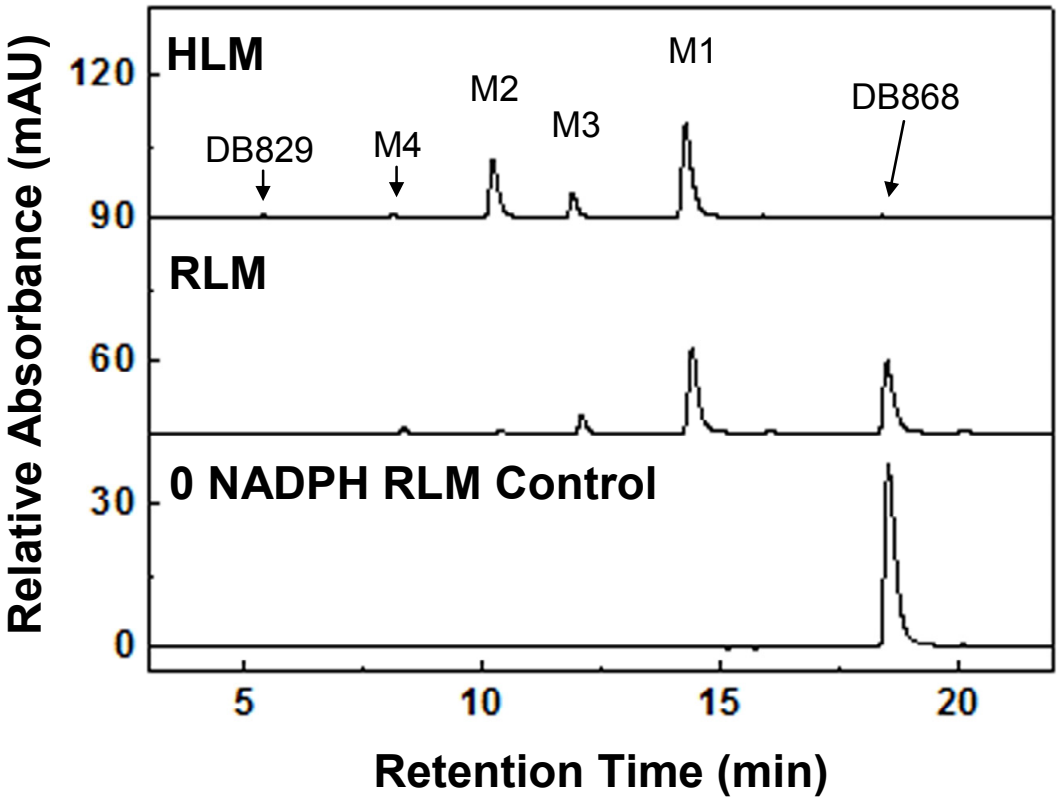

Figure 2.2 Representative HPLC-UV chromatograms depicting peaks for DB868 (18.5 min) and intermediate metabolites M1 (14.5 min), M2 (10.5 min), M3 (12.3 min), and M4 (8.3 min). The chromatograms show analysis of 180 min-incubations of DB868 (10 μM) with human or rat liver microsomal fractions (HLM or RLM respectively; 0.5 mg/mL) in the presence (top and middle) or absence (bottom) of NADPH. Trace amounts of DB829 (5.8 min) are detected in the UV-chromatogram of incubations with HLMs. A similar profile to the RLM control was observed for the 0-NADPH HLM control (not shown).

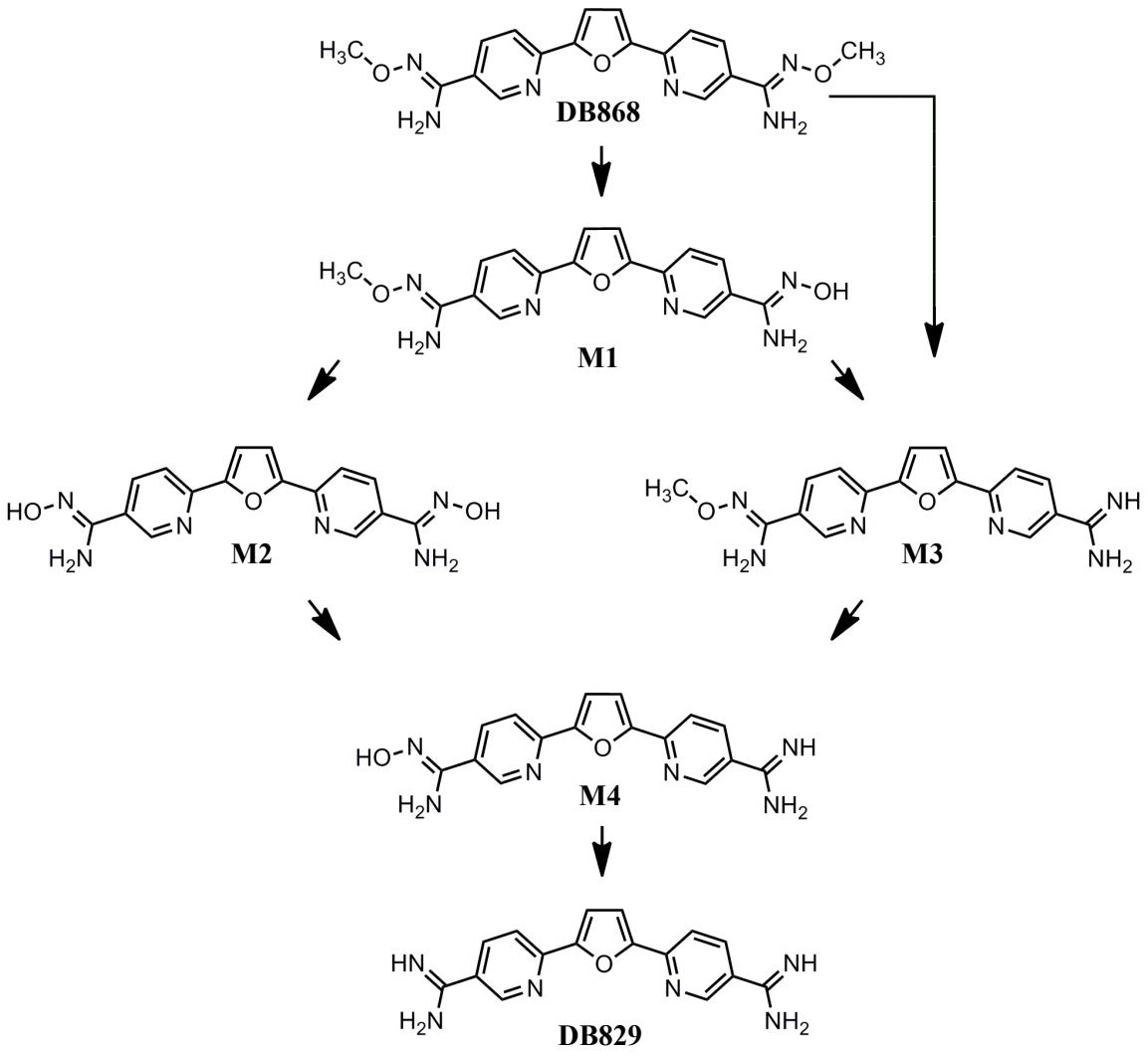

Figure 2.3 Proposed biotransformation of the prodrug DB868 leading to the formation of the active diamidine DB829.

A.

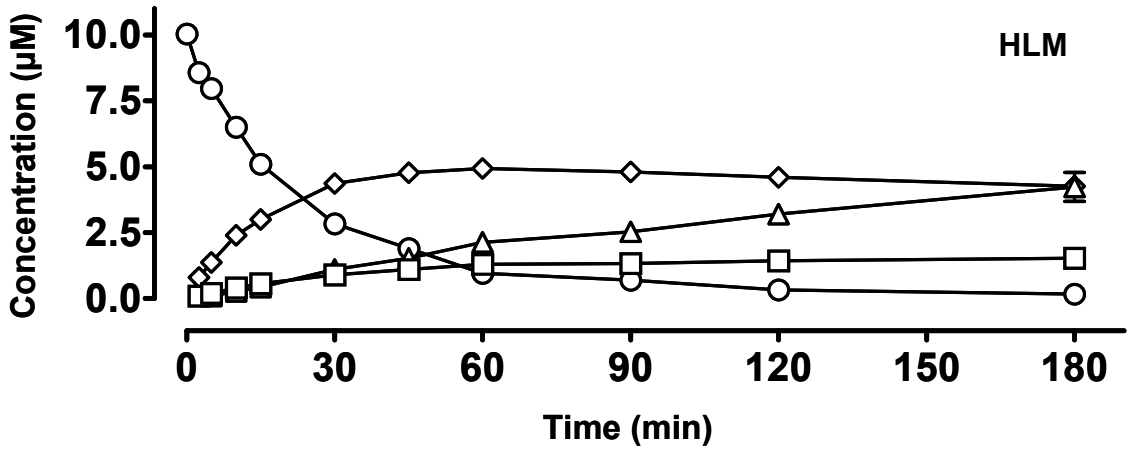

B.

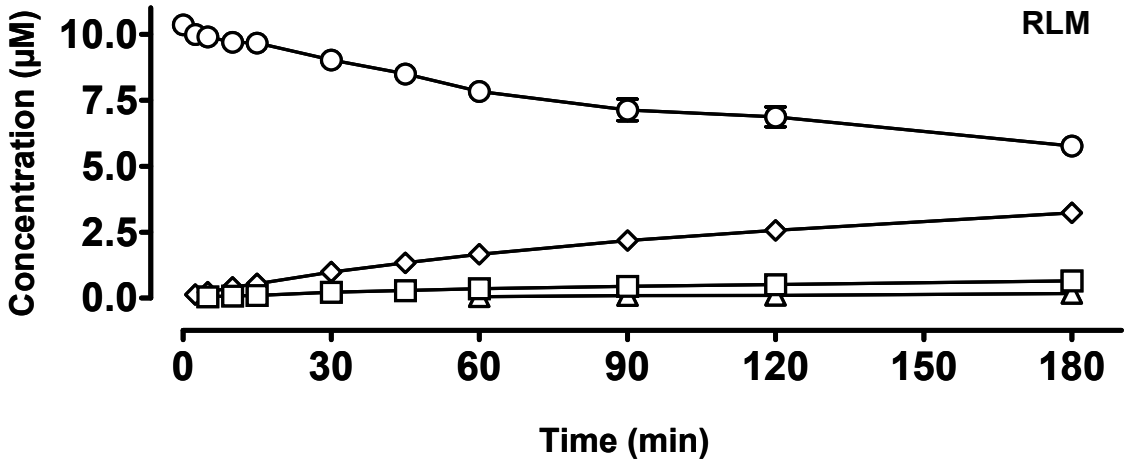

Figure 2.4 Concentration-time profiles of DB868 and intermediate metabolites. DB868 (○) and intermediate metabolites M1 (◊), M2 (Δ), M3 (□) were formed in incubation of DB868 with human and rat liver microsomes (HLMs and RMLs, respectively). HLMs (A) or RLMs (B) were incubated with DB868 (10 μM) for up to 180 min and the intermediate metabolites were quantified by HPLC-UV. Quantification of the M4 metabolite was not possible due to a lack of an authentic standard. Concentrations of DB829 were below the lower limit of quantification. Symbols represent the mean ± SD of triplicate determinations.

A.

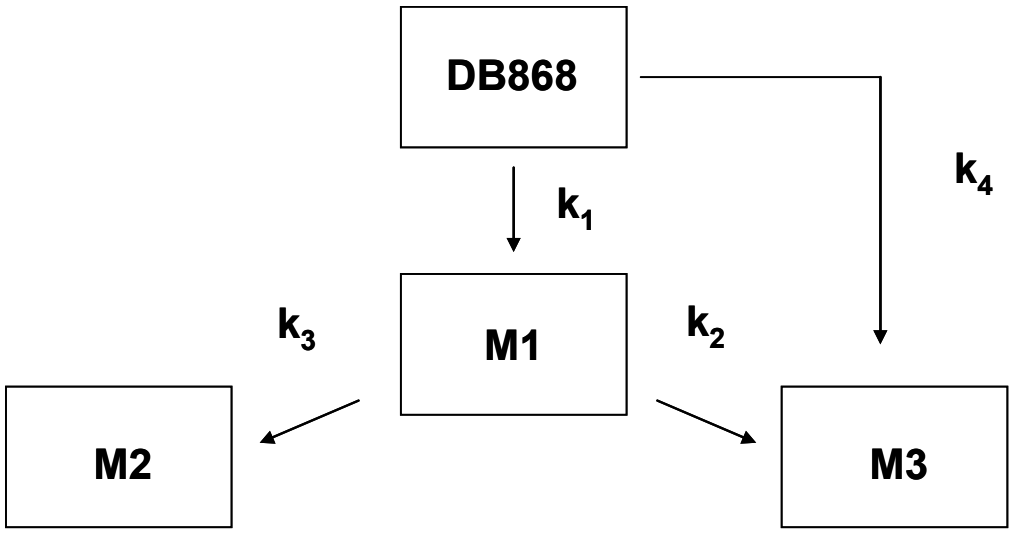

B.

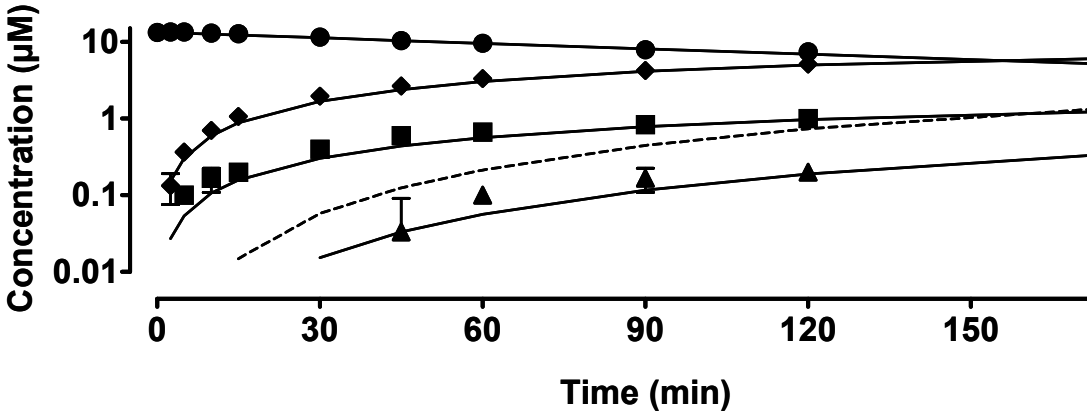

Figure 2.5 Biotransformation of DB868 by liver microsomal fractions. (A) Model scheme representing the biotransformation of DB868 by liver microsomal fractions. The first-order rate constants k_1, k_2, k_3 and k_4 denote the formation of intermediate metabolites M1, M2 and M3, respectively, by RLMs. In incubations with HLMs, the formation of M2 was best described by an allosteric process (B) Concentration-time profile of DB868 (●) and intermediate metabolites (M1(♦), M2(▲), and M3(■)) formed by incubation with rat liver microsomes (RLMs). Symbols represent experimental data ± SD of triplicate determinations. The solid lines indicate the fit of the final rat model (shown above) to the data. The dashed line depicts the large underprediction of M3 when the rate constant k_4 is omitted from the model.

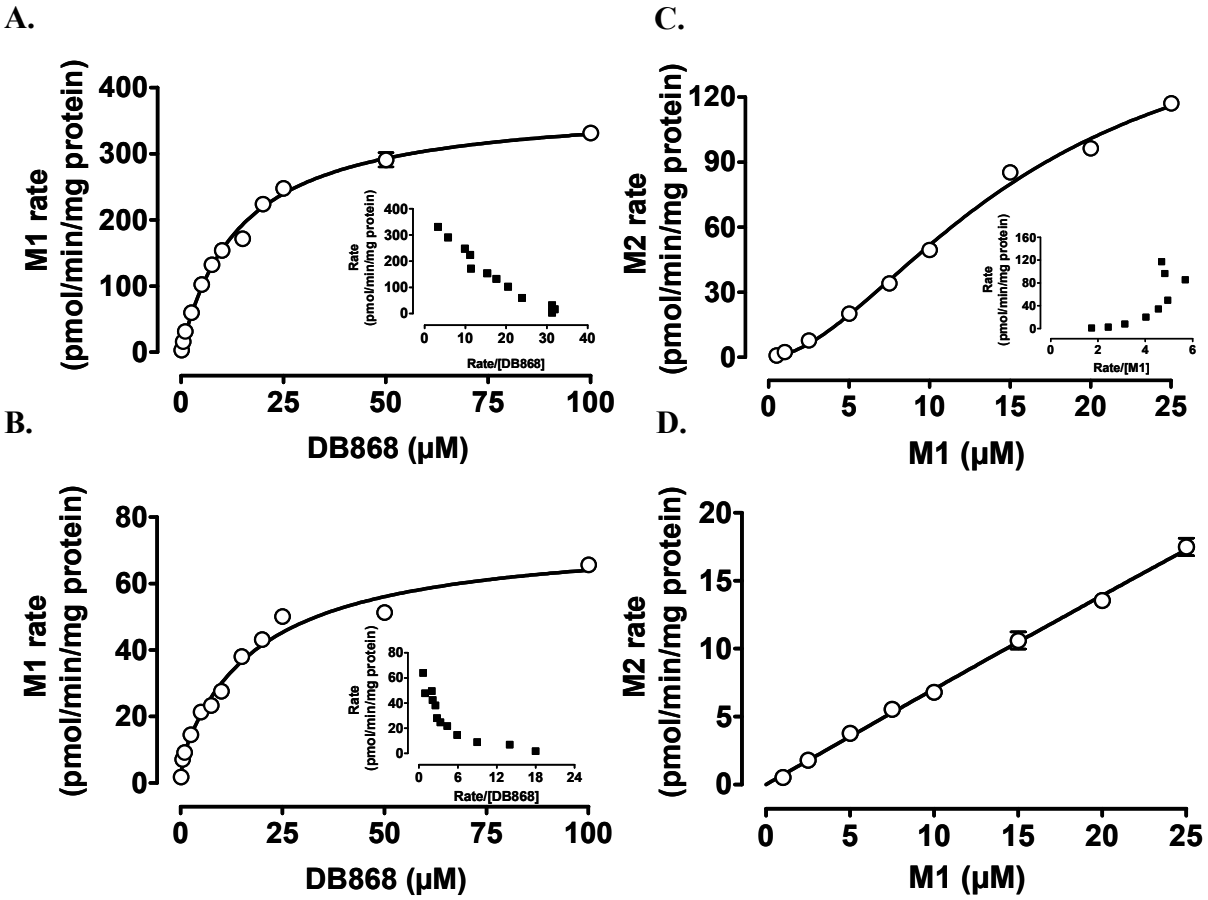

Figure 2.6 Rates of M1 and M2 formation in human and rat liver microsomes. Plots showing the rates of M1 and M2 formation by human liver microsomes (HLMs) (top) and rat liver microsomes (RLMs) (bottom). M1 formation data are from incubations of HLMs or RLMs (0.5 mg/mL) with DB868 (0.1-100 μM) for 5 min or 10 min, respectively. M2 formation data are from incubations of HLMs with M1 (0.1- 25 μM) for 5 min. All reactions were started with NADPH (2 mM). M1 formation by HLMs was best described by a single-enzyme Michaelis-Menten equation while M1 formation by RLMs was best described by a two-enzyme equation. M2 formation by HLMs was best described by the Hill equation. M2 formation by RLMs did not reach saturation at the concentrations examined. Insets show Eadie-Hofstee plots characteristic of a single enzyme system (A), a biphasic system (B), and an allosteric system (C). Symbols represent the mean ± SD of triplicate determinations

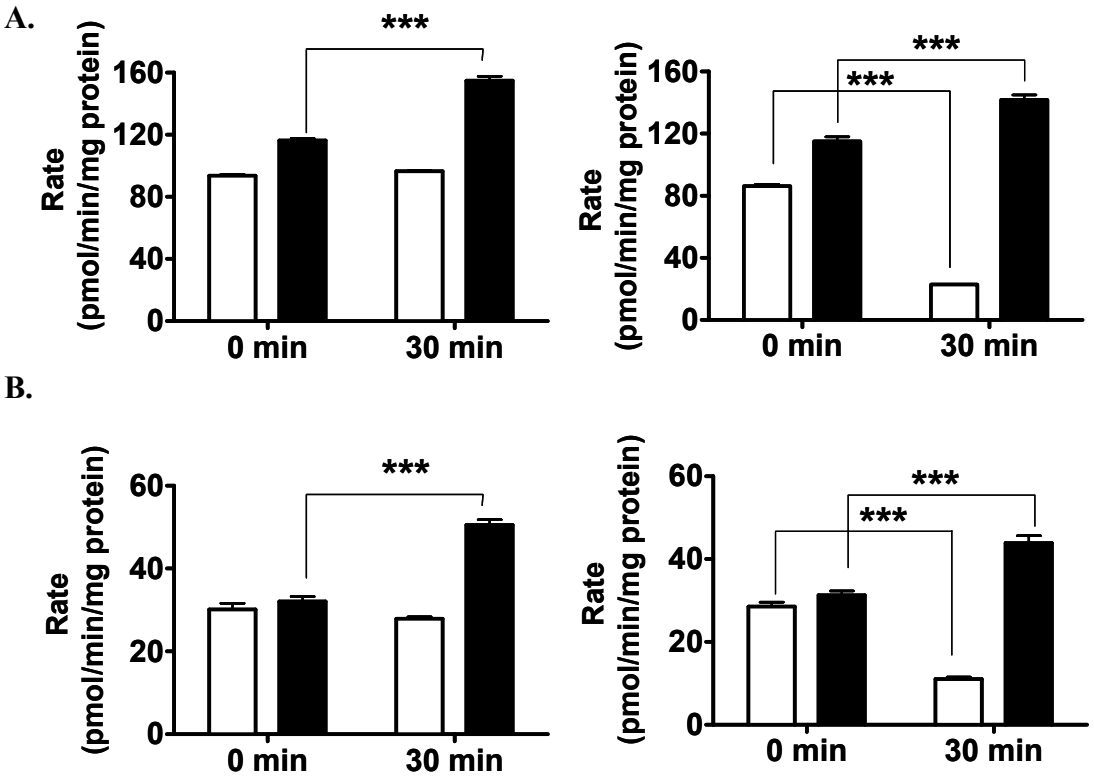

Figure 2.7 Time-dependent inhibition of DB868 *N*-demethoxylation in human and rat liver microsomes. Direct *N*-demethoxylation of DB868 shown by time-dependent inhibition experiments with human liver microsomes (HLMs) (A) or rat liver microsomes (RLMs) (B). HLMs or RLMs (5 mg/ml) were treated with ABT (1 mM) in the absence (left panels) or presence (right panels) of NADPH (2 mM). Aliquots were removed from the primary incubation mixtures at 0 and 30 min and were added to secondary incubations (10-fold dilution) containing DB868 (10 μM) and NADPH (2 mM). Bars represent the rate of formation of M1 (white bars) and M3 (black bars) and are the means ± SD of triplicate determinations (***$p < 0.001$).

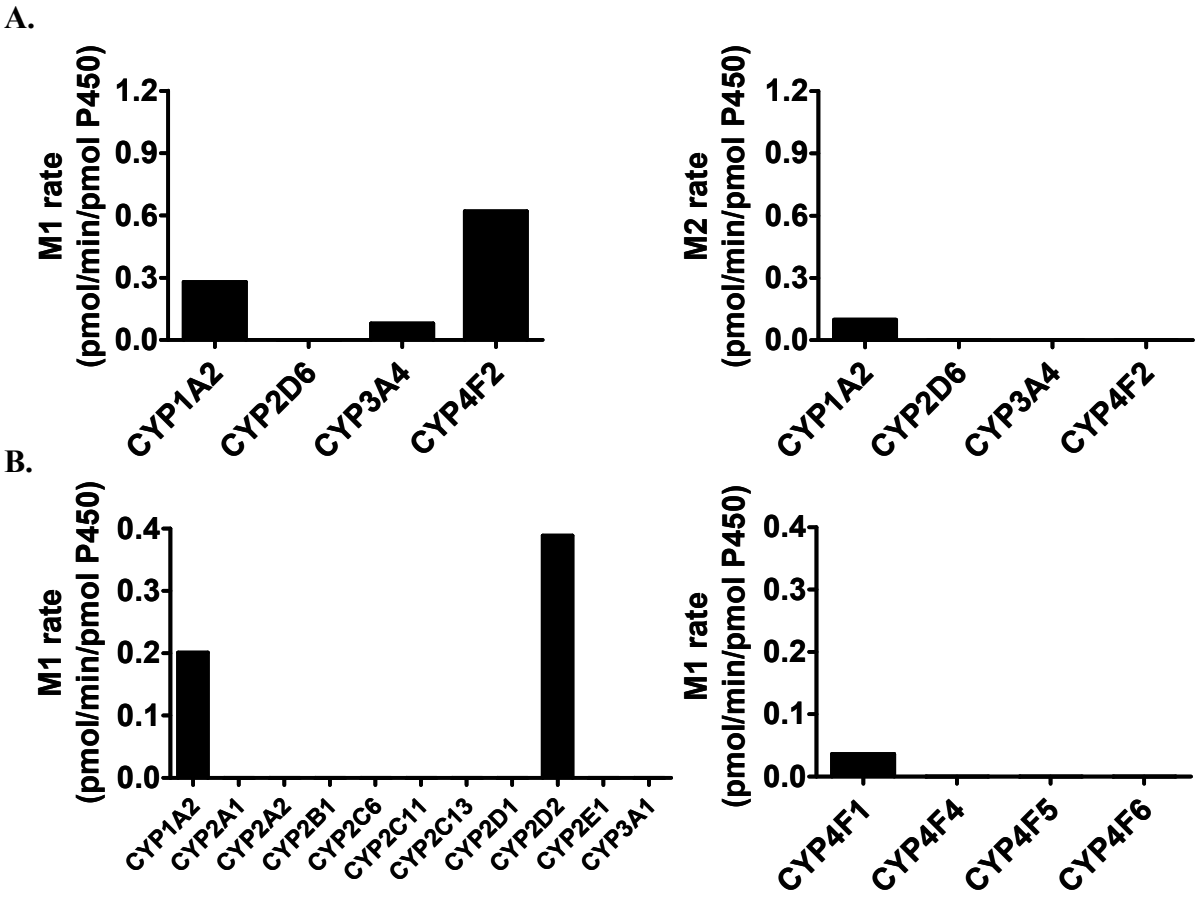

Figure 2.8 Human and rat CYP enzymes responsible for M1 and M2 formation. The top panels show select human recombinant CYP enzymes incubated with DB868 (A; left panel) or M1 (A; right panel) for 15 min. The bottom panels show rat recombinant CYP enzymes incubated with DB868 (B; left panel) for 15 min or purified rat CYP4F enzymes (B; right panel) incubated with DB868 for 30 min. All reactions were started with NADPH (2 mM). Bars represent the mean of duplicate determinations.

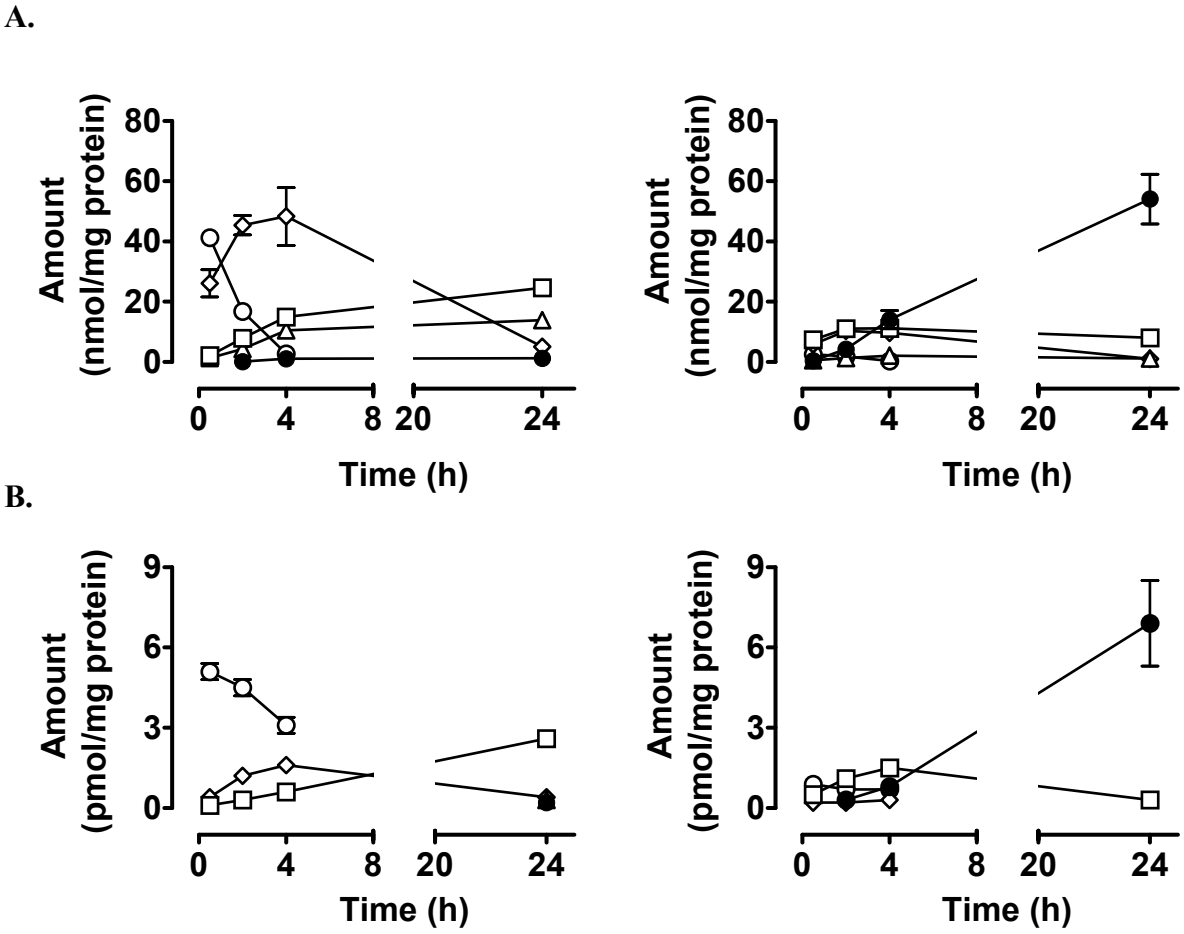

Figure 2.9 DB868 and phase I metabolites in incubations with human and rat sandwich culture hepatocytes. DB868 (10 μM) was incubated with human sandwich culture hepatocytes (HSCHs) (A) or rat sandwich culture hepatocytes (RSCHs) (B) at 37°C for up to 24 h. Amounts of DB868 (○) and metabolites (M1 (◊), M2 (Δ), M3 (□), and DB829 (●)) were quantified from medium (A and B; left panels) and cell lysate (A and B; right panels) removed at select incubation time points (0.5, 2, 4 and 24 h). The data represent the mean ± SD of 4 (RSCHs) to 6 (HSCHs) determinations. Quantification of the M4 metabolite was not possible due to a lack of an authentic standard.

G. TABLES

Table 2.1 Protonated molecular ions of the prodrug DB868 and its metabolites, mass shifts and MS^n fragmentations

Compound	MW	$[M+H]^+$	Δ Mass shift	Proposed Structural Assignment	$MS \rightarrow MS^2, MS^3$
DB868	366	367	NA	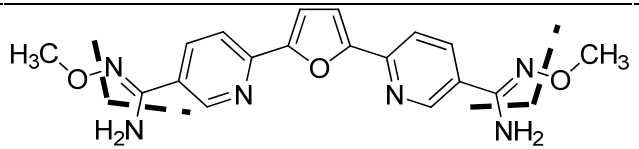	367→**320**, 273
M1	352	353	-14	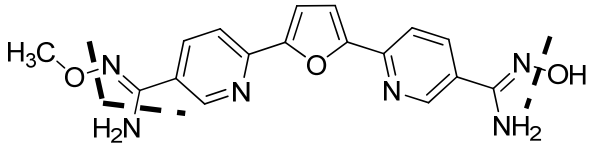	353→**306**, 289
M2	338	339	-28	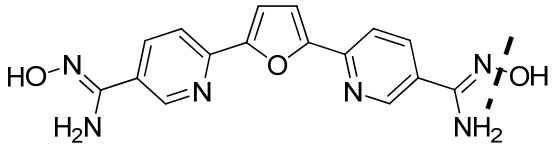	339→**322**,306
M3	336	337	-30	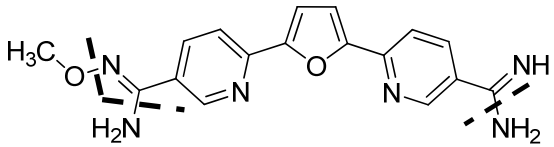	337→**290**, 273
M4	322	323	-44	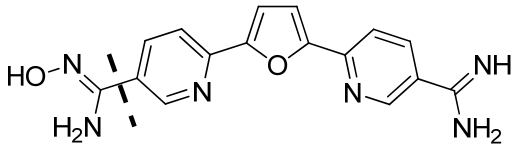	323→306

NA: Not applicable
Dashed lines on structures represent proposed fragmentation sites.

Table 2.2 Apparent first-order rate constants for the metabolism of DB868 (10 μM) in HLM and RLM

Species	Parameter (min^{-1})	Estimate (%CV)	Cl_{app} (μL/min/mg protein)
HLM	k_1	0.0300 (5.6)	15.00
	k_2	0.0002 (18)	0.10
	k_3	0.0060 (7.6)	3.00
	k_4	0.0057 (15)	2.86
RLM	k_1	0.0046 (2.6)	2.32
	k_2	0.0007 (52)	0.32
	k_3	0.0006 (36)	0.30
	k_4	0.0005 (25)	0.28

Data are the mean parameter estimates and their coefficient of variation obtained by non-linear regression using WinNonlin 5.0.1 (Pharsight, Mountain View, CA).

Table 2.3 Enzyme kinetic parameters for the formation of M1 and M2 in HLM and RLM

Species	Pathway	V_{max} (pmol/min/mg protein)	K_m (μM)	S_{50} (μM)	n	Cl_{int} (μL/min/mg protein)	Cl_{max} (μL/min/mg protein)
HLM	868→M1	340 (4.5)	11 (6.7)			30.9	
	M1→M2 (Hill)	184 (12)		18 (3)	1.7 (0.2)		3.2
	M1→M2 (Korzekwa)	82.4 (52)	46.9 (39)			1.8	
	M1→M2 (Korzekwa)	184 (12)	0.15 (23)			1226.6	
RLM	868→M1	11.8(26)	0.5 (34)			23.6	
	868→M1	70 (14)	27 (36)			2.6	

Data are mean parameter estimates and their coefficient of variation obtained by non-linear regression using WinNonlin 5.0.1 (Pharsight, Mountain View, CA). Cl_{max}: Obtained from graphical analysis of Clapp versus substrate (M1) plot (Witherow and Houston, 1999)

H. ACKNOWLEDGEMENTS

The authors thank Dr. Deanna Kroetz (University of California San Francisco) for donating the purified CYP4F proteins and Dr. Thomas Trout (UNC-Department of Biochemistry and Biophysics) for his helpful discussions regarding allosteric kinetics.

I. FOOTNOTES

a. This investigation was supported by the Consortium of Parasitic Drug Development (CPDD).

b. This investigation was originally presented at the Globalization of Pharmaceutics Education Network (GPEN) meeting. Leuven, Belgium (2008).

c. Reprint requests: Mary F. Paine, Ph.D.

2320 Kerr Hall, CB #7569

Eshelman School of Pharmacy University of North Carolina Chapel Hill, NC 27599-7569

Office: (919) 966-9984

Fax: (919) 962-0644

Email: mpaine@unc.edu

J. REFERENCES

Atkins W (2004) Implications of the allosteric kinetics of cytochrome P450s. Drug Discovery Today 9:484.

Badawi N, RÃ¸nhede S, Olsson S, Kragelund B, Johnsen A, Jacobsen O and Aamand J (2009) Metabolites of the phenylurea herbicides chlorotoluron, diuron, isoproturon and linuron produced by the soil fungus Mortierella sp. Environmental Pollution 157:2812.

Balasegaram M, Young H, Chappuis F, Priotto G, Raguenaud ME and Checchi F (2009) Effectiveness of melarsoprol and eflornithine as first-line regimens for gambiense sleeping sickness in nine Medecins Sans Frontieres programmes. Trans R Soc Trop Med Hyg 103:280-290.

Barrett MP, Boykin DW, Brun R and Tidwell RR (2007) Human African trypanosomiasis: pharmacological re-engagement with a neglected disease. Br J Pharmacol 152:1155-1171.

Berger B (1998) Parameters Influencing Biotransformation Rates of Phenylurea Herbicides by Soil Microorganisms. Pesticide Biochemistry and Physiology 60:82.

Bow DA, Perry JL, Miller DS, Pritchard JB and Brouwer KL (2008) Localization of P-gp (Abcb1) and Mrp2 (Abcc2) in freshly isolated rat hepatocytes. Drug Metab Dispos 36:198-202.

Boykin DW, Kumar A, Spychala J, Zhou M, Lombardy RJ, Wilson WD, Dykstra CC, Jones SK, Hall JE, Tidwell RR and et al. (1995) Dicationic diarylfurans as anti-Pneumocystis carinii agents. J Med Chem 38:912-916.

Cameron MD, Wen B, Roberts AG, Atkins WM, Campbell AP and Nelson SD (2007) Cooperative binding of acetaminophen and caffeine within the P450 3A4 active site. Chem Res Toxicol 20:1434-1441.

Chandra P and Brouwer KL (2004) The complexities of hepatic drug transport: current knowledge and emerging concepts. Pharm Res 21:719-735.

Chappuis F, Udayraj N, Stietenroth K, Meussen A and Bovier PA (2005) Eflornithine is safer than melarsoprol for the treatment of second-stage Trypanosoma brucei gambiense human African trypanosomiasis. Clin Infect Dis 41:748-751.

Clement B, Mau S, Deters S and Havemeyer A (2005) Hepatic, extrahepatic, microsomal, and mitochondrial activation of the N-hydroxylated prodrugs benzamidoxime, guanoxabenz, and Ro 48-3656 ([[1-[(2s)-2-[[4-[(hydroxyamino)iminomethyl]benzoyl]amino]-1-oxopropyl]-4-piperid inyl]oxy]-acetic acid). Drug Metab Dispos 33:1740-1747.

Fairlamb AH (2003) Chemotherapy of human African trypanosomiasis: current and future prospects. Trends Parasitol 19:488-494.

Havemeyer A, Bittner F, Wollers S, Mendel R, Kunze T and Clement B (2006) Identification of the missing component in the mitochondrial benzamidoxime prodrug-converting system as a novel molybdenum enzyme. J Biol Chem 281:34796-34802.

Hutzler JM, Hauer MJ and Tracy TS (2001) Dapsone activation of CYP2C9-mediated metabolism: evidence for activation of multiple substrates and a two-site model. Drug Metab Dispos 29:1029-1034.

Isin EM, Sohl CD, Eoff RL and Guengerich FP (2008) Cooperativity of cytochrome P450 1A2: interactions of 1,4-phenylene diisocyanide and 1-isopropoxy-4-nitrobenzene. Arch Biochem Biophys 473:69-75.

Ismail MA, Brun R, Easterbrook JD, Tanious FA, Wilson WD and Boykin DW (2003) Synthesis and antiprotozoal activity of aza-analogues of furamidine. J Med Chem 46:4761-4769.

Kern A, Bader A, Pichlmayr R and Sewing KF (1997) Drug metabolism in hepatocyte sandwich cultures of rats and humans. Biochem Pharmacol 54:761-772.

Korzekwa KR, Krishnamachary N, Shou M, Ogai A, Parise RA, Rettie AE, Gonzalez FJ and Tracy TS (1998) Evaluation of atypical cytochrome P450 kinetics with two-substrate models: evidence that multiple substrates can simultaneously bind to cytochrome P450 active sites. Biochemistry 37:4137-4147.

Legros D, Ollivier G, Gastellu-Etchegorry M, Paquet C, Burri C, Jannin J and Buscher P (2002) Treatment of human African trypanosomiasis--present situation and needs for research and development. Lancet Infect Dis 2:437-440.

Linder CD, Renaud NA and Hutzler JM (2009) Is 1-aminobenzotriazole an appropriate in vitro tool as a nonspecific cytochrome P450 inactivator? Drug Metab Dispos 37:10-13.

Mohamed AI and David WB (2006) Synthesis of deuterium and ^{15}N-labelled 2,5-*Bis*[5-amidino-2-pyridyl]furan and 2,5-*Bis*[5-(methoxyamidino)-2-pyridyl]furan. Journal of Labelled Compounds and Radiopharmaceuticals 49:985-996.

Ortiz de Montellano PR and Mathews JM (1981) Autocatalytic alkylation of the cytochrome P-450 prosthetic haem group by 1-aminobenzotriazole. Isolation of an NN-bridged benzyne-protoporphyrin IX adduct. Biochem J 195:761-764.

Priotto G, Fogg C, Balasegaram M, Erphas O, Louga A, Checchi F, Ghabri S and Piola P (2006) Three Drug Combinations for Late-Stage *Trypanosoma brucei gambiense* Sleeping Sickness: A Randomized Clinical Trial in Uganda. PLOS Clin Trial 1:e39.

Saulter J, Kurian J, Trepanier L, Tidwell R, Bridges A, Boykin D, Stephens C, Anbazhagan M and Hall JE (2005) Unusual Dehydroxylation of Antimicrobial Amidoxime Prodrugs by Cytochrome b5 and NADH Cytochrome b5 Reductase. Drug Metab Dispos 33:1886-1893.

Sohl CD, Isin EM, Eoff RL, Marsch GA, Stec DF and Guengerich FP (2008) Cooperativity in oxidation reactions catalyzed by cytochrome P450 1A2: highly cooperative pyrene hydroxylation and multiphasic kinetics of ligand binding. J Biol Chem 283:7293-7308.

Sternberg JM (2004) Human African trypanosomiasis: clinical presentation and immune response. Parasite Immunology 26:476.

Tracy TS (2006) Atypical cytochrome p450 kinetics: implications for drug discovery. Drugs R D 7:349-363.

Wang MZ, Saulter JY, Usuki E, Cheung YL, Hall M, Bridges AS, Loewen G, Parkinson OT, Stephens CE, Allen JL, Zeldin DC, Boykin DW, Tidwell RR, Parkinson A, Paine MF and Hall JE (2006) CYP4F enzymes are the major enzymes in human liver microsomes that catalyze the O-demethylation of the antiparasitic prodrug DB289 [2,5-bis(4-amidinophenyl)furan-bis-O-methylamidoxime]. Drug Metab Dispos 34:1985-1994.

Wenzler T, Boykin DW, Ismail MA, Hall JE, Tidwell RR and Brun R (2009) New treatment option for second-stage African sleeping sickness: in vitro and in vivo efficacy of aza analogs of DB289. Antimicrob Agents Chemother 53:4185-4192.

WHO. 2010. Http://www.who.int/mediacentre/factsheets/fs259/en/

Witherow LE and Houston JB (1999) Sigmoidal kinetics of CYP3A substrates: an approach for scaling dextromethorphan metabolism in hepatic microsomes and isolated hepatocytes to predict in vivo clearance in rat. J Pharmacol Exp Ther 290:58-65.

Xu F, Falck JR, Ortiz de Montellano PR and Kroetz DL (2004) Catalytic activity and isoform-specific inhibition of rat cytochrome p450 4F enzymes. J Pharmacol Exp Ther 308:887-895.

Zhou L, Thakker DR, Voyksner RD, Anbazhagan M, Boykin DW, Hall JE and Tidwell RR (2004) Metabolites of an orally active antimicrobial prodrug, 2,5-bis(4-amidinophenyl)furan-bis-O-methylamidoxime, identified by liquid chromatography/tandem mass spectrometry. J Mass Spectrom 39:351-360.

Zhou L, Voyksner RD, Thakker DR, Stephens CE, Anbazhagan M, Boykin DW, Hall JE and Tidwell RR (2002) Characterizing the fragmentation of 2,5-bis (4-amidinophenyl)furan-bis-O-methylamidoxime and selected metabolites using ion trap mass spectrometry. Rapid Commun Mass Spectrom 16:1078-1085.

CHAPTER 3

TRYPANOSOMAL INFECTION ALTERS THE PHARMACOKINETICS AND DISPOSITION OF THE ANTIPARASITIC AGENT FURAMIDINE AND ITS PRODRUG PAFURAMIDINE IN RATS

This chapter will be submitted to the journal *Antimicrobial Agents and Chemotherapy* and is formatted in the style of this journal.

A. ABSTRACT

Cytokines generated during infection and inflammation have been demonstrated to mediate down-regulation of many drug metabolizing enzymes (DMEs) and transporters. The consequences of such down-regulation often are manifested as altered drug clearance or exposure, which may lead to untoward, or even toxic, or sub-therapeutic outcomes. A prodrug of the potent antitrypanosomal agent furamidine, evaluated for the treatment of human African trypanosomiasis, requires biotransformation for activation. It was hypothesized that trypanosomal infection would decrease conversion of pafuramidine to furamidine due to down-regulation of DMEs, leading to ineffective concentrations of active metabolite. Pafuramidine systemic exposure (AUC) was 1.3-fold higher in infected animals compared to controls, following an oral dose that saturated metabolism (25 μmol/kg) ($p<0.01$). In contrast, no elevation in AUC was observed in infected animals receiving an oral dose within the linear pharmacokinetic range (7.5 μmol/kg) or when pafuramidine was administered intravenously (1.45 μmol/kg). A marked increase in furamidine systemic AUC (up to 3-fold) and prolonged half-life (up to 2-fold) was observed in infected compared to control animals regardless of route of administration and dose. A significant decrease in the rate of furamidine biliary excretion in infected rats (12-fold from control) ($p<0.05$) may explain the observed increase in systemic furamidine exposure. These results demonstrate that trypanosomal infection can alter the pharmacokinetics of both pafuramidine and furamidine, suggesting down-regulation of both hepatic CYP enzymes involved in pafuramidine clearance and canalicular transporters involved in furamidine biliary excretion. Sub-therapeutic circulating concentrations of furamidine in infected populations may not be of concern.

B. INTRODUCTION

Infection-related changes in pharmacokinetics of drugs were recognized in the clinic more than two decades ago, with a case of reduced theophylline clearance in children infected with influenza. Diminished clearance led to drug-related toxicity and was linked to decreased function of CYP enzymes during infection due to inflammatory cytokines (21). Other clinical examples of altered pharmacokinetics as a result of infection or inflammation have since been reported (23, 29, 30, 36, 37, 45). Numerous *in vitro* studies have focused on understanding mechanisms by which infection alters expression and function of drug metabolizing enzymes. Particular attention has centered on investigating effects of pro-inflammatory cytokines (4, 19, 32, 33). For example, direct challenge with the pro-inflammatory cytokines IL1-β, IL-6, TNF-α and INF-γ suppressed mRNA expression of major CYPs 1A2, 2C, 2E1 and 3A4 in primary cultures of human hepatocytes (1). Similarly, CYP2E1 was down-regulated during LPS-induced inflammation in the rat (2). Inflammatory cytokines also are capable of modulating phase II enzymes and drug transporters (13, 15). TNF-α and IL-1 were associated with significant reduction of sulfotransferase (Sult) 2a1 in a murine model of LPS-inflammation (19). Likewise, TNF-α and IL-6 had profound effects on mRNA expression and function of basolateral and canalicular transporters in human hepatocytes (39).

Human African trypanosomiasis (HAT) is a parasitic disease endemic to sub-Saharan Africa. It is caused by the flagellated protozoan *Trypanosoma brucei*. HAT has two distinct stages: first-stage and second-stage. First-stage is defined by an acute infection and the presence of trypanosomes in the blood and lymph. Second-stage begins once parasites invade the central nervous system, and is diagnosed by the detection of *T. brucei* subspecies

in cerebrospinal fluid. Second-stage symptoms are more severe than first-stage symptoms (e.g., general malaise, fatigue and headaches) and include neurological abnormalities that affect the wake-sleep cycle (38). Without drug treatment, HAT is fatal. Current chemotherapy for treatment of either stage is scarce. In addition, available drugs are associated with impractical dosing regimens and unacceptable toxicity. For example, melarsoprol used until recently as first line treatment for second-stage HAT, must be administered intravenously and requires three or four times daily administration for a period of three or four weeks (3). This arsenic containing compound also causes post-treatment reactive encelopathy in 10% of patients, half of which die. As with other neglected diseases, there is little monetary incentive for pharmaceutical companies to develop new and safer drugs for HAT. Thus, only a few public sector institutions are involved discovery and development of drugs to treat this deadly disease.

Pafuramidine is a prodrug of the potent antitrypanosomal agent, furamidine, which was in development for treatment of first-stage HAT (Figure 3.1). In 2008, phase III clinical trials were completed in which pafuramidine was tested as the first oral treatment for first-stage HAT; however, during an extended phase I clinical trial in healthy volunteers evaluating the safety and tolerability of pafuramidine, development was halted due to liver toxicity and unforeseen delayed nephrotoxicity (28). Nothwithstanding the observed toxicity, pafuramidine and other diamidine prodrugs in development for the treatment of second-stage HAT have suitable pharmacokinetic characteristics for oral administration. Pharmacokinetic studies with rats and monkeys showed that pafuramidine undergoes extensive first-pass metabolism with minor contributions (<10%) by non-hepatic routes (24). Metabolic activation of pafuramidine occurs in the liver, through a complex metabolic

pathway that includes *O*-demethylation and *N*-hydroxylation reactions (47). The primary metabolite of pafuramidine, an *O*-demethylation product, is catalyzed by CYP4F2 in human liver microsomes, while reductive intermediate metabolites were shown to be products of the cytochrome b_5/NADH b_5 reductase system (34, 41). Intestinal first-pass metabolism of pafuramidine is believed to be minimal compared to hepatic first-pass metabolism, as reflected by the reported intrinsic clearance for M1 formation (pafuramidine-*O*-demethylation) of human intestinal and liver microsomes (0.27 and 7.6 ml/min/mg protein, respectively). Additionally, pafuramidine was shown to have high absorptive permeability in Caco-2 cell monolayers (P_{app} = 32.2 x10^{-6} cm/s) (42, 46). The unbound fraction (f_u) of pafuramidine and furamidine in rat plasma was 0.01 and 0.2, respectively (24). After intravenous or oral administration of pafuramidine, furamidine was observed in rats and monkeys as early as 30 min post-dose, indicating rapid formation in the liver. Among the elimination pathways of furamidine, biliary excretion and glucuronidation were reported as important components, with renal excretion having a minor contribution. In both rats and monkeys, tissue binding was shown to be a major component of furamidine disposition, as demonstrated by extensive accumulation of furamidine in tissues, including liver and kidney (24).

Based on the known effects of infection on DMEs, and that furamidine requires biotransformation of pafuramidine, it was hypothesized that down-regulation of DMEs during infection would decrease clearance of pafuramidine and yield sub-therapeutic concentrations of the active metabolite furamidine. This investigation aimed to evaluate the effects of trypanosomal infection on the pharmacokinetics of pafuramidine and furamidine in a rat experimental model of first-stage HAT. An improved understanding of the effects of

trypanosomal infection on the pharmacokinetics of these agents will help guide development of diamidine analogs and prodrugs for the treatment of HAT.

C. MATERIALS AND METHODS

Materials. Pafuramidine and furamidine were synthesized in the laboratory of Dr. David Boykin (Georgia State University, Atlanta, GA) as described previously (18). Heat inactivated fetal bovine serum, (10% v/v), 1% hypoxanthine, L-cysteine, thymidine prepared in sodium hydroxide, penicillin/streptomycin, bathocuproine disulfonic acid, β-mercaptoethanol and pyruvate were purchased from Sigma-Aldrich (St. Louis, MO).

Animals. Cannulated male Sprague-Dawley rats (226-250 g) were purchased from Charles River Laboratories (Raleigh, NC) and were maintained in single cages on standard rodent chow and water *ad libitum*. Animals were acclimated for seven days prior to experiments. All experiments followed protocols in accordance with the guidelines for the use of live animals approved by the Institutional Animal Care and Use Committee of the University of North Carolina at Chapel Hill.

***In vitro* cultivation of parasites.** *T. b. brucei* S427, an isolate from Uganda (1960) (43), was cultivated in modified Iscove's medium (HMI-18) as described by Hirumi and Hirumi (17). Parasites were grown in Corning 10-mL (25-cm^2) cell culture flasks (Corning Inc. Corning, NY) and were passaged every 2-3 days until cell densities reached approximately 10^6 trypanosomes/mL.

Characterization of *T. b. brucei* infection in Sprague-Dawley rats. Histopathology and biochemical markers of liver and kidney function were determined to assess potential biochemical and physiologic changes elicited by the infection. Three groups

of ten jugular vein cannulated (226 - 250 g) rats were separated into control (n=4) and infected animals (n=6). Each group was designed to capture changes in organ function at early, medium and high parasitemia (group 1, 2 and 3, respectively) based on preliminary experiments that defined the time course of the infection. On day 0, rats were inoculated intraperitoneally with *T. b. brucei* S427 (4 x 10^4 cells) or injected with vehicle (400 µL) (HMI-18 medium). To evaluate the time course of the infection, parasitemia was determined daily by counting trypanosomes from a drop of jugular vein blood under a microscope and averaging the counts of least 20 fields at a 400X magnification. Blood was collected daily from the jugular vein. Blood collections were divided between lithium heparin-coated tubes (200 µL) or EDTA-coated tubes (30 µL) for plasma and blood clinical analysis, respectively. Blood in heparin tubes was separated from plasma by centrifugation at 3000 rpm (1500 x g) in a Marathon 8K centrifuge (Fisher Scientific, Pittsburgh, PA) for 10 min. Animals were euthanized with carbon dioxide at days 3, 5 and 6 (groups 1, 2, and 3, respectively), and livers and kidneys were excised. A portion of each organs was sectioned and stored in 10% neutral formalin buffer for hematoxylin and eosin (H&E) staining, ensuring that the same section was obtained from all animals. The remaining portion of each organ was frozen immediately on dry ice and stored at -80°C.

Histology and light microscopy. Liver and kidney sections were immersed in 10% neutral formalin buffer for at least 24 h before processing. Slices of liver or kidney of 3-6 mm in thickness were embedded in paraffin wax and sectioned at 3 µm for H&E staining prior examination by microscopy with an Olympus BX61 fluorescent microscope on bright field mode with color camera (Olympus America, Center Valley, PA). Liver and kidney sections were examined for changes in tissue architecture, presence of focal areas of necrosis,

tissue congestion and inflammation. All histological samples were processed at the UNC Animal Histopathology Core Facility (Chapel Hill, NC).

Hematological and serum markers. Blood collected in EDTA tubes was maintained at 4°C until analysis with a veterinary hematology system (HESKA Corporation, Loveland, CO). Plasma collected in heparin coated tubes was maintained at 4°C until analysis for biochemical markers. Total protein, alanine aminotrasterase (ALT), total bilirubin (BIL), blood urea nitrogen (BUN), and serum creatinine (SCR) were analyzed on a VITRO 350 Chemical Analyzer (Ortho-Clinical Diagnostics, Rochester, NY) by the UNC Animal Clinical Chemistry and Gene Expression Facility (Chapel Hill, NC).

Pharmacokinetic experiments. Double jugular and femoral vein cannulated male Sprague-Dawley rats (n=6) were infected with *T. b. brucei* S427 (10^4 cells) or treated with vehicle (HMI-18). *Intravenous administration of prodrug.* On day four post-inoculation, animals were administered pafuramidine intravenously (1.45 μmol/kg) as a 30-min infusion through the femoral vein cannula. The dose was formulated as a solution of D-α-tocopheryl polyethylene glycol 1000 succinate, citric acid, ethanol, and 0.9% saline according to methods described previously (24). Blood (0.2 mL) was collected from a jugular vein at 0.08, 0.25, 0.5, 1, 2, 4, 6, 8, 12 and 24 h after the infusion was stopped, and the samples were maintained at 4°C until separated from plasma by centrifugation at 3000 rpm (1500 x g) for 10 min. Plasma was removed from red blood cells, taking care to ensure that the buffy coat, which in addition to white blood cells contains trypanosomes in infected samples, was not disrupted. Additionally, an aliquot of the plasma (10 μL) from infected samples was examined microscopically to ensure the absence of trypanosomes. Plasma was stored at -20°C until further processing. Plasma samples were prepared for HPLC/MS/MS analysis by

adding 200 µL of 7:1 (v/v) methanol:water 0.1% trifluoroacetic acid (v/v) containing 30 nM d_8-pafuramidine and d_8-furamidine as internal standards to an aliquot of plasma (25 µL). After vortexing, this mixture was centrifuged at 3000 rpm (1500 x g) for 10 min at 4°C. The supernatant (170 µL) was removed and evaporated for (~25 min) in a 96-well plate nitrogen evaporator (Evaporex EVX-192, Apricot designs, Monrovia, CA). Samples were reconstituted with a mixture of 15% (v/v) methanol: water 0.1% trifluoroacetic acid, vortexed and transferred to vials for quantification of pafuramidine and furamidine by HPLC/MS/MS (described below).

Oral administration of prodrug. Dose escalation studies with pafuramidine were conducted in uninfected animals to assess pharmacokinetic linearity. Jugular vein cannulated rats (n= 4) were administered pafuramidine by oral gavage (2.5, 7.5 and 25 µmol/kg) in a suspension of 70:30 (v/v) acidified water: (70:30 v/v) Tween 80:ethanol. To assess the effects of infection after oral administration of pafuramidine, pharmacokinetic studies with infected and uninfected rats were carried out at two different doses. The doses selected were either within or above the linear range (7.5 and 25 µmol/kg, respectively). Jugular vein cannulated rats (n=6 per group) were infected with *T. b. brucei* S427 (10^4 cells) by intraperitoneal injection or treated with vehicle (HMI-18). Four days post-inoculation, rats were administered pafuramidine by oral gavage at either 7.5 or 25 µmol/kg in the same oral formulation described above. For both dose escalation and experiments with infected animals, blood (0.2 mL) was collected from a jugular vein at 0.08, 0.25, 0.5, 1, 2, 4, 6, 8, 12 and 24 h after pafuramidine administration and was stored at 4°C until separated from plasma by centrifugation at 3000 rpm (1500 x g) for 10 min. Plasma was stored at -20°C until

samples were processed (according to the methods described above) for quantification of pafuramidine, M1 or furamidine by HPLC/MS/MS analysis (described below).

In situ* bile duct cannulation experiments:* To determine whether biliary elimination of furamidine was impaired during trypanosomal infection, *in situ* bile cannulation experiments were conducted according to the methods described by Lee et.al., (2002) with modifications (22). Male Sprague-Dawley rats (n=3) were infected intraperitoneally with *T. b. brucei* S427 (10^4 cells) or treated with vehicle (HMI-18). On day four post-inoculation, animals were anesthetized by intraperitoneal administration of ketamine and xylazine (cocktail) at a dose of 75 mg/kg and 10 mg/kg, respectively. A small polyethylene tube (PE-10) was used to cannulate the common bile duct for bile collection. After bile flow was established, a 7.5 μmol/kg dose of pafuramidine (prepared in the same oral formulation described above) was administered directly into the duodenum. Immediately after dosing, bile was collected at 10 min intervals for 60 min. Body temperature was monitored using a Traceable digital thermometer (Fisher Scientific, Pittsburgh, PA) and was maintained between 36-37°C using a Sunbeam heating pad (Jarden Corporation, Providence, RI). Bile samples were maintained at 4°C for the duration of the experiment and were stored at -20°C until processing for furamidine quantification. Bile collections were prepared for HPLC/MS/MS analysis by diluting 1:50 (v/v) with 7:1 (v/v) methanol:water 0.1% trifluoroacetic acid (v/v) containing 60 nM d_8-furamidine as internal standard.

HPLC-mass spectrometry analysis. Reconstituted samples were analyzed by liquid chromatography with detection by tandem mass spectrometry with no further manipulation. A Shimadzu solvent delivery system (Columbia, MD, USA), a Leap HTC Pal thermostated

autosampler (Carrboro, NC USA), and an Applied Biosystems API 4000 triple quadruple mass spectrometer with a TurboIon ion source (Applied Biosystems, Foster City, CA, USA) were used for these analytical studies. Tuning, operation, integration and data analysis were performed using Analyst® software v.1.4.1 (Applied Biosystems, Foster City, CA, USA). Standard curves for pafuramidine, furamidine, and M1 were prepared for each analytical run using appropriate matrix (i.e., plasma). The standard curves ranged from 1 -1000 nM and the lower limit of quantification was 5 nM. The sample injection volume was 4 µl. Following injection, analytes were eluted from an Aquasil C18 column (d_p = 5 µm, 2.1 x 50 mm; Thermo Electron Corporation, San Jose, CA) using a mobile phase gradient. Mobile phase A consisted of 35 mM formic acid with 15 mM ammonium formate in 100% water, and mobile phase B consisted of 35 mM formic acid with 15 mM ammonium formate in 80:20 v/v acetonitrile: water. The mobile phase gradient was as follows: 0 - 0.8 min hold at 10% B; 0.8 - 7.0 min linear gradient to 80% B; 7.0 - 7.6 min linear gradient to 100% B; 7.6 - 8.5 hold at 100% B, 8.5 - 8.6 min linear gradient to 10% B, 8.6 -10.0 min hold at 10% B. The flow rate was 0.35 ml/min. Total run time, including equilibration, was 10 minutes per injection. All eluent was directed to the mass spectrometer. The mass spectrometer was operated in positive ion mode using multiple reaction monitoring: pafuramidine, 365.1→334.1 *m*/*z*; furamidine, 305.3→288.1 *m*/*z*; M1, 351.1→320.1 *m*/*z*; d_8-furamidine, 313.3→296.1 *m*/*z*; d_8-pafuramidine, 373.1→242.0 *m*/*z*.

Pharmacokinetic Analysis. Pharmacokinetics of pafuramidine and furamidine were evaluated by noncompartmental methods using WinNonlin (v5.2; Pharsight, Mountain View, CA). The first-order elimination rate constant (k) was determined from linear regression of the terminal phase of the concentration-time curve (using a minimum of three data points).

Terminal half-life ($t_{½}$) was calculated as ln 2/k. The linear trapezoidal (linear interpolation) method was used for the calculation of the area under the curve (AUC_{0-t}) from the time of dosing to the last measurable concentration. Area under the curve extrapolated to infinity ($AUC_{0-\infty}$) was calculated as ($AUC_{0-t} + C_{last\ pred}/k$), where ($C_{last\ pred}$) was the last predicted concentration. Systemic clearance (CL) was calculated as dose/$AUC_{0-\infty}$ following intravenous administration. The volume of distribution at steady state (V_{ss}) was estimated using $MRT_{0-\infty}$ * CL, where MRT is the mean residence time extrapolated to infinity. Maximum concentration (C_{max}) and the time to achieve C_{max} (T_{max}) following oral administration were reported as observed median and range. Apparent oral clearance (CL_{po}) was calculated as dose/$AUC_{0-\infty}$. Values of $AUC_{0-\infty}$ that were extrapolated >25% were not reported.

Statistical Analysis. One way ANOVA with a post-hoc Dunnett's test for multiple comparisons was used to evaluate the difference in hematological and serum markers values at different days of infection compared to control. Comparisons between pharmacokinetic parameters between infected and un-infected controls were made using Student's t-tests. Repeated measures ANOVA was used for comparisons of biliary excretion rate and bile flow between infected and uninfected groups. For all statistical methods, differences were deemed significant if p-values were <0.05. Statistical analyses were performed using GraphPad InStat 3.06 (GraphPad Software, San Diego, CA, USA) and R version 2.11.1 (Vienna, Austria)

D. RESULTS

***Trypanosoma brucei brucei* infection in Sprague-Dawley rats.** *Time course of parasitemia.* Blood parasite counts in infected rats from groups 1-3 were recorded daily. Trypanosomes were not visible microscopically until day three post-infection. Parasitemia increased exponentially on days 3 and 4 and peaked on day 5. Only two animals survived to day 6 post-infection, and their parasitemia was lower than peak counts (Figure 3.2).

Histological Evaluation: Minimal changes in the architecture of the liver and kidney tissues of infected animals were observed at day 3 (group 1) or day 5 (group 2) post-infection compared to uninfected controls. Mild infiltration of inflammatory cells was evident in both tissues at day 5 post-infection (Figure 3.3). Tissues from the infected animals of group 3 showed an increased number of inflammatory cells infiltrating the parenchyma; however, no focal areas of necrosis or other pathological signs were evident at this time point (not shown).

Hematological and biochemical markers. In both groups 1 and 2, no significant differences were observed in RBC counts or HCT values between infected and uninfected controls (Tables 3.1 and 3.2). The WBC counts in group 1 showed a marked decrease at day 3 post-infection, with a reduction of about 45% from control values. The WBC counts in group 2 increased up to 63% from control on day 2 followed by a decrease sharp decrease beginning at day 3 resulting in up to 70% decrease from control values by day 5 post-infection. Groups 1 and 2 showed no significant elevations in ALT, BIL, total protein, BUN and SCR until day 3 post-infection (Table 3.2). However, at day 5 post-infection ALT and BUN levels increased 9- and 1.4-fold, respectively. BIL values in infected animals of groups 1 and 2 showed an increasing trend as the infection progressed; however, it was not possible to ascertain whether there was a statistical difference between infected and infected controls

because most of the control values were below the limit of quantification (<0.1) and thus no standard deviation values were available.

Pharmacokinetic experiments. *Dose escalation study.* To determine linearity in the dose-exposure relationship of pafuramidine in uninfected rats, a dose-escalation study was conducted at three dose levels. A proportional increase in exposure (AUC_{0-12}) was observed from 2.5 and 7.5 µmol/kg, whereas a greater than proportional increase was observed at 25 µmol/kg. The mean apparent oral clearance (Cl_{po}) of pafuramidine at 2.5, 7.5, and 25 µmol/kg was 8.0 (0.3), 12 (36), and 4.8 (14) L/h/kg, respectively (presented as geometric means and coefficient of variances). The active metabolite to pafuramidine AUC_{0-12} ratio was relatively constant at approximately 0.5 (Figure 3.4).

Pharmacokinetics of pafuramidine and furamidine after intravenous infusion. A rapid decline of pafuramidine from plasma was observed in both uninfected and infected animals (Figure 3.5). The pafuramidine concentration-time profile of the control animals showed biphasic decay, while a monoexponential decay profile was observed for the infected animals. Significant differences ($p<0.05$) in both the $t_{½}$ and V_{ss} were observed in infected animals compared to controls, where the V_{ss} was 2.1-fold lower and the $t_{½}$ 2.6-fold shorter in infected animals compared to controls. No significant changes in systemic clearance (CL) or exposure (AUC_{0-12}) were observed between groups (Table 3.3). For furamidine, the AUC_{0-6} was significantly greater ($p < 0.01$) in infected animals compared to uninfected controls (Table 3.3).

Pharmacokinetics of pafuramidine and furamidine after oral administration of 7.5 µmol/kg pafuramidine. Pafuramidine was absorbed readily in both uninfected and infected rats, with a median T_{max} of 1 h in both groups (Figure 3.6). Although no statistically

significant differences were observed, there was a tendency for both the median C_{max} and AUC_{0-12} of pafuramidine to be higher in infected animals. Similarly, both the $t_{½}$ and CL_{po} of pafuramidine in infected animals tended to be lower compared to controls. No significant differences were observed when comparing pharmacokinetic parameters of M1 in infected and uninfected animals; however, like pafuramidine there was a tendency toward higher AUC_{0-12} in infected animals. The median C_{max} and T_{max} of furamidine in infected rats were at least twice the corresponding values in control rats; likewise, the geometric mean AUC_{0-12} and $t_{½}$ of furamidine in infected rats were at least twice the corresponding values in control rats (Table 3.4).

Pharmacokinetics of pafuramidine and furamidine after oral administration of 25 µmol/kg pafuramidine. The median C_{max} , T_{max}, and the $t_{½}$ geometric mean of pafuramidine were similar in the both the infected and uninfected groups. In contrast, significant differences in pafuramidine exposure ($p<0.01$) were observed in the infected group compared to uninfected control, with a 1.3-fold higher exposure (AUC_{0-24}) in the infected rats (Figure 3.7). Consistent with the increased pafuramidine exposure in infected animals a significant decrease in the exposure of the M1 metabolite was observed in infected animals compared to controls (AUC_{0-12}) (Figure 3.8). Differences in the pharmacokinetic profiles of furamidine between infected and uninfected animals were also observed. In infected animals the furamidine AUC_{0-24} was significantly ($p<0.001$) higher compared to uninfected controls with a 1.9-fold increase in exposure in the infected animals. The profile of elimination of furamidine changed from formation-rate limited to elimination-rate limited. No meaningful differences were observed in the median C_{max}, T_{max}, and the $t_{½}$ geometric means of furamidine between uninfected and infected rats (Table 3.4).

Biliary excretion of furamidine. Comparison of biliary excretion rate between infected animals and uninfected animals showed significant differences ($p < 0.05$) when averaged across the entire time interval (0 - 60 min). Additionally, the difference in biliary excretion rates changes significantly with respect to time ($p<0.001$) (Figure 3.9). Furthermore, the average bile flow was not significantly different between groups. However, bile flow changed significantly for both groups with respect to time ($p<0.001$) (Figure 3.10).

E. DISCUSSION

Infectious agents have been demonstrated to modulate the clearance of drugs *via* down-regulation or induction of drug metabolizing enzymes (31). The consequences of down-regulation often are exemplified by untoward side effects or drug-related toxicity due to accumulation of systemic drug concentrations (21). *In vitro* studies have demonstrated that pro-inflammatory cytokines are in part responsible for down-regulation of drug metabolizing enzymes, including members of the CYP superfamily (12). The varied effects of down-regulation with respect to the degree and specificity of CYP enzymes affected make it difficult to ascertain what the overall effects of disease and infection would be on pharmacokinetics of a compound (8, 26, 27).

The compound pafuramidine is a prodrug for the potent antitrypanosomal agent furamidine. In liver microsomes it was shown that the biotransformation pathway of pafuramidine consists of a series of oxidative and reductive enzymatic reactions that lead to the generation of furamidine *via* four phase-I intermediates (M1-M4) (34, 41, 47). Pharmacokinetic studies with rats and monkeys also showed extensive pafuramidine metabolism, with detection of intermediate metabolites and furamidine the in plasma of both

species following intravenous and oral administration (24). Since metabolic biotransformation is essential to the formation of the active diamidine, prior to this investigation it was a concern that trypanosomal infection could diminish the formation of furamidine to sub-therapeutic levels. Accordingly, it was hypothesized that infection would decrease the metabolic activation of pafuramidine thus affecting the concentrations of furamidine in infected animals. This hypothesis was tested by conducting pharmacokinetics studies to examine both pafuramidine and furamidine, in a rat model of first-stage HAT.

Characterization of the experimental model of infection was conducted to ascertain that potential pharmacokinetic changes observed in infected animals were not a reflection of major organ damage due to the trypanosomal infection. Accordingly, determination of the time course of the parasitemia was conducted, as well as an evaluation of the histology and biochemical markers of the major eliminating organs liver and kidney. The characterization showed that inoculation with 10^4 cells induced an acute infection that had a single wave of parasitemia peaking at day five, followed by death at day six post-infection. The short course of the infection coupled with the single wave of parasitemia indicated that the S427 strain is highly virulent even when inoculated at a low density of parasites (10^4). This response mimics the short length of infection observed in humans during first-stage HAT and is in contrast to the response of infections with other *T.b. brucei* strains (i.e., AnTat 1.1E) that elicit multiple waves of parasitemia characteristic of second-stage HAT (6, 16, 38).

Despite the virulence, hematological tests at different days of infection showed no evidence of anemia or changes in hematocrit compared to control animals. These observations are in contrast to reports of decreased RBC counts in rat experimental models of trypanosomal infection and may be due to the short duration of the infection in this study (up

to 5 days) compared to studies in other laboratories where measurements were taken at 11-12 days post-infection (11). A significant decrease in WBC was apparent beginning on day 4 post-infection, consistent with reports of leucopenia in other infections due to migration of neutrophils and lymphocytes from the blood to the site of infection. Moderate elevation in ALT was observed at days 4 and 5 post-infection consistent with increased rate of hepatocyte turnover during inflammation in other types of infection (e.g., viral hepatitis) (14). Minor BUN elevations were observed at day 5 post-infection concurrent with inflammation at peak parasitemia. These biochemical changes were not commensurate with the histopathological results, where there were negligible to no effects on organ histology and hence function. Based on these results and the time-course of parasitemia, day four post-infection was selected for the conduct of the pharmacokinetic studies.

Pharmacokinetic dose-escalation studies showed a supra-proportional increase in exposure (AUC_{0-12}) at 25 μmol/kg, indicating saturation of pafuramidine metabolism considering that the predominant clearance mechanism is metabolic. The furamidine to pafuramidine AUC_{0-12} ratio remained relatively constant at ~0.5 for all three doses, suggesting decreased elimination of furamidine at the highest dose. Based on these results, experiments with infected and uninfected animals were carried out at both a sub-saturating and saturating dose of pafuramidine (7.5 and 25 μmol/kg, respectively). The dose for the intravenous administration was selected to match the lowest dose (1 mg/kg or 2.7 μmol/kg) given to rats by Midgley et al. (2007) and was given as an intravenous infusion because a bolus dose led to overt toxicity (24). This dose was likely to be saturating since pafuramidine concentrations approximated the concentrations observed following the 25 μmol/kg from dose escalation studies.

When pafuramidine was given intravenously as a 30 min infusion, no significant differences were observed in systemic exposure (AUC_{0-12}), or CL between the control and infected animals, as expected for a compound whose clearance approaches liver blood flow (44). Consistent with the definition of a compound with blood-flow limited clearance the extraction ratio (E) of pafuramidine was 0.75 (44). This value was obtained using the relationship $E = CL_H/Q$ where Q represents hepatic blood flow in the rat (3.3 L/h/kg) (7) and CL_H is the hepatic clearance of pafuramidine calculated according to the well-stirred model equation.

$$Cl_H = \frac{Q \bullet Cl_{int}}{Q + Cl_{int}}$$

In this equation, Cl_{int} is the total intrinsic clearance ($Cl_{int}=fu \bullet Cl_{int}$) equivalent to the Cl_{po} (11 L/h/kg) (35) from the linear oral dose 7.5 μmol/kg (Table 3.4). These calculations work under the assumption of complete absorption ($f_a=1$) of pafuramidine, which can be inferred from studies in Caco-2 cells that showed that the P_{app} value of pafuramidine is comparable to that of propanolol (32.2×10^{-6} cm/s and 30.8×10^{-6} cm/s, respectively) which was shown to have complete intestinal absorption (40, 46). Hence, because pafuramidine clearance is blood flow limited, a decreased metabolic capacity due to infection was unlikely to cause discernable changes in pafuramidine systemic exposure between control and infected animals following intravenous administration.

Results from oral administration studies showed significant differences in pafuramidine systemic exposure (AUC_{0-24}) between infected and control animals after the 25 μmol/kg dose, where a 1.3-fold higher exposure was observed in infected animals compared to uninfected controls. This difference was attributed to a decreased metabolic clearance in

infected animals induced by the infection. However, after the 7.5 μmol/kg oral dose no statistical meaningful differences were observed in the exposure of pafuramidine (AUC_{0-12}) between infected and uninfected controls animals. The discrepancy between oral doses stems from the fact that the clearance of pafuramidine is capacity limited where small changes in enzyme capacity may not be appreciated under linear conditions but can be more clearly discerned under saturating conditions. Mathematically this can be demonstrated *via* the Michaelis-Menten equation:

$$v = \frac{V_{max} \bullet S}{K_m + S}$$

Where v is velocity, V_{max} is the maximal velocity, S is the substrate concentration, and K_m is the substrate concentration at half the maximal velocity. When S is much less than K_m, v is dependent on $V_{max}/K_m \bullet S$ and it is assumed that the enzyme pool well exceeds the substrate concentration, whereas under saturating conditions ($S >> K_m$) v is dependent on V_{max}. Consistent with the interpretation above, M1 exposure (AUC_{0-12}) in infected animals following a saturating oral dose of pafuramidine was significantly lower ($p < 0.05$) compared to control, whereas M1 exposure between infected and control animals showed no significant difference following a sub-saturating oral dose of pafuramidine.

A reduced pafuramidine metabolic clearance was expected to reduce systemic levels of furamidine. Unexpectedly, an increase in furamidine exposure of as much as a 3-fold was observed in infected animals compared to controls irrespective of the route of administration. These results suggested that a mechanism involved in the hepatic disposition of furamidine is altered during infection. To date the hepatic disposition of furamidine has not been studied in detail. However, mass balance studies with radiolabeled pafuramidine show that various

mechanisms are involved in the hepatic disposition of furamidine including biliary elimination, organ sequestration, metabolic glucuronide conjugation, and basolateral export into systemic circulation. Among these mechanisms biliary elimination and organ sequestration accounted for the most important mechanisms of furamidine disposition (24). As a polar molecule, furamidine relies on drug transporters to enter and exit cells (25). Altered protein expression in one of these transporters was a potential explanation for the observed results. Recently, down-regulation of mRNA and protein expression of the biliary efflux transporters MRP2 and BSEP were shown to be mediated by the pro-inflammatory cytokines IL-6 and TNF-α in human hepatocytes (39), supporting the notion that infection could have an effect on the elimination of furamidine.

In situ bile duct cannulation experiments with control and infected animals showed that trypanosomal infection causes a significant decrease ($p < 0.05$) in the biliary excretion of furamidine (Figure 3.8) indicating that altered biliary excretion due to trypanosomal infection may in part explain the observed increased exposure of furamidine in infected animals. Previous studies have established that significant increases in plasma exposure can result from a reduction in biliary excretion. Studies with Mrp2-deficient rats showed that, compared to control, the major polar metabolites of troglitazone, troglitazone-sulfate (TRO-sulf) and troglitazone-glucuronide (TRO-gluc), were elevated in plasma by 2- and 50-fold, respectively (20). Moreover, it was demonstrated that compensatory up-regulation of basolateral transporters (i.e., Mrp3) occured during cholestatic conditions in response to diminished or abolished canalicular transporters such as Mrp2, indicating that enhanced basolateral excretion is possible under conditions of canalicular transport impairment (9, 10, 48).

Despite the observed changes in furamidine biliary excretion rate during the *in situ* bile cannulation experiments with infected animals, additional mechanisms may also contribute to the increase in plasma exposure of furamidine. Down-regulation of phase II enzymes including UGT1A4, UGT2B4 and UGT2B7 was observed in human liver tissues with extensive inflammation, suggesting that decreased conjugation of furamidine also could occur (5). Furamidine glucuronide conjugates were not detected in either control or infected animals in the *in situ* bile cannulation experiments (0-60 min) perhaps due to the short duration of the study. Another important component in furamidine disposition is hepatic accumulation. Following pafuramidine oral administration (10 mg/kg or 27 μmol/kg) to healthy rats, a 1300:1 furamidine liver to plasma ratio was observed 24 h post dose (24). These results were consistent with large amounts of furamidine detected 24 h pafuramidine post-dose (7.5 μmol/kg) in the livers of both infected and uninfected animals during the present investigation (data not shown). Hence, small perturbations in tissue binding may be expected to increase the unbound fraction of furamidine and have effects on the overall elimination of furamidine (24). To the authors' knowledge, no reports have demonstrated that infection could alter the tissue binding capacity of any chemical.

Results of the current work suggest that trypanosomal infection can alter the pharmacokinetics and disposition of the prodrug pafuramidine and active metabolite, furamidine. As hypothesized, trypanosomal infection decreased metabolic clearance of pafuramidine, resulting in significantly higher exposure compared to control. Despite the enhanced pafuramidine exposure in infected animals, the magnitude of change was modest and is unlikely to be of toxicological concern. Trypanosomal infection also increased the systemic exposure of the active furamidine, alleviating concerns of sub-therapeutic levels of

this active metabolite during infection. This work also highlights that during infection, changes in pharmacokinetics of high extraction compounds would be more readily recognized under saturating conditions and will likely be less discernible when drug concentrations are within the linear range.

F. FIGURES

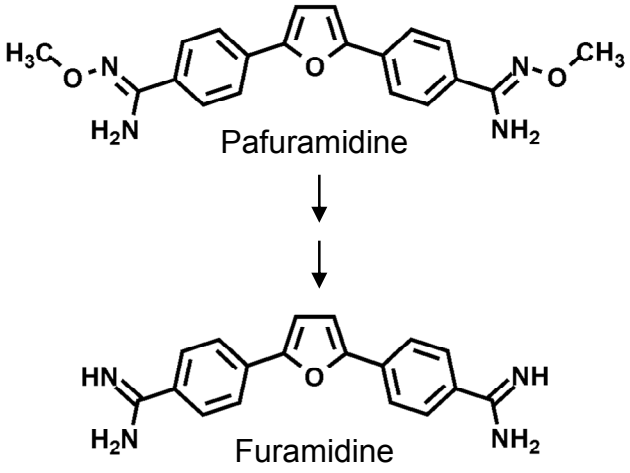

Figure 3.1 Chemical structures of prodrug and active diamidine.

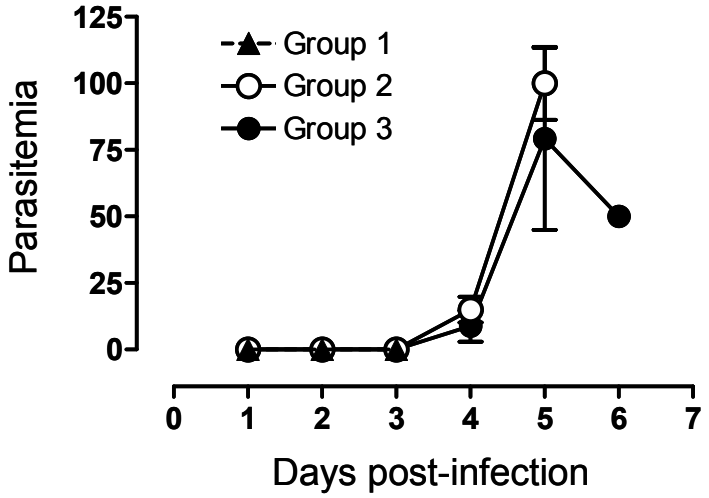

Figure 3.2 Time course of parasitemia in *T. b. brucei* infected Sprague-Dawley rats. Data represent mean parasitemia levels ± SD in rats infected with 4 x 10^4 *T. b. brucei* (S247) three days post infection, (▲) group 1 (n=6); five days post-infection (○) group 2 (n=6); and six days post-infection, (●) group 3 (n=6 except for the last time point n=2). Blood parasites were counted using a light microscope (objective X40).

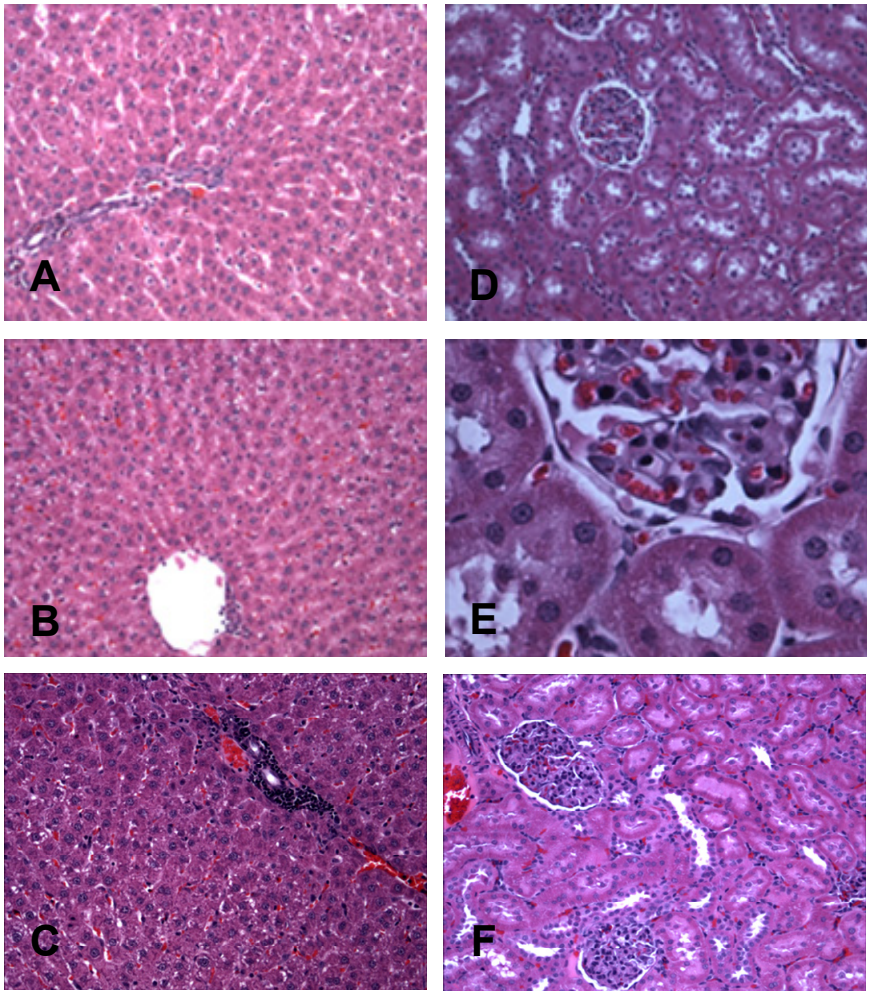

Figure 3.3 Representative histology slides of liver and kidney sections of *T. b. brucei* infected Sprague-Dawley rats and un-infected controls. (A) Liver section of a control rat. Typical architecture of the liver with parenchymal cell chords irradiating from the portal triad. H&E, objective X10. (B) Infected liver at day 3 post-infection (group 1). Parenchymal cells show normal architecture with chords irradiating from central vein. Presence of inflammatory cells is seen in the bottom right corner of the central vein opening. No areas of focal necrosis or tissue damage are observed. H&E, objective X10. (C) Infected liver at day 5 post-infection (group 2). Presence of inflammatory cells is evident around the portal triad with mild infiltration into the parenchymal tissue. H&E, objective X10. (D) Section of the renal cortex of a control rat. Glomerulus and proximal tubules show normal architecture. H&E, objective X10. (E) Infected kidney at day 3 post-infection (group 1). No changes are observed from control. H&E, objective X40. (F) Infected kidney at day 5 post-infection (group 2). Minimal presence of interstitial inflammation. H&E, objective X10.

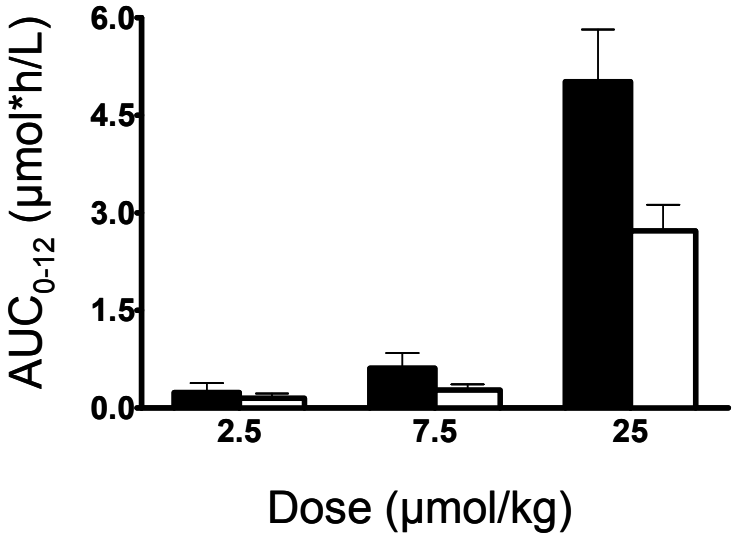

Figure 3.4 Relationship between pafuramidine and furamidine exposure (AUC_{0-12}) and dose in control and *T. b. brucei* infected Sprague-Dawley rats. Black bars (pafuramidine) and white bars (furamidine) represent the mean ± SD.

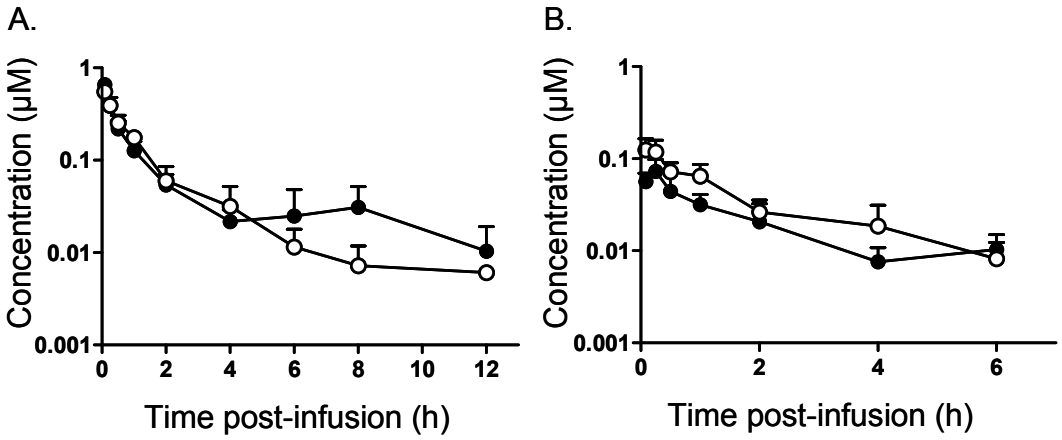

Figure 3.5 Pafuramidine (A) and furamidine (B) mean plasma concentration-time profiles in control (●) or *T. b. brucei* infected (○) Sprague-Dawley rats following a 1.45 µmol/kg intravenous infusion (30 min). The data represent mean ± SD of at least four animals.

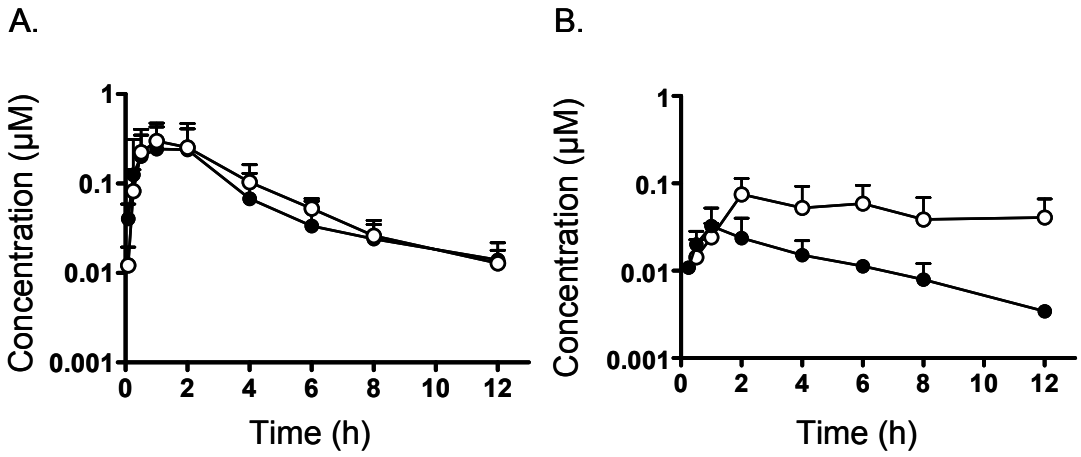

Figure 3.6 Pafuramidine (A) and furamidine (B) mean plasma concentration-time profiles in control (●) or *T. b. brucei* infected (○) Sprague-Dawley rats following oral administration of a 7.5 μmol/kg dose. The data represent mean ± SD of at least four animals.

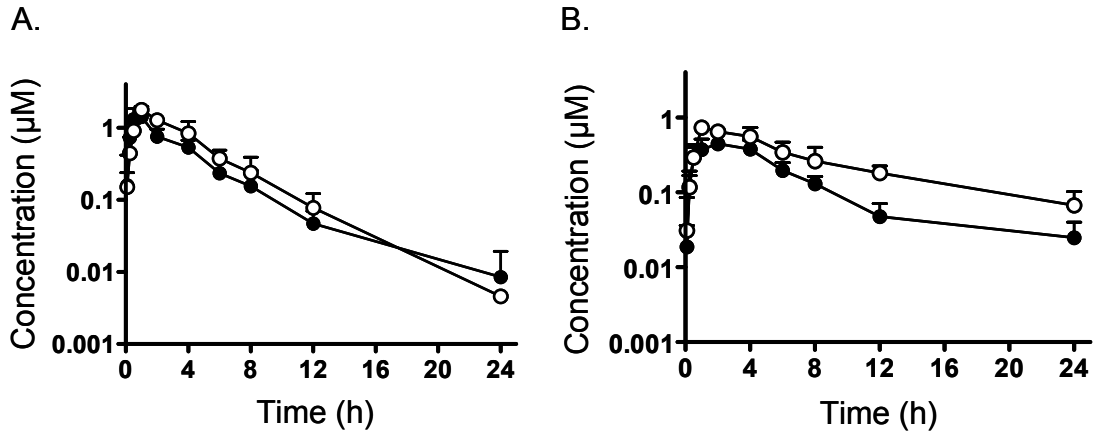

Figure 3.7 Pafuramidine (A) and furamidine (B) mean plasma concentration-time profiles in control (●) or *T. b. brucei* infected (○) Sprague-Dawley rats following oral administration of a 25 µmol/kg dose. The data represent mean ± SD of at least five animals.

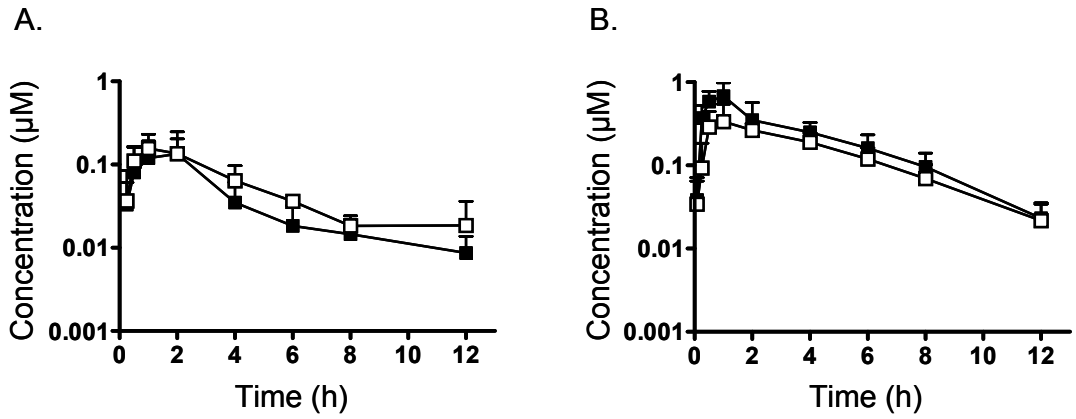

Figure 3.8 Mean M1 plasma concentration-time profiles in control (■) or *T. b. brucei* infected (□) Sprague-Dawley rats following oral administration of a 7.5 µmol/kg (A) or a 25 µmol/kg (B) pafuramidine dose. The data represent mean ± SD of at least four animals.

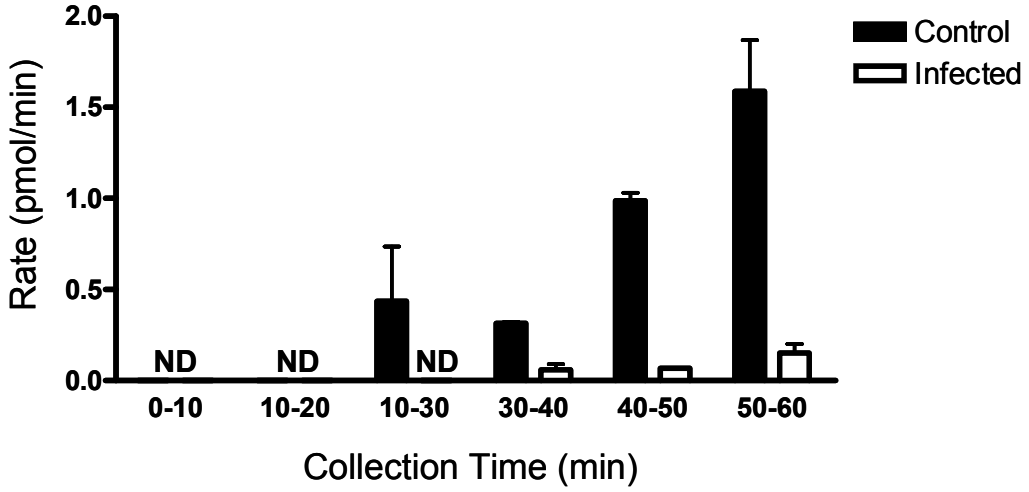

Figure 3.9 Biliary excretion rates of furamidine in control and infected Sprague-Dawley rats following intraduodenal administration of 7.5 μmol/kg pafuramidine. Bars represent the mean excretion rate ± SD of n=3 rats at each collection interval (with the exception of 40-50 n=2). Significantly lower biliary excretion rates were seen in infected rats compared to controls $p < 0.01$. ND. Not detected.

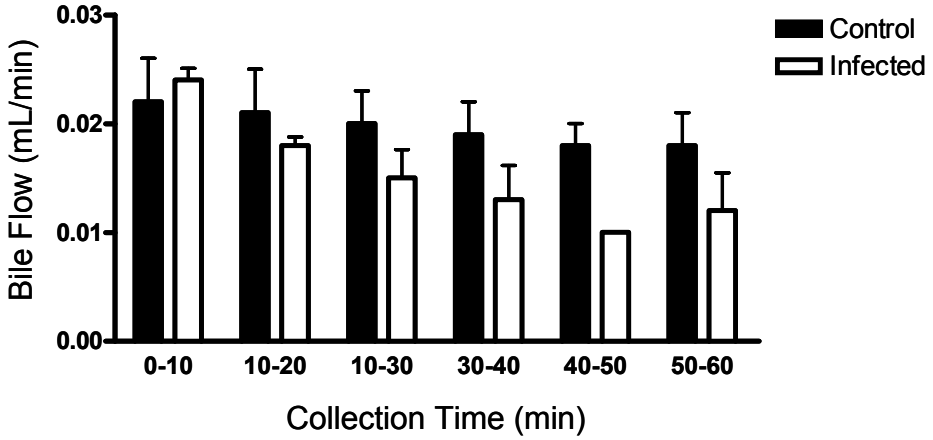

Figure 3.10 Bile flow in control and infected Sprague-Dawley rats. Bars represent the mean bile flow ± SD of n=3 rats at each collection interval (with the exception of 40-50 n=2).

G. TABLES

Table 3.1 Summary of hematological and biochemical marker values of liver and kidney function in control and *T. b. brucei* infected Sprague-Dawley rats (group1).

Marker (unit)	Day of Infection			
	Control[a]	Day 1[b]	Day 2[b]	Day 3[b]
White Blood Cells ($10^3/\mu L$)	11.3 (2.5)	11.1 (2.6)	10.7 (2.1)	6.2 (2.4)**
Red Blood Cells ($10^6/\mu L$)	6.6 (0.4)	6.8 (0.6)	6.8 (0.4)	6.2 (1.5)
Hematocrit (%)	36.0 (2.2)	36.7 (2.3)	36.2 (1.5)	33.6 (7.7)
Alanine Aminotransferase (IU/L)	39.9 (7.2)	56.3 (25.6)	51.7 (26.9)	42.2 (12.6)
Total Bilirubin (mg/dL)	<0.1 (ND)	0.3 (0.2)	0.2 (0.0)	0.5 (0.6)
Total Protein (g/dL)	5.4 (0.5)	5.6 (0.7)	5.6 (0.7)	5.6 (0.8)
Blood Urea Nitrogen (mg/dL)	13.8 (1.6)	16.2 (3.1)	14.8 (3.0)	14.2 (3.7)
Serum Creatinine (mg/dL)	0.3 (0.1)	0.3 (0.2)	0.3 (0.1)	0.3 (0.1)

a. Data represent mean of n=12 animals (±SD).
b. Data represent mean of n=6 animals (±SD).
ND: Not determined (the values of ten out of 12 rats were <0.1).
** Significant at $p < 0.01$.

Table 3.2 Summary of hematological and biochemical marker values of liver and kidney function in control and *T. b. brucei* infected Sprague-Dawley rats (group 2).

	Day of Infection					
Marker (unit)	Control[a]	Day 1[b]	Day 2[b]	Day 3[b]	Day 4[b]	Day 5[b]
White Blood Cells (10^3/uL)	11.3 (2.5)	16.4(7.8)	18.4 (9.4)*	7.9 (2.6)	7.1 (1.7)	3.4 (2.3)*
Red Blood Cells (10^6/uL)	6.6 (0.4)	6.6 (0.2)	6.9 (0.3)	6.6 (1.3)	6.6 (0.6)	6.1 (0.8)
Hematocrit (%)	36.0 (2.2)	35.7 (1.1)	37.7 (1.6)	36.4 (7.1)	35.6 (2.6)	33.0 (4.1)
Alanine Aminotransferase (IU/L)	39.9 (7.2)	49.0 (10.7)	42.3 (10.7)	47.7 (16.8)	144.7 (54.4)*	358 (178)**
Total Bilirubin (mg/dL)	<0.1 (ND)	<0.1 (ND)	0.2 (0.0)	0.6 (0.7)	0.4 (0.4)	0.2 (0.1)
Total Protein (g/dL)	5.4 (0.5)	5.5 (0.9)	6.6 (3.5)	5.8 (0.9)	5.6 (0.7)	5.9 (0.7)
Blood Urea Nitrogen (mg/dL)	13.8 (1.6)	14.8 (2.3)	13.5 (1.6)	12.5 (1.9)	17.2 (2.9)	20.4 (5.4)**
Serum Creatinine (mg/dL)	0.3 (0.1)	0.4 (0.1)	0.3 (0.1)	0.3 (0.1)	0.2 (0.0)	0.3 (0.1)

a. Data represent mean of n=12 animals (±SD).
b. Data represent mean of n=6 animals (±SD).
ND: Not determined (the values of ten out of 12 rats were <0.1).
* Significant at $p < 0.05$.
** Significant at $p < 0.01$.

Table 3.3 Pharmacokinetic parameters of pafuramidine and furamidine after intravenous administration of 1.45 µmol/kg pafuramidine to control and infected rats

	Control[a]	Infected[a]
Pafuramidine		
AUC_{0-12} (µmol*h/L)	0.65 (17)	0.58 (23)
$AUC_{0-\infty}$ (µmol*h/L)	0.74 (13)	0.59 (24)
V_{ss} (L/kg)	8.11 (50)	3.85 (18)*
CL (L/h/kg)	1.95 (12)	2.45 (22)
$t_{½}$ (h)	4.67 (59)	1.80 (36)*
Furamidine		
C_{max} (µmol/L) [median (range)]	0.08 (0.06-0.11)	0.13 (0.10-0.20)**
T_{max} (h) [median (range)]	0.25 (0.08-0.5)	0.25 (0.08-1)
AUC_{0-6}(µmol*h/L)	0.12 (23)	0.19 (23)**
$AUC_{0-\infty}$ (µmol*h/L)	0.17 (40)	ND
V_{ss} (L/kg)	N/A	N/A
CL (L/h/kg)	N/A	N/A
$t_{½}$ (h)	4.07 (66)	1.78 (8.2)**

a. Data represents the geometric mean and CV% of n=6 unless otherwise indicated.
ND: Not determined. Estimated parameter did not meet acceptance criterion (extrapolated area >25%).
N/A: Not applicable
* Significant at $p < 0.05$.
** Significant at $p < 0.01$.

Table 3.4 Pharmacokinetic parameters of pafuramidine, M1 and furamidine after oral administration of 7.5 and 25 µmol/kg pafuramidine to control and infected rats

	Control[a]	Infected[a]
Pafuramidine		
Dose (µmol/kg)	7.5	7.5
C_{max} (µmol/L) [median (range)]	0.24 (0.09 - 0.5)	0.33 (0.13 - 0.62)
T_{max} (h) [median (range)]	1 (0.5 - 2)	1 (0.5 - 2)
AUC_{0-12} (µmol*h/L)	0.58 (88)	1.00 (42)
$AUC_{0-\infty}$ (µmol*h/L)	0.67 (82)	1.09 (37)
CL_{po} (L/h/kg)	11 (90)	6.9 (45)
$t_{½}$ (h)	3.9 (87)	2.4 (44)
M1		
C_{max} (µmol/L) [median (range)]	0.17 (0.03 - 0.27)	0.19 (0.076-0.26)
T_{max} (h) [median (range)]	2 (1 – 4)	1 (0.5 – 2)
AUC_{0-12} (µmol*h/L)	0.37 (71)	0.63 (26)
$AUC_{0-\infty}$ (µmol*h/L)	0.45 (64)	0.75 (16)
$t_{½}$ (h)	2.8 (40)	3.2 (69)
Furamidine		
C_{max} (µmol/L) [median (range)]	0.03 (0.01 - 0.05)	0.08 (0.05 -0.15)
T_{max} (h) [median (range)]	1 (0.5 -1)	2 (2 -12)
AUC_{0-12} (µmol*h/L)	0.15[b]	0.47 (53)
$AUC_{0-\infty}$ (µmol*h/L)	0.17[b]	ND
$t_{½}$ (h)	3.7[b]	8.8 (80)
Pafuramidine		
Dose (µmol/kg)	25	25
C_{max} (µmol/L) [median (range)]	1.88 (1.00 - 2.07)	1.72 (1.5 - 2.2)
T_{max} (h) [median (range)]	1 (0.5-1)	1(1-1)
AUC_{0-24}(µmol*h/L)	5.49 (9)	7.41 (16)**
$AUC_{0-\infty}$ (µmol*h/L)	5.55 (8.1)	7.43 (15)**
CL_{po} (L/h/kg)	4.50 (7.4)	3.37(14)
$t_{½}$ (h)	3.3 (41)	2.8 (13)
M1		
C_{max} (µmol/L) [median (range)]	0.78 (0.55-0.97)	0.31 (0.29-0.76)
T_{max} (h) [median (range)]	1 (0.5-1)	1 (0.5-2)
AUC_{0-12} (µmol*h/L)	2.40 (21)	1.64 (10)**
$AUC_{0-\infty}$ (µmol*h/L)	2.54 (22)	1.74 (15)*
$t_{½}$ (h)	2.4 (34)	2.6 (57)
Furamidine		
C_{max} (µmol/L) [median (range)]	0.57 (0.33-0.77)	0.72 (0.62 - 1.0)
T_{max} (h) [median (range)]	2 (1 - 4)	1 (1 - 4)
AUC_{0-24}(µmol*h/L)	3.13 (15)	6.01 (19)***
$AUC_{0-\infty}$ (µmol*h/L)	3.28 (14)	6.76 (19)***
$t_{½}$ (h)	5.3 (25)	7.3 (34)

a. Data represents the geometric mean and CV% of at least six animals unless otherwise indicated.
b. Data was obtained from mean analysis of n=4. At 12 h the data of only two rats was above the lower limit of quantification.
ND: Estimated parameter did not meet acceptance criteria (extrapolated area >25%).
* $p<0.05$, ** $p<0.01$, *** $p<0.001$

H. ACKNOWLEDGEMENTS

The authors would like to thank the pathologists Dr. Tara Rubinas and Dr. Dan Kleven for their guidance interpreting the histological samples.

I. FOOTNOTES

a. This investigation was supported by a grant from the Consortium of Parasitic Drug Development (CPDD).

b. This investigation was originally presented at the American Association of Pharmaceutical Sciences (AAPS) meeting. Los Angeles, CA (2009).

c. Reprint requests: Dhiren R. Thakker, Ph.D.

100F Beard Hall, CB #7355

UNC Eshelman School of Pharmacy

University of North Carolina Chapel Hill, NC 27599-7569

Telephone: (919) 962-0092

FAX: 919-966-6919

E-mail: dhiren_thakker@unc.edu

J. REFERENCES

1. **Abdel-Razzak, Z., P. Loyer, A. Fautrel, J. C. Gautier, L. Corcos, B. Turlin, P. Beaune, and A. Guillouzo.** 1993. Cytokines down-regulate expression of major cytochrome P-450 enzymes in adult human hepatocytes in primary culture. Mol Pharmacol **44:**715.

2. **Abdulla, D., K. B. Goralski, and K. W. Renton.** 2006. The regulation of cytochrome P450 2E1 during LPS-induced inflammation in the rat. Toxicol Appl Pharmacol **216:**1-10.

3. **Barrett, M. P., D. W. Boykin, R. Brun, and R. R. Tidwell.** 2007. Human African trypanosomiasis: pharmacological re-engagement with a neglected disease. Br J Pharmacol **152:**1155-71.

4. **Chen, J. Q., A. Strom, J. A. Gustafsson, and E. T. Morgan.** 1995. Suppression of the constitutive expression of cytochrome P-450 2C11 by cytokines and interferons in primary cultures of rat hepatocytes: comparison with induction of acute-phase genes and demonstration that CYP2C11 promoter sequences are involved in the suppressive response to interleukins 1 and 6. Mol Pharmacol **47:**940-7.

5. **Congiu, M., M. L. Mashford, J. L. Slavin, and P. V. Desmond.** 2002. UDP glucuronosyltransferase mRNA levels in human liver disease. Drug Metab Dispos **30:**129-34.

6. **Darsaud, A., L. Bourdon, C. Chevrier, M. Keita, B. Bouteille, A. Queyroy, F. Canini, R. Cespuglio, M. Dumas, and A. Buguet.** 2003. Clinical Follow-Up in the Rat Experimental Model of African-Trypanosomiasis. Experimental Biology and Medicine **228:**1362.

7. **Davies, B., and T. Morris.** 1993. Physiological Parameters in Laboratory Animals and Humans. Pharmaceutical Research **10:**1095.

8. **De-Oliveira, A. C., R. S. Carvalho, F. H. Paixao, H. S. Tavares, L. S. Gueiros, C. M. Siqueira, and F. J. Paumgartten.** 2010. Up- and down-modulation of liver cytochrome P450 activities and associated events in two murine malaria models. Malar J **9:**81.

9. **Donner, M. G., and D. Keppler.** 2001. Up-regulation of basolateral multidrug resistance protein 3 (Mrp3) in cholestatic rat liver. Hepatology **34:**351-9.

10. **Donner, M. G., U. Warskulat, N. Saha, and D. Haussinger.** 2004. Enhanced expression of basolateral multidrug resistance protein isoforms Mrp3 and Mrp5 in rat liver by LPS. Biol Chem **385:**331-9.

11. **Ekanem, J., and O. Yusuf.** 2008. Some biochemical and haematological effects of black seed (Nigella sativa) oil on Trypanosoma brucei-infected rats. African Journal of Biotechnology **7:**157.

12. **Ferrari, L., J. Y. Jouzeau, P. Gillet, R. Herber, P. Fener, A. M. Batt, and P. Netter.** 1993. Interleukin-1 beta differentially represses drug-metabolizing enzymes in arthritic female rats. J Pharmacol Exp Ther **264:**1012-20.

13. **Geier, A., C. G. Dietrich, S. Voigt, M. Ananthanarayanan, F. Lammert, A. Schmitz, M. Trauner, H. E. Wasmuth, D. Boraschi, N. Balasubramaniyan, F. J. Suchy, S. Matern, and C. Gartung.** 2005. Cytokine-dependent regulation of hepatic organic anion transporter gene transactivators in mouse liver. Am J Physiol Gastrointest Liver Physiol **289:**G831-41.

14. **Getachew, Y., L. James, W. M. Lee, D. L. Thiele, and B. C. Miller.** Susceptibility to acetaminophen (APAP) toxicity unexpectedly is decreased during acute viral hepatitis in mice. Biochem Pharmacol **79:**1363-71.

15. **Gharavi, N., and A. O. El-Kadi.** 2007. Role of nitric oxide in downregulation of cytochrome P450 1a1 and NADPH: Quinone oxidoreductase 1 by tumor necrosis factor-alpha and lipopolysaccharide. J Pharm Sci **96:**2795-807.

16. **Giroud, C., F. Ottones, V. Coustou, D. Dacheux, N. Biteau, B. Miezan, N. Van Reet, M. Carrington, F. Doua, and T. o. Baltz.** 2009. Murine Models for *Trypanosoma brucei gambiense* Disease Progressionâ€"From Silent to Chronic Infections and Early Brain Tropism. PLoS Negl Trop Dis **3:**e509.

17. **Hirumi, H., and K. Hirumi.** 1989. Continuous Cultivation of Trypanosoma brucei Blood Stream Forms in a Medium Containing a Low Concentration of Serum Protein without Feeder Cell Layers. The Journal of Parasitology **75:**985.

18. **Ismail, M. A., R. Brun, J. D. Easterbrook, F. A. Tanious, W. D. Wilson, and D. W. Boykin.** 2003. Synthesis and antiprotozoal activity of aza-analogues of furamidine. J Med Chem **46:**4761-9.

19. **Kim, M. S., J. Shigenaga, A. Moser, C. Grunfeld, and K. R. Feingold.** 2004. Suppression of DHEA sulfotransferase (Sult2A1) during the acute-phase response. Am J Physiol Endocrinol Metab **287:**E731-8.

20. **Kostrubsky, V. E., M. Vore, E. Kindt, J. Burliegh, K. Rogers, G. Peter, D. Altrogge, and M. W. Sinz.** 2001. The effect of troglitazone biliary excretion on metabolite distribution and cholestasis in transporter-deficient rats. Drug Metab Dispos **29:**1561-6.

21. **Kraemer, M. J., C. T. Furukawa, J. R. Koup, G. G. Shapiro, W. E. Pierson, and C. W. Bierman.** 1982. Altered theophylline clearance during an influenza B outbreak. Pediatrics **69:**476-80.

22. **Lee, I. K., Y. M. Lee, I. S. Song, S. J. Chung, S. G. Kim, M. G. Lee, and C. K. Shim.** 2002. Hepatobiliary excretion of tributylmethylamonium in rats with lipopolysaccharide-induced acute inflammation. Arch Pharm Res **25:**969-72.

23. **Mayo, P. R., K. Skeith, A. S. Russell, and F. Jamali.** 2000. Decreased dromotropic response to verapamil despite pronounced increased drug concentration in rheumatoid arthritis. Br J Clin Pharmacol **50:**605-13.

24. **Midgley, I., K. Fitzpatrick, L. M. Taylor, T. L. Houchen, S. J. Henderson, S. J. Wright, Z. R. Cybulski, B. A. John, A. McBurney, D. W. Boykin, and K. L. Trendler.** 2007. Pharmacokinetics and metabolism of the prodrug DB289 (2,5-bis[4-(N-methoxyamidino)phenyl]furan monomaleate) in rat and monkey and its conversion to the antiprotozoal/antifungal drug DB75 (2,5-bis(4-guanylphenyl)furan dihydrochloride). Drug Metab Dispos **35:**955-67.

25. **Ming, X., W. Ju, H. Wu, R. R. Tidwell, J. E. Hall, and D. R. Thakker.** 2009. Transport of dicationic drugs pentamidine and furamidine by human organic cation transporters. Drug Metab Dispos **37:**424-30.

26. **Montero, R., L. Serrano, V. M. Davila, A. Ito, and A. Plancarte.** 2003. Infection of rats with Taenia taeniformis metacestodes increases hepatic CYP450, induces the activity of CYP1A1, CYP2B1 and COH isoforms and increases the genotoxicity of the procarcinogens benzo[a]pyrene, cyclophosphamide and aflatoxin B(1). Mutagenesis **18:**211-6.

27. **Piquette-Miller, M., and F. Jamali.** 1995. Influence of severity of inflammation on the disposition kinetics of propranolol enantiomers in ketoprofen-treated and untreated adjuvant arthritis. Drug Metab Dispos **23:**240-5.

28. **Pohlig G, B. S., Blum J, Burri C, Kabeya AM, Lubaki J-P F, Mpoto AM, Munungu BF, Deo GKM, Mutantu PN, Kuikumbi FM, Mintwo AF, Munungi AK, Dala A, Macharia S, Bilenge CMM, MesuVKBK, J Franco JR, Dituvanga ND, Olson CA.** 2008. Phase 3 trial of pafuramidine maleate (DB289), a novel, oral drug, for treatment of first stage sleeping sickness: safety and efficacy. 57th American Society for Tropical Medicine and Hygiene. New Orleans, LA.

29. **Pukrittayakamee, S., S. Looareesuwan, D. Keeratithakul, T. M. Davis, P. Teja-Isavadharm, B. Nagachinta, A. Weber, A. L. Smith, D. Kyle, and N. J. White.** 1997. A study of the factors affecting the metabolic clearance of quinine in malaria. Eur J Clin Pharmacol **52:**487-93.

30. **Raaska, K., V. Raitasuo, M. Arstila, and P. J. Neuvonen.** 2002. Bacterial pneumonia can increase serum concentration of clozapine. Eur J Clin Pharmacol **58:**321-2.

31. **Renton, K. W.** 2005. Regulation of drug metabolism and disposition during inflammation and infection. Expert Opin Drug Metab Toxicol **1:**629-40.

32. **Richardson, T. A., and E. T. Morgan.** 2005. Hepatic cytochrome P450 gene regulation during endotoxin-induced inflammation in nuclear receptor knockout mice. J Pharmacol Exp Ther **314:**703-9.

33. **Rockich, K., and R. Blouin.** 1999. Effect of the acute-phase response on the pharmacokinetics of chlorzoxazone and cytochrome P-450 2E1 in vitro activity in rats. Drug Metab Dispos **27:**1074-7.

34. **Saulter, J., J. Kurian, L. Trepanier, R. Tidwell, A. Bridges, D. Boykin, C. Stephens, M. Anbazhagan, and J. E. Hall.** 2005. Unusual Dehydroxylation of Antimicrobial Amidoxime Prodrugs by Cytochrome b5 and NADH Cytochrome b5 Reductase. Drug Metab Dispos **33:**1886-93.

35. **Shand, D. G., D. M. Kornhauser, and G. R. Wilkinson.** 1975. Effects of route of administration and blood flow on hepatic drug elimination. J Pharmacol Exp Ther **195:**424-32.

36. **Shedlofsky, S. I., B. C. Israel, R. Tosheva, and R. A. Blouin.** 1997. Endotoxin depresses hepatic cytochrome P450-mediated drug metabolism in women. Br J Clin Pharmacol **43:**627-32.

37. **Sonne, J., M. Dossing, S. Loft, and P. B. Andreasen.** 1985. Antipyrine clearance in pneumonia. Clin Pharmacol Ther **37:**701-4.

38. **Sternberg, J. M.** 2004. Human African trypanosomiasis: clinical presentation and immune response. Parasite Immunology **26:**476.

39. **Vee, M. L., V. Lecureur, B. Stieger, and O. Fardel.** 2009. Regulation of drug transporter expression in human hepatocytes exposed to the proinflammatory cytokines tumor necrosis factor-alpha or interleukin-6. Drug Metab Dispos **37:**685-93.

40. **Volpe, D., P. Faustino, A. Ciavarella, E. Asafu-Adjaye, C. Ellison, L. Yu, and A. Hussain.** 2007. Classification of Drug Permeability with a Caco-2 Cell Monolayer Assay. Clinical Research and Regulatory Affairs **24:**47.

41. **Wang, M. Z., J. Y. Saulter, E. Usuki, Y. L. Cheung, M. Hall, A. S. Bridges, G. Loewen, O. T. Parkinson, C. E. Stephens, J. L. Allen, D. C. Zeldin, D. W. Boykin, R. R. Tidwell, A. Parkinson, M. F. Paine, and J. E. Hall.** 2006. CYP4F enzymes are the major enzymes in human liver microsomes that catalyze the O-demethylation of the antiparasitic prodrug DB289 [2,5-bis(4-amidinophenyl)furan-bis-O-methylamidoxime]. Drug Metab Dispos **34:**1985-94.

42. **Wang, M. Z., J. Q. Wu, A. S. Bridges, D. C. Zeldin, S. Kornbluth, R. R. Tidwell, J. E. Hall, and M. F. Paine.** 2007. Human enteric microsomal CYP4F enzymes O-demethylate the antiparasitic prodrug pafuramidine. Drug Metab Dispos **35:**2067-75.

43. **Wenzler, T., D. W. Boykin, M. A. Ismail, J. E. Hall, R. R. Tidwell, and R. Brun.** 2009. New treatment option for second-stage African sleeping sickness: in vitro and in vivo efficacy of aza analogs of DB289. Antimicrob Agents Chemother **53:**4185-92.

44. **Wilkinson, G. R.** 1987. Clearance approaches in pharmacology. Pharmacol Rev **39:**1-47.

45. **Winstanley, P. A., D. J. Back, and A. M. Breckenridge.** 1987. Inhibition of theophylline metabolism by interferon. Lancet **2:**1340.

46. **Zhou, L., K. Lee, D. R. Thakker, D. W. Boykin, R. R. Tidwell, and J. E. Hall.** 2002. Enhanced permeability of the antimicrobial agent 2,5-bis(4-amidinophenyl)furan across Caco-2 cell monolayers via its methylamidoidme prodrug. Pharm Res **19:**1689-95.

47. **Zhou, L., D. R. Thakker, R. D. Voyksner, M. Anbazhagan, D. W. Boykin, J. E. Hall, and R. R. Tidwell.** 2004. Metabolites of an orally active antimicrobial prodrug, 2,5-bis(4-amidinophenyl)furan-bis-O-methylamidoxime, identified by liquid chromatography/tandem mass spectrometry. J Mass Spectrom **39:**351-60.

48. **Zollner, G., P. Fickert, A. Fuchsbichler, D. Silbert, M. Wagner, S. Arbeiter, F. J. Gonzalez, H. U. Marschall, K. Zatloukal, H. Denk, and M. Trauner.** 2003. Role of nuclear bile acid receptor, FXR, in adaptive ABC transporter regulation by cholic and ursodeoxycholic acid in mouse liver, kidney and intestine. J Hepatol **39:**480-8.

CHAPTER 4

A SEMI-PHYSIOLOGIC PHARMACOKINETIC MODEL PREDICTS THE EFFECTS OF DECREASED ENZYME CAPACITY ON DRUG EXPOSURE

A. INTRODUCTION

Pharmacokinetic studies described in this dissertation (Chapter 3) showed that dose and route of administration were important factors to discern the effects of decreased enzyme capacity triggered by infection, resulting in altered pharmacokinetics. The observations conformed to the concepts of the well-stirred model of hepatic clearance (Shand et al., 1975). With these concepts, predictions of the effects of decreased enzyme capacity, due to infection or inflammation, on systemic exposure were generated by simulating different scenarios where doses in the linear and saturating range of metabolism were administered orally or intravenously. Predictions from simulations representing impaired metabolism were compared to simulations representing baseline metabolic capacity. Results supported our experimental observations, where the maximum change in magnitude of exposure occurred when a compound was given orally and the dose given saturated metabolism.

B. METHODS

A semi-physiologic pharmacokinetic model was developed according to methods described by Kanamitsu et al. with modifications (Kanamitsu et al., 2000). For simulations of intravenous administration, the model included three compartments representing the portal vein, liver and blood (Figure 4.1). For simulations of oral administration the same model was used with the exception that the gut lumen compartment was added (Figure 4.2). The rat physiologic parameters used were obtained from available literature and are listed in Table 4.1, and the pharmacokinetic parameters are listed in Table 4.2. Drug doses were selected to represent drugs with high hepatic extraction ($E > 0.7$) or low hepatic extraction ($E < 0.3$), where extraction (E) represents the ratio of hepatic clearance to blood flow (Shand et al.,

1975). The value of liver blood flow (Q) used to calculate hepatic clearance was 20 mL/min (Houston and Carlile, 1997). High and low intrinsic clearance (Cl_{int}) values were according to the ranges defined by Houston (1997), where a high extraction drug Cl_{int} ranged from 50-10000 mL/min, and a low extraction drug Cl_{int} ranged from 0.1-10 mL/min, normalized to the standard weight of a rat (0.25 kg) (Houston and Carlile, 1997). Values for V_{max} and K_m were selected to generate either high or low Cl_{int} values (Table 4.2). Since the model included a liver compartment, a temporal description of the drug concentration in this compartment was incorporated. Metabolic saturation was defined when concentrations in the liver reached values above the set K_m. The following assumptions were made: 1) absorption was a first-order process, 2) hepatic metabolism was the sole means of systemic clearance, 3) metabolism was governed by Michaelis-Menten kinetics, 4) drug partitions to blood and tissue equally (K_p =1), and 5) plasma protein binding was negligible (f_u=1). Simulations were performed using the software Berkeley Madonna v8.3.18 (University of California at Berkeley, Berkely, CA).

C. RESULTS

Simulations suggested that the most drastic changes in systemic exposure will occur when a high extraction drug is administered orally at concentrations that saturate metabolic clearance. Modest changes are expected to occur for drugs that are high or low extraction, and are dosed orally, with resulting systemic concentrations that do not saturate metabolism. Minimal changes are expected to occur in most scenarios when drugs are administered intravenously. Results for all simulations are presented in Tables 4.3 and 4.4, and a scheme summarizing all possible scenarios is presented in Figure 4.3.

D. DISCUSSION

It has been widely recognized that infectious disease and inflammation elicits down-regulation of DMEs, resulting in decreased protein expression or decreased enzyme capacity. The consequences of DME down-regulation have clinical implications and were recently reported to affect drug development. In the clinic down-regulation of DMEs is often manifested as decreased drug clearance/increased exposure of drugs with the potential of causing untoward side effects or toxicity (Kraemer et al., 1982; de Leon and Diaz, 2003). In drug development down-regulation of DMEs has been reported as a source of increased pharmacokinetic variability (Schmith and Foss, 2010). Despite the significant progress that has been made to understand the molecular mechanisms of DME down-regulation, to date there is not a strategy to predict the changes that this phenomenon will have on drug pharmacokinetics. Based on results obtained from pharmacokinetic studies described in this dissertation work and pharmacokinetic concepts of the well-stirred model of hepatic clearance, predictions of relative changes in systemic drug exposure were generated by simulating different scenarios of dose and route of drug administration. Simulations were focused on predicting changes in systemic exposure as opposed to systemic clearance, since systemic exposure is most often associated with driving pharmacological drug action or side effects. Predictions of systemic drug exposure in a system where enzyme capacity was decreased by 25% were compared to predictions from a system working at baseline enzyme capacity. A 25% decrease in enzyme capacity was selected as a conservative estimate of DME down-regulation during inflammation or infection; however, studies have shown that decreased CYP protein expression induced by different infectious stimuli could range from 20-90% (Table 1.1). Thus the exposure changes obtained from these predictions potentially

underestimate the degree of exposure change that may occur in cases of greater enzyme down-regulation.

Model predictions showed that the largest changes in systemic exposure (2.3-fold) are expected when a high extraction drug is administered orally at a dose that saturates metabolic clearance. These results were consistent with the experimental observations described in Chapter 3, where significant increases in pafuramidine (a high extraction drug) exposure was observed in infected animals compared to uninfected controls when this agent was administered at an oral dose that saturated metabolism. To the authors' knowledge there are no examples in the literature describing similar observations, potentially due to the large number of low extraction or metabolically stable drugs, which often have favorable pharmacokinetic properties as therapies for oral administration.

Model predictions for high or low extraction drugs given orally at sub-saturating doses of metabolism showed modest changes in systemic drug exposure, consistent with exposure changes reported in the literature. For example, a modest elevation in systemic exposure (1.3-fold) was reported for the low extraction drug quinine when it was administered to patients with chronic liver disease at a dose that achieved systemic concentrations that did not saturate metabolism (C_{max} =10 μM; K_m=105 μM) (Auprayoon et al., 1995; Zhao and Ishizaki, 1997). Although systemic exposure values were not reported, three independent studies showed modest transient elevations in the steady-state concentration of clozapine (2- to 3-fold) in patients temporarily afflicted with infectious disease. In the case of pafuramidine, there was a trend for increased systemic exposure in infected animals compared to controls when the drug was dosed at sub-saturating concentrations; however, the increase was not statistically significant.

Model predictions showed minimal changes in systemic exposure for either low or high extraction drugs that were dosed intravenously, suggesting that in most cases down-regulation of DMEs will not have effects on the exposure of drugs whose dose regimen is *via* intravenous injection. The simulations were consistent with experimental observations for pafuramidine when it was dosed intravenously, where no changes in systemic exposure were observed in infected animals compared to controls.

The implications of altered systemic exposure of drugs need to be made in the context of therapeutic index. For example, even in cases in which large systemic exposure changes are expected, if the therapeutic index of a drug is large the clinical implications of the changes will be negligible. Conversely, in cases where small or modest changes in systemic exposure are expected, untoward effects may be experienced in the case of a narrow therapeutic index drug, thus making the modest changes predicted by these simulations for low extraction drugs potentially important. This was exemplified by two clinical examples involving theophylline and clozapine, both low extraction compounds, where decreased metabolism due to infectious disease resulted in moderate to severe toxicity, despite exhibiting only modest changes (2- to 3-fold) in steady-state concentrations.

Simulations conducted to predict the effect of decreased enzyme capacity on drug systemic exposure supported experimental observations described in this dissertation (Chapter 3). Predictions show that minimal effects on pharmacokinetics will be observed when drugs are given intravenously, regardless of whether the drug is high or low extraction. Modest to significant changes will be observed when a drug is dosed orally, with the most significant effects on drugs that are high extraction and are given at doses that saturate metabolism. Taken together, this analysis shows that, impaired drug metabolism due to

decreased enzyme capacity (25%) modestly affects drug exposure (maximum observed change 2.3-fold). These results may explain why there are few examples of altered pharmacokinetics of drugs in the clinic taking into consideration the promiscuity of infection and inflammation in human disease.

E. FIGURES

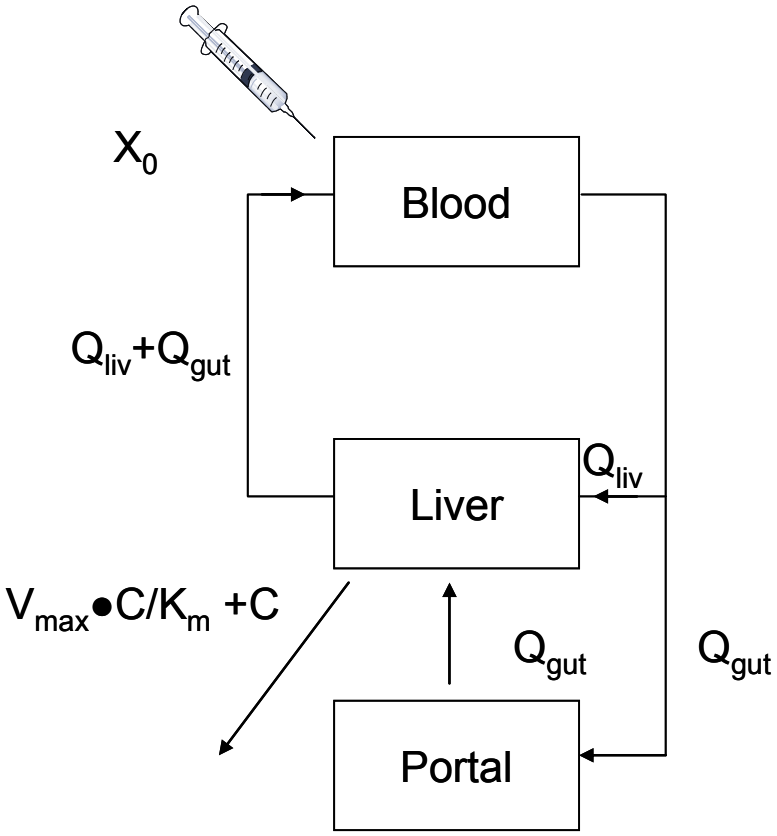

Figure 4.1 Model used for simulations of intravenous administration of drug. X_0 represents dose, Q represents blood flow, V_{max} represents the maximum velocity and K_m represents the half maximum velocity.

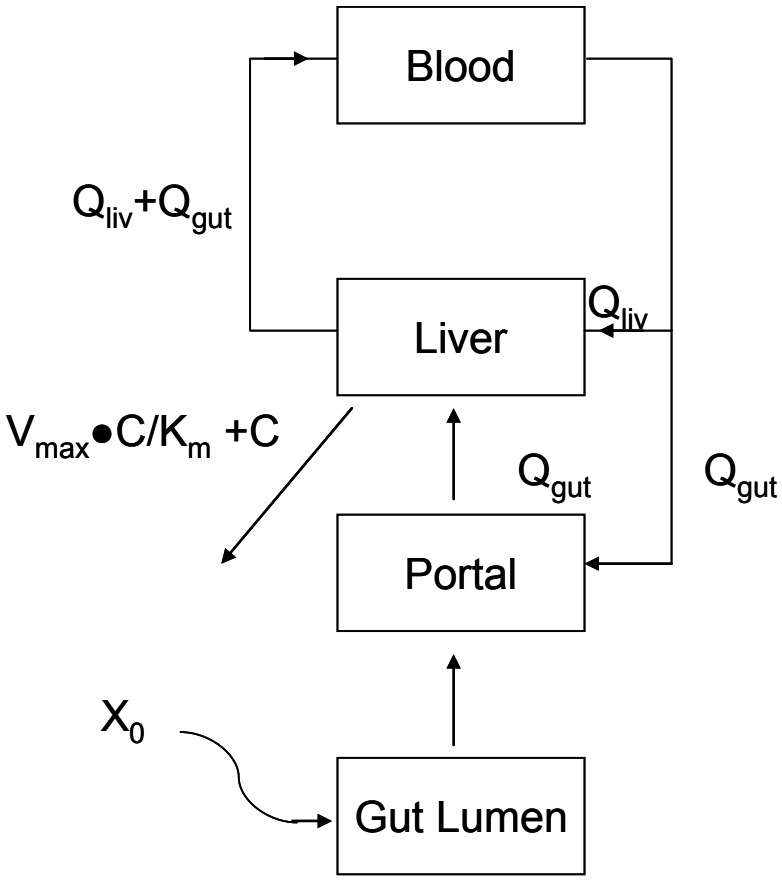

Figure 4.2 Model used for simulations of oral administration of drug. X_0 represents dose, Q represents blood flow, V_{max} represents the maximum velocity and K_m represents the half maximum velocity.

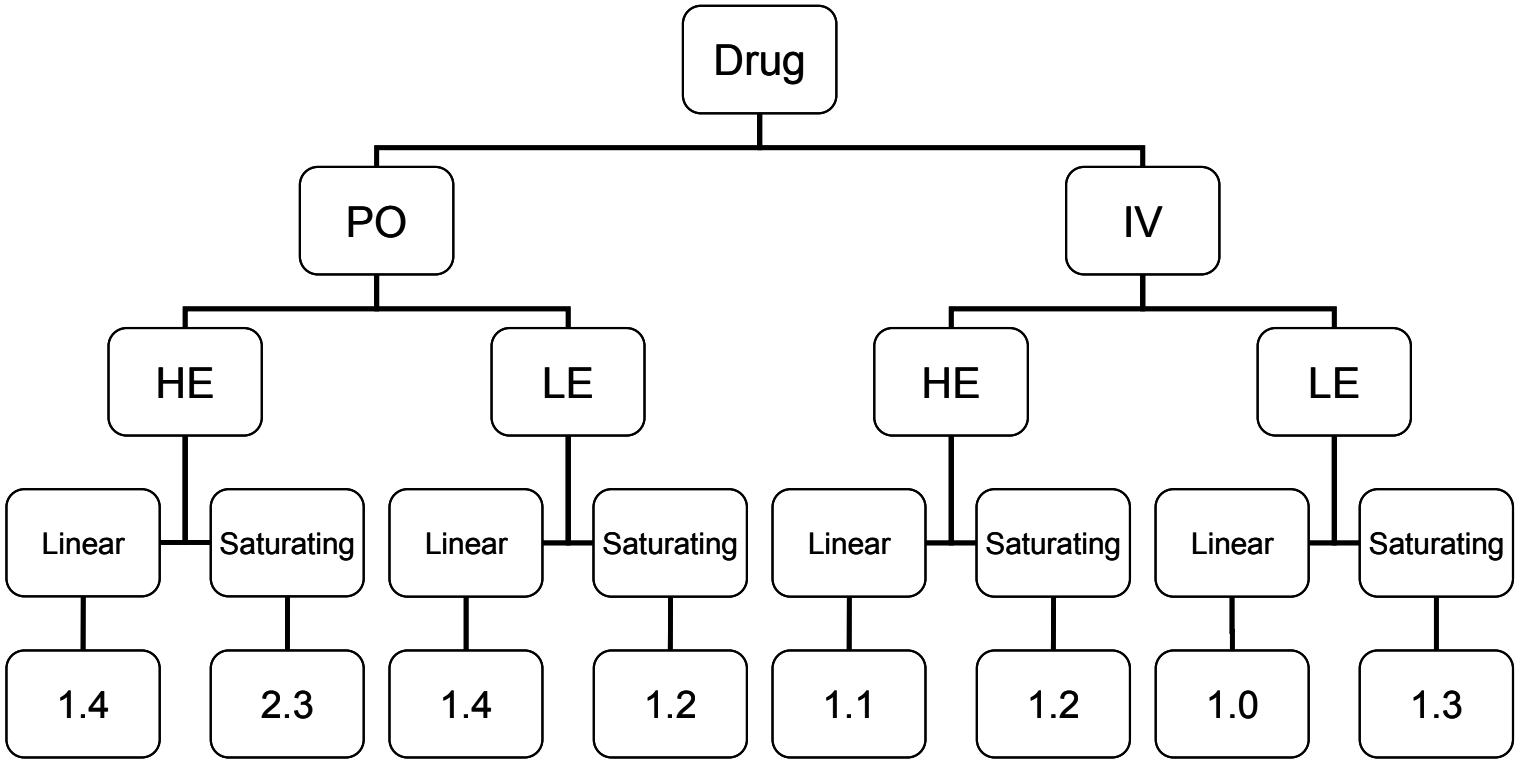

Figure 4.3 Scheme depicting the effects of decreased enzyme capacity (25%) on the AUC of drugs. Values represent $AUC_{infected}/AUC_{control.}$ IV: Intravenous administration, PO: Oral administration, HE: High Extraction and LE: Low Extraction

F. TABLES

Table 4.1 Physiological parameters used for semi-physiologic pharmacokinetic model

Parameter	Value	Units	Reference
Body weight (BW)	0.250	Kg	
Liver blood flow (Q_{liv})	17.08	mL/min	(Brown et al., 1997)
Gastrointestinal blood flow (Q_{gut})	7.32	mL/min	(Brown et al., 1997)
Liver Partition Coefficient (K_p)	1		
Liver Volume (V_{liv})	9.15	mL	(Brown et al., 1997)
Portal Volume (V_{portal})	1	mL	(Kanamitsu et al., 2000)
Systemic Volume (V_{syst})	18.5	mL	(Brown et al., 1997)

Table 4.2 Pharmacokinetic parameters used for simulations of oral and intravenous administration

	Control Enzyme Capacity		25% Decrease Enzyme Capacity	
	HE	LE	HE	LE
V_{max}(μmol/min)	120	10	90	7.5
K_m (μmol/mL)	2	2	2	2
Cl_{int} (mL/min)	60	5	45	3.75
f_a	1	1	1	1
f_u	1	1	1	1
k_a (1/min)	0.03	0.03	0.03	0.03

HE High Extraction
LE Low Extraction
V_{max} Maximum velocity
K_m Half maximum velocity
Cl_{int} Intrinsic clearance
f_a Fraction absored
f_u Unbound fraction
k_a First-order rate constant for absorption

Table 4.3 Results of simulation for intravenous administration

Control Enzyme Capacity						
Dose (μmol/kg)	Saturating or Linear Dose	Hepatic Extraction	$C_{max,\ liver}$ (μmol/mL)	$C_{max,\ blood}$ (μmol/mL)	AUC_{blood} (μmol•min/mL)	AUC ratio
35	Linear	HE[a]	0.10	0.47	0.51	-
700	Saturating		3.05	9.46	13	-
35	Linear	LE[b]	0.25	0.47	2.2	-
700	Saturating		5.6	9.5	93	-
25% Decrease Enzyme Capacity						
Dose (μmol/kg)	Saturating or Linear Dose	Hepatic Extraction	$C_{max,\ liver}$ (μmol/mL)	$C_{max,\ blood}$ (μmol/mL)	AUC_{blood} (μmol•min/mL)	AUC ratio[e]
35	Linear	HE[c]	0.12	0.47	0.57	1.12
700	Saturating		3.55	9.46	15	1.15
35	Linear	LE[d]	0.25	0.47	2.2	1.00
700	Saturating		5.7	9.5	123	1.32

HE High Extraction
LE Low Extraction
a. V_{max} = 120 μmol/min, K_m = 2 μmol/mL
b. V_{max} = 10 μmol/min, K_m = 2 μmol/mL
c. V_{max} = 90 μmol/min, K_m = 2 μmol/mL
d. V_{max} = 7.5 μmol/min, K_m = 2 μmol/mL
e. Ratio of AUC for 25% decreased enzyme capacity over AUC for matched control

Table 4.4 Results of simulation for oral administration

Control Enzyme Capacity						
Dose (μmol/kg)	Saturating or Linear Dose	Hepatic Extraction	$C_{max,\ liver}$ (μmol/mL)	$C_{max,\ blood}$ (μmol/mL)	AUC_{blood} (μmol•min/mL)	AUC ratio
800	Linear	HE[a]	0.09	0.09	3.2	-
16000	Saturating		6.55	6.52	157	-
800	Linear	LE[b]	1.10	1.10	50	-
16000	Saturating		100.2	100.2	6220	-
25% Decrease Enzyme Capacity						
Dose (μmol/kg)	Saturating or Linear Dose	Hepatic Extraction	$C_{max,\ liver}$ (μmol/mL)	$C_{max,\ blood}$ (μmol/mL)	AUC_{blood} (μmol•min/mL)	AUC ratio[e]
800	Linear	HE[c]	0.13	0.12	4.4	1.38
16000	Saturating		12.7	12.7	355	2.26
800	Linear	LE[d]	1.43	1.43	72	1.44
16000	Saturating		107.4	107.4	7175	1.15

HE High Extraction
LE Low Extraction
a. V_{max} = 120 μmol/min, K_m = 2 μmol/mL
b. V_{max} = 10 μmol/min, K_m = 2 μmol/mL
c. V_{max} = 90 μmol/min, K_m = 2 μmol/mL
d. V_{max} = 7.5 μmol/min, K_m = 2 μmol/mL
e. Ratio of AUC for 25% decreased enzyme capacity over AUC for matched control

G. REFERENCES

Auprayoon P, Sukontason K, Na-Bangchang K, Banmairuroi V, Molunto P and Karbwang J (1995) Pharmacokinetics of quinine in chronic liver disease. Br J Clin Pharmacol 40:494-497.

Brown RP, Delp MD, Lindstedt SL, Rhomberg LR and Beliles RP (1997) Physiological parameter values for physiologically based pharmacokinetic models. Toxicol Ind Health 13:407-484.

de Leon J and Diaz FJ (2003) Serious respiratory infections can increase clozapine levels and contribute to side effects: a case report. Prog Neuropsychopharmacol Biol Psychiatry 27:1059-1063.

Houston JB and Carlile DJ (1997) Prediction of hepatic clearance from microsomes, hepatocytes, and liver slices. Drug Metab Rev 29:891-922.

Kanamitsu S, Ito K and Sugiyama Y (2000) Quantitative prediction of in vivo drug-drug interactions from in vitro data based on physiological pharmacokinetics: use of maximum unbound concentration of inhibitor at the inlet to the liver. Pharm Res 17:336-343.

Kraemer MJ, Furukawa CT, Koup JR, Shapiro GG, Pierson WE and Bierman CW (1982) Altered theophylline clearance during an influenza B outbreak. Pediatrics 69:476-480.

Schmith VD and Foss JF (2010) Inflammation: planning for a source of pharmacokinetic/pharmacodynamic variability in translational studies. Clin Pharmacol Ther 87:488-491.

Shand DG, Kornhauser DM and Wilkinson GR (1975) Effects of route of administration and blood flow on hepatic drug elimination. J Pharmacol Exp Ther 195:424-432.

Zhao XJ and Ishizaki T (1997) The In vitro hepatic metabolism of quinine in mice, rats and dogs: comparison with human liver microsomes. J Pharmacol Exp Ther 283:1168-1176.

CHAPTER 5

CONCLUSIONS

Inflammation is an important component of the immune response, which is triggered upon tissue injury or invasion of a host by an infectious organism. Inflammation also plays an integral role in the pathophysiology of many chronic diseases, including diabetes, cardiovascular disease, advanced cancer and rheumatoid arthritis (Libby, 2007). Data accumulated over the past three decades demonstrate that molecular effectors of inflammation (i.e., cytokines and nitric oxide) can modulate expression and function of DMEs and DTs (Aitken et al., 2006; Morgan et al., 2008). The degree of modulation of particular DMEs and DTs depends on the inflammatory molecular effector imposing the challenge and/or infectious agent examined (Abdel-Razzak et al., 1993; Le Vee et al., 2009). In some cases, modulatory effects were shown to differentially alter (i.e., up- or down-regulate) particular CYPs, even in response to the same stimuli (Richardson et al., 2006; Yang and Lee, 2008). In spite of these differences in response, the general effect of inflammation and infection on DMEs and DTs is down-regulation of mRNA/protein expression and/or decreased protein function (Renton, 2005).

Human African trypanosomiasis (HAT) is a parasitic disease that afflicts one of the poorest regions of the world, sub-Saharan Africa. Chemotherapies for treatment of HAT are limited to a handful of drugs that are associated with moderate to severe toxicities, as well as impractical dosing regimens (Chapter 1). Despite problems with these drugs, the last registration of a drug against HAT occurred over 30 years ago (Fairlamb, 2003). As with other neglected diseases, efforts for discovery and development of new agents for treatment of HAT are undertaken largely by non-profit organizations and academic institutions. Among the few classes of compounds currently in development for first- and second-stage HAT are diamidine analogs of pentamidine, a drug that has long been used for treatment of

first-stage HAT. Diamidines and their bis-*O*-methylamidoxime prodrugs have shown efficacy for both first-stage HAT (when parasites are confined to the hemolymphatic system) and the more challenging second-stage HAT (when parasites invade the central nervous system). Metabolic activation of prodrugs is essential for generation of the pharmacologically active compounds (Ettmayer et al., 2004). For example, the bis-*O*-methylamidoxime prodrug pafuramidine, which was in development for treatment of first-stage HAT, was shown to undergo complex biotransformation to generate the active diamidine metabolite, furamidine, in humans (Zhou et al., 2004). This biotransformation pathway involved oxidative reactions catalyzed by CYP enzymes and reductive reactions catalyzed by cytochrome b_5/NADPH b_5 reductases (Saulter et al., 2005; Wang et al., 2007). Prior to this dissertation project, it was not known whether the bis-*O*-methylamidoxime prodrug, DB868, under investigation for second-stage HAT, required similar biotransformation as pafuramidine to generate the active diamidine metabolite, DB829, or whether the metabolic profile in humans would be similar to that in rats, a common pre-clinical species used for drug development. Additionally, because bioactivation of diamidine prodrugs would occur during active trypanosomal infection, it was not known whether down-regulation of DMEs would have an effect on bis-*O*-methylamidoxime prodrug biotransformation to the corresponding active diamidine metabolite with observable effects on the pharmacokinetics of these agents.

In vitro and *in vivo* approaches were utilized in this dissertation project to address the following objectives: 1) characterize the biotransformation of the bis-*O*-methylamidoxime prodrug, DB868, to the pharmacologically active metabolite, DB829 and 2) ascertain, in a rat model of first-stage trypanosomiasis, whether trypanosomal infection diminishes conversion

of bis-*O*-methylamidoxime prodrugs to corresponding active diamidine metabolites using the prodrug, pafuramidine, and active metabolite, furamidine, as model compounds. The central hypothesis was that trypanosomal infection will down-regulate metabolic bioconversion of bis-*O*-methylamidoxime prodrugs, thereby increasing systemic exposure to the prodrug and decreasing systemic exposure to the pharmacologically active diamidine.

Using human and rat liver microsomes and hepatocytes, the phase I biotransformation pathway of the bis-*O*-methylamidoxime prodrug, DB868, was elucidated (Figure 2.3). It was demonstrated that DB868 was metabolized extensively by both human and rat liver enzymes. Four phase I intermediate metabolites were detected (M1-M4) in both species. The M1 and M2 metabolites were formed by sequential *O*-demethylation reactions of DB868 and M1, respectively. The M3, M4 and active DB829 metabolites were formed by *N*-dehydroxylation of M1, M2 and M4, respectively. Additionally, a novel *N*-demethoxylation reductive reaction was identified, which produced the metabolite *O*-methylamidoxime/amidine (M3) directly from DB868. These results showed that the biotransformation pathway of DB868 mirrored that of the analog bis-*O*-methylamidoxime prodrug, pafuramidine, where similar sequential *O*-demethylation and *N*- dehydroxylation reactions preceded formation of the active diamidine, furamidine. The only difference between the pafuramidine and DB868 biotransformation pathways was the discovery of an *N*-demethoxylation reduction, contributing to the direct formation of the *O*-methylamidoxime/amidine metabolite M3 from DB868. Insight into this unrecognized reaction was derived from kinetic analysis of intermediate metabolite formation, which was not carried out during characterization of pafuramidine biotransformation. Hence, the possibility exists that this reaction also is part of the pafuramidine biotransformation pathway but was not recognized using traditional

methods (e.g., mass spectrometric methods and knowledge of common metabolic pathways), which highlights the value of kinetic modeling for identification of novel metabolic pathways. Marked species differences were observed in the kinetics of M2 formation (M1-*O*-demethylation), which may be of concern from a toxicologic perspective. Formation of M2, the diamidoxime prodruct of M1, using both liver microsomes and hepatocytes of rats was minimal compared to humans. This finding was consistent with different kinetics of M2 formation, which was described in humans by an allosteric process and in rats by a linear process. Allosteric formation of M2 in humans correlated with involvement of CYP1A2, known to have other substrates that exhibit allosteric kinetics (e.g., α-napthoflavone, pyrene, and 1-hydroxypyrene) (Sohl et al., 2008). Despite the different kinetics observed for M2 formation between species, based on the large S_{50} (18 μM) observed for allosteric formation of M2 in humans, it is unlikely that these kinetics will be observed clinically.

Formation of M2 (M1-*O*-demethylation) was catalyzed by CYP1A2 in humans, unlike formation of M1 (DB868-*O*-demethylation) which involved catalysis by both CYP4F and CYP1A2 in both human and rat liver microsomes. The involvement of CYP4F in M1 formation was in agreement with findings by Wang et.al., who demonstrated, with human liver microsomes, that pafuramidine-*O*-demethylation was catalyzed primarily by CYP4F isoforms (Wang et al., 2006). Collectively, these results suggested that bis-*O*-methylamidoxime prodrugs show similarities in both biotransformation pathways and enzymes that catalyze these reactions.

Formation of the active diamidine, DB829, was negligible when DB868 was incubated with microsomes, whereas DB289 was detected readily when DB868 was incubated with hepatocytes from both species. However, once formed in hepatocytes,

DB829 was exported slowly to the culture medium over time, with the majority of compound remaining trapped intracellularly. This key finding suggested a temporal disconnect between rate of formation and appearance of DB829 in hepatocyte culture medium. Because diamidines are dications at physiologic pH, they are unable to diffuse passively through membranes, and have been shown to rely on drug transporters to reach the site of action and/or to be eliminated (Ming et al., 2009). Extensive accumulation of DB289 within hepatocytes suggested low affinity for carrier-mediated basolateral export or tight intracellular binding or sequestration. Because the extent of DB829 accumulation/sequestration was significant (relative to dose), and this process affected the kinetics of DB829 appearance in the medium, this phenomenon appeared characteristic of target-mediated drug disposition as described by Levy (Levy, 1994), who suggested that sequestration of drugs due to capacity-limited binding processes can affect the pharmacokinetics of drugs. Results from these *in vitro* studies confirmed that in both humans and rats, biotransformation of the bis-*O*-methylamidoxime prodrug DB868 was similar to that of pafuramidine and that it relies on CYP- and cytochrome b_5/NADPH b_5 reductase-mediated processes to generate the active diamidine, DB829. Additionally, these studies served to recognize that aside from metabolism, basolateral export and/or intracellular accumulation/sequestration appeared to play an important role in the disposition of DB829.

To determine whether trypanosomal infection would have an effect on the pharmacokinetic behavior of bis-*O*-methylamidoxime prodrugs and their corresponding diamidines, the prodrug, pafuramidine, and metabolically formed diamidine, furamidine, were utilized as model compounds. Initial studies focused on development and characterization of a rat experimental model of first-stage trypanosomiasis (Chapter 3).

Characterization of this model was conducted to determine that potential pharmacokinetic changes observed in infected animals were not a reflection of organ damage due to trypanosomal infection. Sprague-Dawley rats were infected with the S427 strain of trypanosomes to mimic human first-stage infection. The time-course of parasitemia was determined by blood counts following intraperitoneal inoculation with 10^4 cells. A short (acute) infection was observed, with parasitemia peaking at day five, followed by death at day six. Infection did not damage liver and kidney function, as reflected by histological evaluation during the course of infection. Moderate elevation of biochemical markers of liver and kidney function (i.e., ALT and BUN, respectively) was observed as infection progressed, with the highest changes (9- and 1.4-fold, respectively) observed at day five of infection, concurrent with maximal parasitemia. Marked elevation in ALT was not a concern, as it has been shown that inflammation induced by other infectious agents also has led to elevations in ALT (e.g., viral hepatitis) (Getachew et al., 2010). Understanding of the time-course of parasitemia, and of any related biochemical and histological changes, served to select the optimal day to conduct pharmacokinetic studies. Day four post-infection was chosen based on the criteria of active parasitic growth and minimal biochemical and histological changes. These results suggest that this rat model of first-stage trypanosomal infection could be used to study effects of infection on pharmacokinetics of drugs other than diamidine analogs and their bis-*O*-methylamidoxime prodrugs.

Upon characterization of a rat experimental model of first-stage trypanosomiasis, studies were conducted to evaluate the pharmacokinetics of intravenously and orally administered pafuramidine and metabolically formed furamidine. When pafuramidine was administered as a 30-min intravenous infusion to control (uninfected) and infected rats, no

changes in pafuramidine clearance or systemic exposure (AUC_{0-12}) were observed. When pafuramidine was administered by oral gavage at a sub-saturating dose (7.5 μg/kg), there was a trend for decreased apparent oral clearance/increased systemic exposure (AUC_{0-12}) in infected animals compared to uninfected animals. In contrast, a significant increase in systemic exposure (AUC_{0-24}) (1.3-fold) was observed in infected animals when pafuramidine was administered at an oral dose known to saturate pafuramidine clearance (25 μmol/kg). These dose and route-discrepant results were explained by the fact that pafuramidine was determined to be a high extraction ratio, or hepatic blood flow-limited, drug. In this case, hepatic metabolism is so efficient (greater than 70% upon a single pass through the liver) that the limiting factor for pafuramidine clearance is the rate at which the agent is delivered to the liver *via* blood flow. Therefore, when pafuramidine is given intravenously to control or infected animals, pafuramidine clearance and exposure would not be affected by down-regulation of DMEs due to infection. Similarly, when pafuramidine is administered orally at sub-saturating concentrations, down-regulation of DMEs due to infection are likely to cause minimal to no changes in pafuramidine systemic clearance/exposure. At sub-saturating concentrations of substrate, the amount of DMEs is expected to greatly exceed substrate, regardless of the presence or absence of infection. Thus, even if a portion of the enzyme pool is decreased in infected animals, changes in drug clearance may not be discernable under these conditions. However, when administered orally at saturating doses, pafuramidine clearance will be limited by enzyme capacity. Under these saturating conditions, diminished enzyme capacity due to infection will be reflected in increased pafuramidine systemic exposure (Chapter 3). Together, results with pafuramidine suggested that infection decreased the metabolism of pafuramidine, suggesting down-regulation of the

enzyme(s) involved in pafuramidine-*O*-demethylation. In humans, metabolism of pafuramidine was shown to be catalyzed by members of the CYP4F family (Wang et al., 2006). Preliminary data obtained during this investigation showed that pafuramidine-*O*-demethylation also is catalyzed by members of the Cyp4f family in rats (unpublished results). Consistent with results presented in this dissertation, down-regulation of mRNA expression of Cyps 4f1, 4f4, 4f5, and 4f6 in primary rat hepatocytes has been shown upon direct stimulation with LPS (Kalsotra et al., 2003). However, conflicting data regarding Cyp4f regulation during inflammation has been reported depending on the source of inflammatory stimulus. For example, another investigation using rat hepatocytes demonstrated up-regulation of Cyps 4f1, 4f4, 4f5, and 4f6 mRNA expression upon challenge with pro-inflammatory cytokines IL-1, IL-6, and TNF-α (Kalsotra et al., 2007). In contrast, challenge with the inflammatory mediators LPS or $BaSO_4$ to rats had no effect on mRNA expression of Cyp4f1 and Cyp4f6 (Kalsotra et al., 2003).

The observed differences in pafuramidine exposure after oral and intravenous administration prompted a systematic analysis of the effects of infection on drug systemic exposure using a semiphysiologic-pharmacokinetic model (Chapter 4). This approach, based on concepts of the well-stirred model of hepatic clearance, served to confirm the interpretation of the dose and route-discrepant results observed for pafuramidine experimentally. Additionally, this model was expanded to predict outcomes for low extraction, or capacity-limited compounds, which are characterized by inefficient metabolism (less than 20% upon a single pass through the liver) (Shand et al., 1975). The variables in the model included high or low intrinsic clearance (corresponding to drugs with high or low hepatic extraction), doses in the linear (sub-saturating) or saturating range of drug

metabolism, and intravenous or oral administration. This analysis not only supported findings in this investigation, but provided a framework from which the impact of infection on drug development can be considered, through illustration of different scenarios in which the pharmacokinetics of a given drug will be more or less sensitive to effects of infection or inflammation. For example, the analysis showed that the largest effects of infection and inflammation (due to diminished enzyme/transporter capacity) will occur with a high extraction drug given at oral doses that will saturate metabolic/distributive clearance. In contrast, little to no effect will be observed on the pharmacokinetics of a low extraction compound when administered intravenously (Chapter 4). Unlike drug-drug interactions, where large (up to 300-fold) changes in drug systemic exposure have been reported (Fichtenbaum et al., 2002), the current analysis suggests that infection and inflammation are less likely to cause such marked effects. This limited effect is supported by several observations in the clinic, in which the largest changes in pharmacokinetics (e.g., clearance) ranged between 2- to 4-fold (Table 1.3). These modest changes in systemic exposure and clearance *in vivo* can be explained by the mechanism of the interaction at the molecular level. For example, decreased enzyme capacity results in changes in V_{max} through suppression of the enzyme pool available for metabolic reactions. Based on the Michaelis-Menten premise that the enzyme pool available for metabolism is much larger than the substrate to be consumed (Voet and Voet, 2004), modest reductions in the enzyme pool (mediated through cytokine or NO responses) are unlikely to have significant effects on the overall clearance of a substrate (see Chapter 3 for further discussion). Moreover, depending on the contribution of a pathway to overall systemic clearance, compounds with multiple routes of clearance will be affected minimally if parallel pathways of clearance are unaffected by inflammation.

Accordingly, as also recognized by Renton (Renton, 2005), the largest effects of decreased enzyme/transporter capacity, due to infection or inflammation, on systemic exposure or clearance of a compound will be observed in instances where 1) the enzyme/transporter is the major contributor to systemic clearance, and 2) the decreased enzyme/transporter capacity is coupled with genetic polymorphisms or drug-drug interactions. Furthermore, untoward effects or toxicity will be more likely when infection affects compounds with a narrow therapeutic window.

According to the central hypothesis underlying this work, reduction in metabolic clearance of pafuramidine in infected animals was expected to reduce systemic concentrations of furamidine, raising concerns about potential sub-therapeutic concentrations. Unexpectedly, significant increases in furamidine systemic exposure were observed in infected animals compared to controls (up to 3-fold). These increases were independent of dose and route of pafuramidine administration. This outcome suggested that a mechanism involved in hepatic disposition of furamidine also was impaired during infection. Although the mechanisms of furamidine disposition are not fully elucidated, rat mass balance excretion studies in which pafuramidine was dosed orally at 10 mg/kg (27 μmol/kg) suggested that, second to tissue sequestration (29% of the dose at 48 h), biliary excretion of furamidine was an important contributor to its elimination (approximately 25% of the dose at 72 h), followed by glucuronidation of furamidine (10% of the dose at 48 h) and renal elimination (4% of the dose at 48 h) (Midgley et al., 2007). To investigate potential mechanisms involved in the increased systemic exposure observed in infected animals, *in situ* bile cannulation experiments were conducted in control and infected animals. Results from these experiments showed a significant decrease (12-fold) in biliary excretion of

furamidine in infected animals compared to controls, suggesting impairment of canalicular transporters involved in biliary excretion of furamidine as a potential mechanism that may explain the observed increased exposure of furamidine in infected animals (Chapter 3). The transporters involved in biliary excretion of furamidine are not known; however, examples of down-regulation of mRNA and protein expression of the biliary efflux transporters MRP2 and BSEP were shown to be mediated by the pro-inflammatory cytokines IL-6 and TNF-α in human hepatocytes (Vee et al., 2009), supporting the notion that infection could have an effect on elimination of furamidine.

Based on mass balance studies reported by Midgley et. al. (2007), another important component in furamidine disposition is hepatic accumulation. To date, the mechanism of accumulation/sequestration of furamidine remains elusive. It is possible that small perturbations in tissue sequestration/binding could increase systemic exposure during episodes of infection; however, this hypothesis has not been tested and merits further investigation. During *in situ* bile cannulation experiments (0-60 min), the effects of infection on phase II metabolism was not ascertained since glucuronide conjugates of furamidine were not detected in bile from either control or infected animals . Absence of furamidine glucuronides in bile was due, potentially, to the short duration of the experiment; however, changes in glucuronide formation during infection is not expected to play a significant role in the increased furamidine exposure of infected animals, as glucuronidation is not a major contributor to furamidine disposition in rats.

Assuming that mechanisms of furamidine elimination in both rats and humans are similar, the increased systemic exposure of furamidine in infected animals could have positive implications, as it would alleviate concern that sub-therapeutic concentrations of

active diamidine will be achieved in the infected population. Data from mass balance studies in uninfected rats and humans showed that, although biliary excretion was the second most important contributor to furamidine disposition in both species, the extent of biliary excretion between these two species differs, with biliary excretion in rats accounting for greater than 70% of furamidine disposition compared to approximately 30% in humans at 168 h post dose (10 mg/kg and 100 mg/kg in rat and human, respectively) (Midgley et al., 2007; Huntingdon, 2008). This suggests that humans will be less sensitive to the effect of infection on biliary excretion of furamidine compared to rats, further reducing concern about the impact of infection on efficacy. Unlike increased furamidine exposure observed in infected rats, human data from Phase IIa clinical trials (Immtech International, 2008) indicated that furamidine systemic exposure after 6 days of dosing in infected patients was comparable to that observed in healthy subjects that participated in Phase I trials, in which pafuramidine was dosed orally at 100 mg twice daily (Immtech International, 2002). These results contrast the up to 3-fold increase in furamidine exposure observed in infected rats and may be explained by the lower contribution of biliary excretion to furamidine disposition in humans, which potentially is due to species differences in canalicular hepatic transporters. Evidence for canalicular transporter differences between species was highlighted for Mrp2/MRP2, which was shown to play a more significant role in rats than in any other species (10-fold higher protein expression compared to human) (Li et al., 2009). Comparable furamidine systemic concentrations during infection in patients did not appear to be due to compensation *via* increased renal elimination, which is a minor component of systemic furamidine elimination in the absence of infection, as similar amounts of furamidine in urine were reported between infected patients and healthy subjects.

In addition to an impact on furamidine pharmacokinetics and efficacy, infection also may have implications for toxicity observed during extended Phase I trials with healthy volunteers (Pohlig G, 2008). Assuming that the mechanism of toxicity was driven by tissue sequestration, an increase in furamidine exposure due to decreased biliary excretion during infection would not be expected to impact liver toxicity, as tissue levels within the liver will, potentially, remain unchanged and decreased biliary excretion/increased furamidine exposure would be driven largely by unbound furamidine concentrations. In this scenario, kidney toxicity could be increased or remain unchanged depending on whether increased systemic furamidine concentrations lead to increased sequestration in the kidney. If, however, the increase in furamidine systemic exposure during infection was due to a decrease in tissue sequestration, toxicity in both liver and kidney may be lessened in infected populations.

In contrast to results presented in this work, data from a Phase IIa study in African patients demonstrated that pafuramidine systemic exposure was reduced greatly (10-fold) compared to healthy subjects from a separate Phase I study. A potential explanation for this discrepancy is differential regulation of CYP4F enzymes during infection between humans and rats, in which CYP4Fs appeared to be induced in humans during infection compared to apparent suppression observed in rats in the current investigation. Differential regulation of CYP4Fs in rats between different experimental systems were highlighted above, where *in vitro* results of down-regulation for these enzymes was not reproduced *in vivo* using the same inflammatory stimulus. The effects of inflammatory or infectious stimuli on regulation of CYP4Fs in humans have not been described and require further investigation.

The differential behavior of pafuramidine and furamidine between rats and humans during trypanosomal infection suggests that rats may not be a suitable model for anticipating

the impact of infection on human toxicity; however, the rat model of first-stage HAT infection can still be useful for development of compounds that do not undergo metabolic catalysis by CYP4Fs and that do not have biliary excretion as a major component of elimination.

In summary, prior to the studies described in this dissertation project, it was unknown whether bioconversion of bis-*O*-methylamidoxime prodrugs would be affected during active trypanosomal infection, thereby altering their pharmacokinetic profile and that of their corresponding active diamidine metabolites. Based on literature knowledge, it was anticipated that impaired metabolism caused by infection would decrease clearance/increase systemic exposure of bis-*O*-methylamidoxime prodrugs of diamidine, resulting in diminished levels of the pharmacologically active diamidine metabolite. Initial studies with the bis-*O*-methylamidoxime prodrug DB868, currently under development for second-stage HAT, confirmed that metabolic bioconversion by at least two enzyme systems (e.g., CYP and cytochrome b_5/NADPH b_5 reductase) was an integral component in the generation of active diamidines. Due to a lack of oral formulation for DB868, studies investigating effects of infection on the pharmacokinetics of bis-*O*-methylamidoxime prodrugs and their corresponding diamidines were conducted with the prodrug, pafuramidine, and the active diamidine, furamidine, whose pharmacokinetics were characterized previously. To address this question, a rat model of first-stage trypanosomal infection was developed and characterized. This model demonstrated that trypanosomal infection has an effect on the pharmacokinetics of bis-*O*-methylamidoxime prodrugs and their active diamidines, as shown by the increase in pafuramidine exposure (AUC) (<2-fold) following a 25 μmol/kg oral dose of pafuramidine, which appeared to be mediated by decreased metabolism *via* impaired

enzyme capacity elicited by infection. The effects of decreased metabolism in infected animals on the pharmacokinetics of pafuramidine were discernable only when pafuramidine was administered orally at a saturating dose. This observation was confirmed using a semiphysiologic model that produced results similar to experimental observations. Additionally, evidence presented in this investigation suggests that transport processes mediating the biliary excretion of the diamidine, furamidine, also are impaired during trypanosomiasis.

Although effects of infection on DMEs is widely recognized, there is little discussion within the literature on why changes in pharmacokinetics and pharmacodynamics are not observed more often in the clinic, despite the prominence of these conditions in humans. The findings of this dissertation project begin to address this gap by furthering the knowledge of which pharmacokinetic characteristics influence how a compound will behave in the presence of inflammation or infection. A quantitative framework is provided for anticipating the impact of inflammation and infection during drug development or drug therapy management.

A. FUTURE DIRECTIONS

In spite of the insights gained regarding how infection affects the disposition of pafuramidine and furamidine, additional studies examining the role of trypanosomal infection on the different mechanisms involved in the disposition of furamidine are needed. For example, identification of the transporters involved in basolateral and biliary export of furamidine is integral to understanding furamidine disposition. Additionally, little data are

available on the mechanism of diamidine tissue binding and consequent effects on pharmacokinetics. The following studies are proposed:

Identify transport protein(s) involved in the hepatobiliary disposition of furamidine.

In vitro, studies in this investigation showed that once generated from prodrug in the liver, the charged diamidine is unable to exit the hepatocyte *via* passive diffusion. Transporters localized on basolateral and canalicular membranes are likely to be involved in the translocation of diamidines into plasma and bile, respectively. To date, the transporters responsible for furamidine basolateral export and biliary excretion remain unknown. To understand fully the disposition of furamidine, studies determining the transporters involved in hepatobiliary disposition of furamidine are warranted. Although not known to transport organic cations, candidate basolateral efflux transporters include the ATP-dependent MRP4 and MRP5 (Konig et al., 1999; Madon et al., 2000; Assem et al., 2004; Ritter et al., 2005). These transporters may play a role in furamidine basolateral export, as it was recently demonstrated that in *mdr1* deficient mice, pentamidine was removed from the brain by a member of the Mrp family (Sanderson et al., 2009). Additionally, involvement of a bidirectional carrier-mediated mechanism should be examined with a special focus on transporters of small organic cations, such as OCT1, which was demonstrated to be localized on the basolateral membrane of hepatocytes (Meyer-Wentrup et al., 1998; Proctor et al., 2008; Ming et al., 2009).

Evaluation of transporters involved in the biliary excretion of furamidine may include, but not be limited to, the canalicular efflux transporters MRP2, MATE1 and P-gp (Paulusma et al., 2000; Scheffer et al., 2000; Otsuka et al., 2005; Hiasa et al., 2006). Focus should center on MATE1, as this transporter was shown recently to mediate the transport of

4',6-diamidino-2-phenylindole (DAPI), a structurally-related diamidine analog (Yasujima et al., 2010). Another transporter that is a likely candidate for furamidine transport is the efflux transporter P-gp, since this transporter has wide substrate specificity (van der Sandt et al., 2000; Mahar Doan et al., 2002). Additionally, P-gp was shown recently to be involved in the biliary export of the organic cation tributylmethylammonium (TBuMa) through ion-pair complexation with bile salts (Song et al., 2010). After identification of biliary transporter(s) involved in biliary excretion of furamidine, determination of relative changes in protein expression of these transporters could be evaluated in infected animals.

Elucidate the mechanism of furamidine intracellular accumulation and effects on pharmacokinetics

Consistent with another report (Midgley et al., 2007), studies in this dissertation project showed that an important component of furamidine disposition is tissue accumulation (Chapter 3). Intracellular accumulation of drugs could involve multiple mechanisms, including organelle sequestration or binding to intracellular components such as proteins or DNA. For furamidine, the mechanism of accumulation in the liver and other organs is unknown but has been shown to have appreciable effects on disposition, as exemplified by a long terminal tissue half-life (~7 days, kidney) (Goldsmith, 2010). Accumulation of diamidines in tissues poses challenges to dose selection and has implications for toxicity depending on the mechanism of accumulation (Kleiner et al., 1997; Santos et al., 2008). *In vitro* studies should be undertaken to elucidate the mechanism of sequestration, including experiments examining lysosomal trapping (Gong et al., 2007; Kaufmann and Krise, 2007), mitochondrial sequestration (Duvvuri et al., 2004), and nuclear accumulation (Wilson et al., 2005). These studies could take advantage of the fluorescent properties of furamidine to

enable characterization of intracellular distribution and accumulation. It is possible that tight binding to macromolecules such as DNA drives the pharmacokinetics of furamidine, in a similar manner to the mechanism known as target-mediated drug disposition, where capacity limited binding drives the overall disposition of an agent (Mager and Jusko, 2001; Levy et al., 2003; Mager, 2006). Therefore, complimentary pharmacokinetic studies comprising intravenous dose escalation studies could be conducted to determine whether a dose-dependent decrease in volume of distribution occurs, as is expected for drugs exhibiting target-mediated disposition.

B. REFERENCES

Abdel-Razzak Z, Loyer P, Fautrel A, Gautier JC, Corcos L, Turlin B, Beaune P and Guillouzo A (1993) Cytokines down-regulate expression of major cytochrome P-450 enzymes in adult human hepatocytes in primary culture. *Mol Pharmacol* **44:**707-715.

Aitken AE, Richardson TA and Morgan ET (2006) Regulation of drug-metabolizing enzymes and transporters in inflammation. *Annu Rev Pharmacol Toxicol* **46:**123-149.

Assem M, Schuetz EG, Leggas M, Sun D, Yasuda K, Reid G, Zelcer N, Adachi M, Strom S, Evans RM, Moore DD, Borst P and Schuetz JD (2004) Interactions between hepatic Mrp4 and Sult2a as revealed by the constitutive androstane receptor and Mrp4 knockout mice. *J Biol Chem* **279:**22250-22257.

Duvvuri M, Gong Y, Chatterji D and Krise JP (2004) Weak base permeability characteristics influence the intracellular sequestration site in the multidrug-resistant human leukemic cell line HL-60. *J Biol Chem* **279:**32367-32372.

Ettmayer P, Amidon GL, Clement B and Testa B (2004) Lessons learned from marketed and investigational prodrugs. *J Med Chem* **47:**2393-2404.

Fairlamb AH (2003) Chemotherapy of human African trypanosomiasis: current and future prospects. *Trends Parasitol* **19:**488-494.

Fichtenbaum CJ, Gerber JG, Rosenkranz SL, Segal Y, Aberg JA, Blaschke T, Alston B, Fang F, Kosel B, Aweeka F and Group NACT (2002) Pharmacokinetic interactions between protease inhibitors and statins in HIV seronegative volunteers: ACTG Study A5047. *AIDS* **16:**569-577.

Getachew Y, James L, Lee WM, Thiele DL and Miller BC (2010) Susceptibility to acetaminophen (APAP) toxicity unexpectedly is decreased during acute viral hepatitis in mice. *Biochem Pharmacol* **79:**1363-1371.

Goldsmith R (2010) Renal Excretion of Anti-Trypanosomal Compounds as a Method of Predicting Potential Nephrotoxicity. *Poster Presentation. World Pharmaceutical Congress: New Tools for Detecting Nephrotoxicity*

Gong Y, Zhao Z, McConn DJ, Beaudet B, Tallman M, Speake JD, Ignar DM and Krise JP (2007) Lysosomes contribute to anomalous pharmacokinetic behavior of melanocortin-4 receptor agonists. *Pharm Res* **24:**1138-1144.

Hiasa M, Matsumoto T, Komatsu T and Moriyama Y (2006) Wide variety of locations for rodent MATE1, a transporter protein that mediates the final excretion step for toxic organic cations. *Am J Physiol Cell Physiol* **291:**C678-686.

Huntingdon (2008) 14C- Pafuramidine Maleate, Absorption, Metabolism and Excretion in Healthy Men After a Single Oral Dose-a Summary of the Plasma Pharmacokinetics, Excretion and Metabolism Data.

Immtech International (2002) Clinical Report for a Phase I Study of Multiple Dose Administration of DB289 to Healthy Volunteers. *289-C-041-002*.

Immtech International (2008) Multiple Dose Pharmacokinetics of DB289 and DB75 in Patients Participating in Immtech International Study 289-C-003. .

Kalsotra A, Anakk S, Brommer CL, Kikuta Y, Morgan ET and Strobel HW (2007) Catalytic characterization and cytokine mediated regulation of cytochrome P450 4Fs in rat hepatocytes. *Arch Biochem Biophys* **461:**104-112.

Kalsotra A, Cui X, Antonovic L, Robida AM, Morgan ET and Strobel HW (2003) Inflammatory prompts produce isoform-specific changes in the expression of leukotriene B(4) omega-hydroxylases in rat liver and kidney. *FEBS Lett* **555:**236-242.

Kaufmann AM and Krise JP (2007) Lysosomal sequestration of amine-containing drugs: analysis and therapeutic implications. *J Pharm Sci* **96:**729-746.

Kleiner DE, Gaffey MJ, Sallie R, Tsokos M, Nichols L, McKenzie R, Straus SE and Hoofnagle JH (1997) Histopathologic changes associated with fialuridine hepatotoxicity. *Mod Pathol* **10:**192-199.

Konig J, Rost D, Cui Y and Keppler D (1999) Characterization of the human multidrug resistance protein isoform MRP3 localized to the basolateral hepatocyte membrane. *Hepatology* **29:**1156-1163.

Le Vee M, Lecureur V, Moreau A, Stieger B, Fardel O, Fardel O, Le Vee M, Le Vee M, Jouan E, Moreau A, Fardel O, Jigorel E, Le Vee M, Boursier-Neyret C, Parmentier Y and Fardel O (2009) Differential regulation of drug transporter expression by hepatocyte growth factor in primary human hepatocytes

Levy G (1994) Pharmacologic target-mediated drug disposition. *Clin Pharmacol Ther* **56:**248-252.

Levy G, Mager DE, Cheung WK and Jusko WJ (2003) Comparative pharmacokinetics of coumarin anticoagulants L: Physiologic modeling of S-warfarin in rats and pharmacologic target-mediated warfarin disposition in man. *J Pharm Sci* **92:**985-994.

Li N, Zhang Y, Hua F and Lai Y (2009) Absolute difference of hepatobiliary transporter multidrug resistance-associated protein (MRP2/Mrp2) in liver tissues and isolated hepatocytes from rat, dog, monkey, and human. *Drug Metab Dispos* **37:**66-73.

Libby P (2007) Inflammatory mechanisms: the molecular basis of inflammation and disease. *Nutr Rev* **65:**S140-146.

Madon J, Hagenbuch B, Landmann L, Meier PJ and Stieger B (2000) Transport function and hepatocellular localization of mrp6 in rat liver. *Mol Pharmacol* **57:**634-641.

Mager DE (2006) Target-mediated drug disposition and dynamics. *Biochem Pharmacol* **72:**1-10.

Mager DE and Jusko WJ (2001) General pharmacokinetic model for drugs exhibiting target-mediated drug disposition. *J Pharmacokinet Pharmacodyn* **28:**507-532.

Mahar Doan KM, Humphreys JE, Webster LO, Wring SA, Shampine LJ, Serabjit-Singh CJ, Adkison KK and Polli JW (2002) Passive permeability and P-glycoprotein-mediated efflux differentiate central nervous system (CNS) and non-CNS marketed drugs. *J Pharmacol Exp Ther* **303:**1029-1037.

Meyer-Wentrup F, Karbach U, Gorboulev V, Arndt P and Koepsell H (1998) Membrane localization of the electrogenic cation transporter rOCT1 in rat liver. *Biochem Biophys Res Commun* **248:**673-678.

Midgley I, Fitzpatrick K, Taylor LM, Houchen TL, Henderson SJ, Wright SJ, Cybulski ZR, John BA, McBurney A, Boykin DW and Trendler KL (2007) Pharmacokinetics and metabolism of the prodrug DB289 (2,5-bis[4-(N-methoxyamidino)phenyl]furan monomaleate) in rat and monkey and its conversion to the antiprotozoal/antifungal drug DB75 (2,5-bis(4-guanylphenyl)furan dihydrochloride). *Drug Metab Dispos* **35:**955-967.

Ming X, Ju W, Wu H, Tidwell RR, Hall JE and Thakker DR (2009) Transport of dicationic drugs pentamidine and furamidine by human organic cation transporters. *Drug Metab Dispos* **37:**424-430.

Morgan ET, Goralski KB, Piquette-Miller M, Renton KW, Robertson GR, Chaluvadi MR, Charles KA, Clarke SJ, Kacevska M, Liddle C, Richardson TA, Sharma R and Sinal CJ (2008) Regulation of drug-metabolizing enzymes and transporters in infection, inflammation, and cancer. *Drug Metab Dispos* **36:**205-216.

Otsuka M, Matsumoto T, Morimoto R, Arioka S, Omote H and Moriyama Y (2005) A human transporter protein that mediates the final excretion step for toxic organic cations. *Proc Natl Acad Sci U S A* **102:**17923-17928.

Paulusma CC, Kothe MJ, Bakker CT, Bosma PJ, van Bokhoven I, van Marle J, Bolder U, Tytgat GN and Oude Elferink RP (2000) Zonal down-regulation and redistribution of the multidrug resistance protein 2 during bile duct ligation in rat liver. *Hepatology* **31:**684-693.

Pohlig G BS, Blum J, Burri C, Kabeya AM, Lubaki J-P F, Mpoto AM, Mununga BF, Deo GKM, Mutantu PN, Kuikumbi FM, Mintwo AF, Mununga AK, Dala A, Macharia S, Bilenge CMM, MesuVKBK, J Franco JR, Dituvanga ND, Olson CA. (2008) Phase 3 trial of pafuramidine maleate (DB289), a novel, oral drug, for treatment of first stage

sleeping sickness: safety and efficacy. *57th American Society for Tropical Medicine and Hygiene. New Orleans, LA.*

Proctor WR, Bourdet DL and Thakker DR (2008) Mechanisms underlying saturable intestinal absorption of metformin. *Drug Metab Dispos* **36:**1650-1658.

Renton KW (2005) Regulation of drug metabolism and disposition during inflammation and infection. *Expert Opin Drug Metab Toxicol* **1:**629-640.

Richardson TA, Sherman M, Antonovic L, Kardar SS, Strobel HW, Kalman D and Morgan ET (2006) Hepatic and renal cytochrome p450 gene regulation during citrobacter rodentium infection in wild-type and toll-like receptor 4 mutant mice. *Drug Metab Dispos* **34:**354-360.

Ritter CA, Jedlitschky G, Meyer zu Schwabedissen H, Grube M, Kock K and Kroemer HK (2005) Cellular export of drugs and signaling molecules by the ATP-binding cassette transporters MRP4 (ABCC4) and MRP5 (ABCC5). *Drug Metab Rev* **37:**253-278.

Sanderson L, Dogruel M, Rodgers J, De Koning HP and Thomas SA (2009) Pentamidine movement across the murine blood-brain and blood-cerebrospinal fluid barriers: effect of trypanosome infection, combination therapy, P-glycoprotein, and multidrug resistance-associated protein. *J Pharmacol Exp Ther* **329:**967-977.

Santos NA, Medina WS, Martins NM, Mingatto FE, Curti C and Santos AC (2008) Aromatic antiepileptic drugs and mitochondrial toxicity: effects on mitochondria isolated from rat liver. *Toxicol In Vitro* **22:**1143-1152.

Saulter J, Kurian J, Trepanier L, Tidwell R, Bridges A, Boykin D, Stephens C, Anbazhagan M and Hall JE (2005) Unusual Dehydroxylation of Antimicrobial Amidoxime Prodrugs by Cytochrome b5 and NADH Cytochrome b5 Reductase. *Drug Metab Dispos* **33:**1886-1893.

Scheffer GL, Kool M, Heijn M, de Haas M, Pijnenborg AC, Wijnholds J, van Helvoort A, de Jong MC, Hooijberg JH, Mol CA, van der Linden M, de Vree JM, van der Valk P, Elferink RP, Borst P and Scheper RJ (2000) Specific detection of multidrug resistance proteins MRP1, MRP2, MRP3, MRP5, and MDR3 P-glycoprotein with a panel of monoclonal antibodies. *Cancer Res* **60:**5269-5277.

Shand DG, Kornhauser DM and Wilkinson GR (1975) Effects of route of administration and blood flow on hepatic drug elimination. *J Pharmacol Exp Ther* **195:**424-432.

Sohl CD, Isin EM, Eoff RL, Marsch GA, Stec DF and Guengerich FP (2008) Cooperativity in oxidation reactions catalyzed by cytochrome P450 1A2: highly cooperative pyrene hydroxylation and multiphasic kinetics of ligand binding. *J Biol Chem* **283:**7293-7308.

Song IS, Choi MK, Jin QR, Shim WS and Shim CK (2010) Increased affinity to canalicular P-gp via formation of lipophilic ion-pair complexes with endogenous bile salts is

associated with mw threshold in hepatobiliary excretion of quaternary ammonium compounds. *Pharm Res* **27:**823-831.

van der Sandt IC, Blom-Roosemalen MC, de Boer AG and Breimer DD (2000) Specificity of doxorubicin versus rhodamine-123 in assessing P-glycoprotein functionality in the LLC-PK1, LLC-PK1:MDR1 and Caco-2 cell lines. *Eur J Pharm Sci* **11:**207-214.

Vee ML, Lecureur V, Stieger B and Fardel O (2009) Regulation of drug transporter expression in human hepatocytes exposed to the proinflammatory cytokines tumor necrosis factor-alpha or interleukin-6. *Drug Metab Dispos* **37:**685-693.

Voet D and Voet JG (2004) *Biochemistry*. J. Wiley & Sons, Hoboken, NJ.

Wang MZ, Saulter JY, Usuki E, Cheung YL, Hall M, Bridges AS, Loewen G, Parkinson OT, Stephens CE, Allen JL, Zeldin DC, Boykin DW, Tidwell RR, Parkinson A, Paine MF and Hall JE (2006) CYP4F enzymes are the major enzymes in human liver microsomes that catalyze the O-demethylation of the antiparasitic prodrug DB289 [2,5-bis(4-amidinophenyl)furan-bis-O-methylamidoxime]. *Drug Metab Dispos* **34:**1985-1994.

Wang MZ, Wu JQ, Bridges AS, Zeldin DC, Kornbluth S, Tidwell RR, Hall JE and Paine MF (2007) Human enteric microsomal CYP4F enzymes O-demethylate the antiparasitic prodrug pafuramidine. *Drug Metab Dispos* **35:**2067-2075.

Wilson WD, Nguyen B, Tanious FA, Mathis A, Hall JE, Stephens CE and Boykin DW (2005) Dications that target the DNA minor groove: compound design and preparation, DNA interactions, cellular distribution and biological activity. *Curr Med Chem Anticancer Agents* **5:**389-408.

Yang KH and Lee MG (2008) Effects of endotoxin derived from Escherichia coli lipopolysaccharide on the pharmacokinetics of drugs. *Arch Pharm Res* **31:**1073-1086.

Yasujima T, Ohta KY, Inoue K, Ishimaru M and Yuasa H (2010) Evaluation of 4',6-diamidino-2-phenylindole as a fluorescent probe substrate for rapid assays of the functionality of human multidrug and toxin extrusion proteins. *Drug Metab Dispos* **38:**715-721.

Zhou L, Thakker DR, Voyksner RD, Anbazhagan M, Boykin DW, Hall JE and Tidwell RR (2004) Metabolites of an orally active antimicrobial prodrug, 2,5-bis(4-amidinophenyl)furan-bis-O-methylamidoxime, identified by liquid chromatography/tandem mass spectrometry. *J Mass Spectrom* **39:**351-360.

APPENDIX I

CONTRIBUTIONS TO SCIENTIFIC PUBLICATIONS

Title: Synthesis, DNA affinity, and antiprotozoal activity of linear dications: Terphenyl diamidines and analogues.

Journal: Journal of Medicinal Chemistry 49:5324-5332. (2006)

Authors: Ismail MA, Arafa RK, Brun R, Wenzler T, Miao Y, Wilson WD, **Generaux C**, Bridges A, Hall JE and Boykin DW (2006)

Abstract: Diamidines 10a-g and 18a,b were obtained from dinitriles 9a-g and 15a,b by treatment with lithium trimethylsilylamide or upon hydrogenation of bis-*O*-acetoxyamidoximes. Dinitriles 9a-g were prepared via Suzuki reactions between arylboronic acids and arylnitriles. Potential prodrugs 12a-f and 17 were prepared via methylation of the diamidoximes 11a-f and 16a. Significant DNA affinities for rigid-rod molecules were observed. Compounds 10a, 10b, 10d, 18a, and 18b show IC50 values of 5 nM or less against *Trypanosoma brucei rhodesiense* (T. b. r.) and 10a, 10b, 10e, 18a, and 18b gave similar ones against *Plasmodium falciparum* (P.f.). The dications, 10a, 10d, 10f, and 10g are more active than furamidine in vivo. The prodrugs are only moderately effective on oral administration. Mouse liver microsome bioconversion of the methamidoxime prodrugs is significantly reduced from that of pafuramidine and suggests that the *in vivo* efficacy of these prodrugs is, in part, due to poor bioconversion.

Contribution: Metabolic Stability Experiments

Title: *In vitro* and *In vivo* determination of Piperacillin Metabolism in Humans.

Journal: Drug Metabolism and Dispositon 35: 345-349. (2007)

Authors: Ghibellini G, Bridges AS, **Generaux CN** and Brouwer KL

Abstract: Piperacillin metabolism and biliary excretion are different between humans and preclinical species. In the present study, piperacillin metabolites were characterized in bile and urine of healthy humans and compared with metabolites formed in vitro. Volunteers were administered 2 g of piperacillin IV; blood, urine, and duodenal aspirates (obtained via a custom-made oroenteric catheter) were collected. The metabolism of piperacillin in humans also was investigated *in vitro* using pooled human liver microsomes and sandwich-cultured human hepatocytes. Piperacillin and metabolites were estimated by high-performance liquid chromatography with tandem mass spectrometry detection. Piperacillin, desethylpiperacillin, and desethylpiperacillin glucuronide were detected in bile, urine, and human liver microsomal incubates. Similar to the *in vivo* results, desethylpiperacillin was formed and excreted into bile canaliculi of sandwich-cultured human hepatocytes. This is the first report of glucuronidation of desethylpiperacillin *in vitro* or *in vivo*. The clinical method employed in this study to determine biliary clearance of drugs also facilitates bile collection as soon as bile is excreted from the gallbladder, thereby minimizing the exposure of labile metabolites to the intestinal environment. This study exemplifies how a combination of *in vitro* and *in vivo* tools can aid in the identification of metabolites unique to the human species.

Contribution: Phase I and Phase II metabolism experiments including microsomal, cytosolic and glucuronidation experiments.

Title: Application of monoclonal antibodies to measure metabolism of an anti-trypanosomal compound *in vitro* and *in vivo*.

Journal: Journal of clinical laboratory analysis 24(3):187-94. (2010)

Authors: Goldsmith RB, Gray DR, Yan Z, **Generaux CN**, Tidwell RR, Reisner HM.

Abstract: Human African trypanosomiasis (HAT), also called African sleeping sickness, is a neglected tropical parasitic disease indigenous to sub-Saharan Africa. Diamidine compounds, including pentamidine and CPD-0801, are potent anti-trypanosomal molecules. The latter is a potential drug in the development at the UNC based Consortium for Parasitic Drug Development. An orally bioavailable prodrug of CPD-0801, DB868, is metabolized primarily in the liver to the active form. A monoclonal antibody developed against a pentamidine derivative has shown significant reactivity with CPD-0801 (EC_{50} 65.1 nM), but not with the prodrug (EC_{50} >18,000 nM). An inhibitory enzyme-linked immunosorbent assay (IELISA) has been used to quantitatively monitor prodrug metabolism by detecting the production of the active compound over time in a sandwich culture rat hepatocyte system and in rats. These results were compared with the results of the standard LC/MS/MS assay. Spearman coefficients of 0.96 and 0.933 (*in vitro* and *in vivo*, respectively) indicate a high correlation between these two measurement methods. This novel IELISA provides a facile, inexpensive, and accurate method for drug detection that may aide in elucidating the mechanisms of action and toxicity of existing and future diamidine compounds.

Contribution: Rat pharmacokinetic experiments following oral administration of 25 μmol/kg DB868

DIAMIDINES FOR HUMAN AFRICAN TRYPANOSOMIASIS

Mary F. Paine, Michael Zhuo Wang, **Claudia N. Generaux**, David W. Boykin, W. David Wilson, Harry P. De Koning, Carol A. Olson, Gabriele Pohlig, Christian Burri, Reto Brun, Grace A. Murilla, John K. Thuita, Michael P. Barrett, Richard R. Tidwell

Eshelman School of Pharmacy (MFP, MZW, CNG) and Department of Pathology and Laboratory Medicine (RRT), The University of North Carolina at Chapel Hill, Chapel Hill, NC 27599, USA

Department of Chemistry, Georgia State University, Atlanta, GA 30302, USA (DWB, WDW)

University of Glasgow, Faculty of Biomedical and Life Sciences and Wellcome Trust Centre for Molecular and Biochemical Parasitology, Glasgow Biomedical Research Centre, Glasgow G12 8TA, UK (HDK, MPB)

Sapphire Oak Consultants, Lindenhurst, IL 60046, USA (CAO)

Swiss Tropical Institute, Pharmaceutical Medicine Unit (GP, CB) and Parasite Chemotherapy Unit, Basel, Switzerland

Kenya Agricultural Research Institute-Trypanosomiasis Research Centre (KARI-TRC), Kikuyu, Kenya (GAM, JKT)

This chapter was submitted to the journal *Current Opinion in Investigational Drugs* and is formatted in the style of this journal.

Abstract

Aromatic diamidines are potent trypanocides. Pentamidine has been used for more than 60 years to treat human African trypanosomiasis (HAT). However, the drug must be administered parenterally and is active only against first stage HAT, prior to the parasites causing neurological deterioration through invasion of the central nervous system (CNS). A major effort to design novel diamidines has led to the development of orally active prodrugs and, remarkably, a new generation of compounds that can penetrate the CNS. Here we outline progress in the development of diamidines against HAT.

Key words

Pentamidine, furamidine, diamidine, human African trypanosomiasis, sleeping sickness, drug metabolism, drug transport, blood brain barrier, clinical trial

Introduction

Human African trypanosomiasis (HAT) is caused by parasitic protozoa of the brucei group of the genus *Trypanosoma* [1]. The disease is endemic in sub-Saharan Africa, where its distribution is determined by the habitat range of the tsetse fly vector that transmits the parasite. HAT has two defined stages. The first stage involves trypanosomes in the haemolymphatic system. The late (or second) stage begins once parasites become manifest in the central nervous system (CNS), where their presence initiates a deterioration in neurological function, including disruptions to sleep/wake patterns that lend the name "sleeping sickness" to this stage of the disease.

Since a process of antigenic variation [2] has so far precluded vaccines against HAT, chemotherapy remains the only option in disease intervention at the level of affected individuals [3]. The concept of integrated control, diminishing transmission by tsetse flies

and reducing the infected population (the primary reservoir for infection) by active surveillance and drug treatment, is attractive [1]. However, HAT, which afflicts exclusively the world's poorest populations, is largely neglected, and many challenges constrain progress.

Current drugs are generally unsatisfactory due to varying degrees of toxicity, a need for parenteral administration, prohibitive cost and distribution difficulties, all of which negatively impact use [3]. For first stage disease, prior to CNS involvement, two drugs are used: pentamidine for *T. b. gambiense* and suramin, largely for *T. b. rhodesiense*. For late stage disease, melarsoprol (a melaminophenyl arsenical) has until recently been the first line drug of choice against gambiense disease and the only remedy for rhodesiense disease. Eflornithine has recently replaced melarsoprol as first line for late stage gambiense disease in many foci, but is of insufficient efficacy to treat the rhodesiense form. In 2009, a combination therapy, eflornithine at reduced dose plus nifurtimox, has been placed on the WHO list of essential medicines. The reduced dosing with improved tolerability, coupled with a perceived reduction in the risk for selecting drug resistance, has led to its recommendation as the first line treatment for late stage gambiense disease (P. Simarro, WHO personal communication). However, new and improved drugs are still urgently needed.

The last few years have shown progress in seeking new drugs for HAT. Several not-for-profit initiatives followed a major campaign against HAT by WHO and Medecins Sans Frontieres (MSF), including the establishment of the Drugs for Neglected Diseases initiative (DNDi), a drug discovery unit for neglected diseases at the University of Dundee (Scotland,

UK), and the Consortium for Parasitic Drug Development (CPDD) centred at the University of North Carolina, USA [3].

Sir James Black, the Nobel prize-winning discoverer of beta blockers, noted insightfully that "the most fruitful basis for the discovery of a new drug is to start with an old drug". For HAT, the aromatic diamidine, pentamidine (fig 1), was introduced as the best of a relatively small number of this class in the 1930s. Pentamidine, however, suffers several drawbacks. The drug is inactive against late stage disease, must be administered by intramuscular injection and causes significant side effects, including hepatic toxicity and hyper- and hypoglycaemia. The success of pentamidine, however, discouraged further work into diamidines until use of the drug against AIDS-associated Pneumocystis pneumonia rekindled interest in the class in the 1980s. Numerous diamidines with pharmacological benefits over pentamidine have been identified, including orally available *N*-methoxy prodrugs. One of these diamidines, furamidine (DB75, fig 1), which in its prodrug form, pafuramidine (DB289, fig 1), became the first HAT drug to enter a clinical trial pathway that conformed to contemporary standards in drug development. Unfortunately, renal toxicity that became evident in a cohort of volunteers in an extended Phase 1 safety trial several weeks after treatment halted development of pafuramidine (and its development is discontinued). The recent discovery of CNS-permeable diamidines offers hope for development of new drugs to potentially treat both first and second stage HAT.

In this article, we review our understanding of how diamidines enter and kill trypanosomes, how they distribute within the body and how they offer great potential as new drugs for use in the battle to eliminate HAT.

Figure 1 Structures of various aromatic diamidines

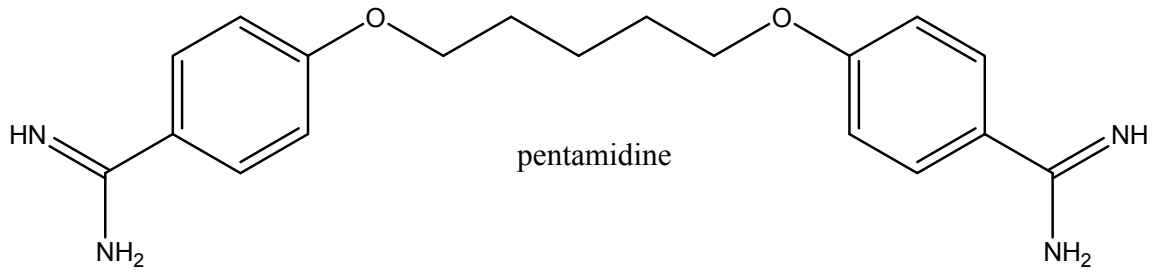

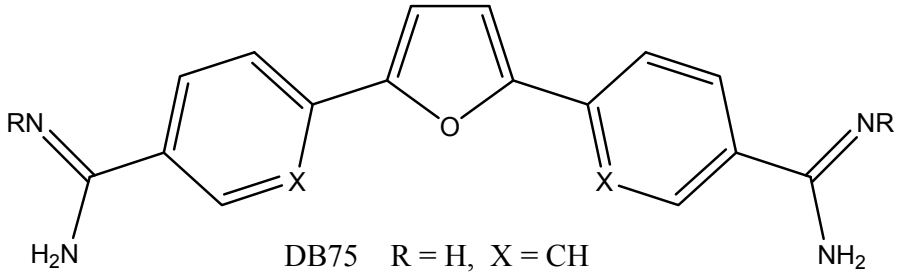

DB75 R = H, X = CH
DB289 R = OCH_3, X = CH
DB820 R = H, X= N, CH
DB844 R = H, X= N, CH
DB829 R = H, X = N
DB868 R = OCH_3, X = N

Diamidine modes of action and mechanisms of resistance

A definitive intracellular target, whose inhibition by diamidines underlies anti-trypanosomal activity, remains elusive [3]. It is, however, clear that diamidines bind with high affinity to DNA and much work has focused on this interaction some of which we discuss here. An extraordinary complex of intercatenated circular DNA that comprises the mitochondrial genome, the so-called kinetoplast that defines the Kinetoplastid taxon to which trypanosomes belong [4,5], has been proposed as a possible target. Fluorescent diamidines bind to the kinetoplast within seconds of the parasite's exposure to these compounds [6], and the kinetoplast disintegrates in diamidine-treated trypanosomes.

Kinetoplast DNA comprises both minicircles and maxicircles. The minicircles contain repeated AT base pair sequences that are in phase (i.e., on the same side of the DNA double helix), producing a bent helical conformation [7-9] that can be disrupted by diamidines [9]. Minicircles encode the small guide RNA molecules that template the remarkable process of RNA editing of precursor transcripts encoded by the maxicircles [10-11]. Aromatic diamidines generally bind to the DNA minor groove in AT sequences of 4-5 base pairs [12,13]. The amidines hydrogen-bond to the thymidine keto or adenosine N3 groups at the floor of the minor groove, and the aromatic systems (or aliphatic with pentamidine) make van der Waals contacts with the groove walls. Electrostatic interactions between the two amidine charges and anionic charges on the DNA backbone provide additional stabilization for the complex. GC-containing sequences bind diamidines less well due to steric interferences from the guanosine amino group.

Recent experiments [14,15] have revealed both the mitochondrion per se and the kinetoplast serve essential roles. A caveat, however, arises in considering dyskinetoplastic strains of *T. evansi*, which have lost condensed kDNA and yet remain almost as sensitive to diamidine drugs as trypanosomes with an intact kinetoplast (R Brun, personal communication). It is certain that key mitochondrial genes remain in these organisms, and detailed studies of diamidine action are needed.

Although questions remain regarding intracellular targets of diamidines, trypanocidal activity is slow, taking several days after exposure to kill parasites in vitro. Trypanosomes accumulate diamidines to high concentrations (millimolar overall, although the proportion bound to cellular macromolecules is not known [16,17]). *T. brucei* pentamidine-resistant parasites were shown [17] to be sensitive to the same intracellular concentrations, but these

concentrations took much longer to achieve than in wild type organisms, suggesting that resistance was associated with a change in the mechanism of uptake.

Diamidines are dications that enter cells via plasma membrane transporters. Trypanocidal specificity likely arises due to the vastly higher rate of influx in trypanosomes relative to mammalian cells, against the transmembrane gradient. Disabling mutations in the transporters responsible for uptake would be expected to lead to diamidine resistance.

Pentamidine, discovered in the 1930s, is used to treat >90% of all first stage HAT cases and also has been used as prophylaxis on a population scale [18]. Despite long-term, widespread use, clinical resistance rarely has been reported. Persistence of efficacy over time may relate to pentamidine's uptake through multiple transporters. The main trypanosome transporter for diamidines is the P2 aminopurine transporter [19-22]. The recognition motif for this transporter is shared between adenine, adenosine, amidines and melamine-containing compounds [23-25]. While loss of this transporter underlies resistance to some diamidines [26-28], it leads to only minor loss of sensitivity to pentamidine [29]. High-level resistance to pentamidine (and melaminophenyl arsenicals) requires loss of at least one other transporter, the so-called high affinity pentamidine transporter (HAPT), as well as P2 [30,31]. Knowledge of the kinetic parameters for each transporter allows the prediction of their exact contribution to the net transmembrane flux for each diamidine [31,32].

Knowledge of the contribution of each transporter to drug accumulation is a key component of the drug development process. For example, furamidine was shown to enter the trypanosome principally via the P2 transporter. However, residual uptake was still measureable in P2 transporter knockout cells, revealing a secondary minor route of uptake

which was, nevertheless, able to sustain sufficient uptake to kill trypanosomes in mice [27]. Difficulties in obtaining crystal structures for transporter proteins have restricted protein-based modeling for structure-activity relationships. As such, a complementary modeling approach based on substrate recognition has been developed that models the substrate-transporter interaction without the need for structural information of the transporter involved [33,34]. Advanced CoMFA and CoMSIA software has been used to create a quantitative and predictive computational model of substrate recognition by the P2 transporter [25]. Similar work is underway for the other known diamidine transporters. This approach will allow the design of multi-transporter selectivity into the next generation of diamidines, thus potentially avoiding early onset resistance and cross-resistance with existing drugs.

Prodrugs, biotransformation, and brain permeant diamidines

With pK_a values ranging from 9-11 (MarvinSketch 5.1.3-2, 2008, ChemAxon http://www.chemaxon.com), the diamidines are charged at physiological pH, resulting in poor oral bioavailability [35]. Oral administration is preferred for drugs used in resource-poor rural African clinics, and a prodrug strategy (where inactive precursors are biotransformed to active metabolites [36]) was devised to determine whether diamidine derivatives could be administered orally.

Pafuramidine (DB289) and the aza analogs DB844 and DB868 were designed as prodrugs of the diamidines furamidine (DB75), DB820, and CPD-0801 (DB829), respectively [37]. These prodrugs involved masking the positive charge of the amidine functional group with *O*-alkyl moieties (Figure 2), resulting in increased lipophilicity and intestinal permeability [38-40].

Figure 2 Schemes for prodrug synthesis

Scheme 1.

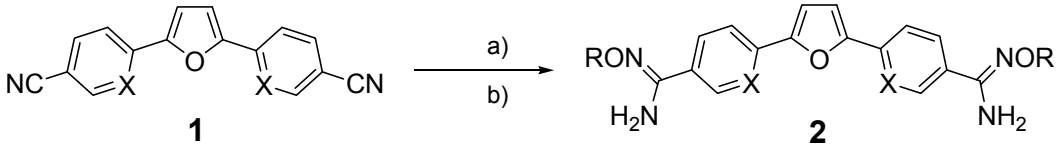

Reagents and conditions: a)EtOH, HCl(gas),rt b)NH_2OR, EtOH, rt

The original procedure used to make the amidoxime and the *O*-methylamidoxime of furamidine involved a Pinner approach as outlined in Scheme 1 [41]. In principal, the imidate ester intermediate can be allowed to react with hydroxylamine or any *O*-alkylhydroxylamine to form the corresponding *O*-alkylamidoxime. This approach has the well-known drawbacks of the Pinner method, primarily the necessity for rigorous exclusion of water to prevent amide formation and the requirement of long reaction times due to very low solubility of the bis-nitriles.

Scheme 2.

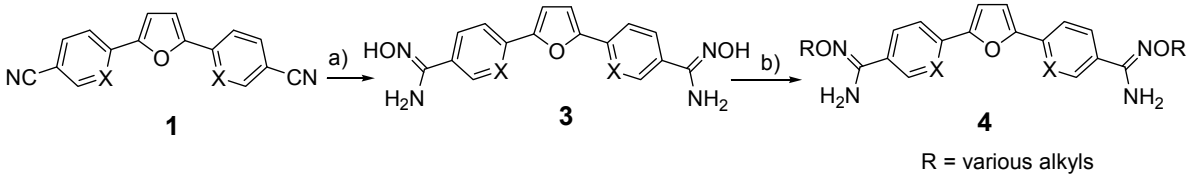

Reagents and conditions: a)NH_2OH, DMSO, rt b)NH_2OR, EtOH, rt b)alkyl halides or sulfonates, LiOH, DMF,H_2O, rt or NaOH, dioxane, H_2O, rt.

O-Alkylation of the bis-amdioximes 3 (Scheme 2) can be readily achieved by base mediated alkylation with alkyl halides or sulfonates at room temperature [37]. In each case, alkylation conditions should be optimized to minimize multi-alkylation (N-alkylation).

Biotransformation of prodrugs to the active diamidines requires a series of enzymatic reactions. The biotransformation of pafuramidine to furamidine involves oxidative catalysis by cytochrome P450 enzymes and reductive catalysis by the cytochrome b_5/NADH-cytochrome b_5 reductase system. Four intermediate metabolites (M1-M4) precede the formation of furamidine [42,43]. Prodrug biotransformation occurs primarily in the liver, and elimination of furamidine occurs via biliary excretion [40]. Tissue distribution data from rats

given a single oral dose (10 mg/kg) of pafuramidine indicated that furamidine was retained extensively in liver, as exemplified by a liver to plasma concentration ratio of 1300:1 [40].

Pafuramidine has shown efficacy in models of first stage infection in mice [44] and vervet monkeys [45], as well as in clinical trials (discussed below). The aza analogs DB844 and DB868 have shown efficacy in models of first and second stage infection in mice [44]. However, DB844 was associated with dose-limiting gastrointestinal toxicity in uninfected vervet monkeys (GA Murilla and JK Thuita, unpublished observation), and further work with this compound has been discontinued. An efficacy study of DB868 in the late stage vervet monkey model of HAT is underway.

The discovery that prodrugs of some diamidines treat disease in the CNS has offered hope for new drugs for late stage HAT. The mechanism(s) by which the diamidines enter the CNS and elicit anti-trypanosomal activity is (are) not fully elucidated. Furamidine [46] and the aza analogs DB820 and DB829 (CPD-0801) (MZ Wang, unpublished observations) have been shown to be substrates of the human facilitative organic cation transporter 1 (OCT1) in Chinese hamster ovary cells stably transfected with OCT1. However, since expression of OCT1/Oct1 in the BBB of humans and mice is reportedly low [47,48], different transporters may facilitate the entry of certain diamidines (i.e., DB820, CPD-0801) into the brain to produce cures in the mouse model of late stage disease.

A preliminary pharmacokinetic study in rats given a single intravenous dose (3 mg/kg) of furamidine or CPD-0801 showed biphasic plasma concentration-time profiles for both diamidines (MF Paine and JP Jones, unpublished observations). The systemic exposure (area under the curve) of CPD-0801 was twice that of furamidine, a reflection of a lower systemic clearance for CPD-0801, and may imply that CPD-0801 has a higher likelihood of

entering the brain. The steady-state volume of distribution was similar between the two compounds. Although the elimination half-life of CPD-0801 was twice that of furamidine, the distribution half-life of CPD-0801 was thrice that of furamidine, indicating that CPD-0801 distributed to tissues more slowly than furamidine. Indeed, the accumulation of CPD-0801 in both the liver and kidney was much less than that of furamidine. Taken together, these data show promise for parenteral CPD-0801 as treatment for second stage HAT. A study of the safety of an acetate salt of this compound (CPD-0802), given intravenously to uninfected vervet monkeys, is underway. If successful, it is expected to trigger entry into a clinical development pathway.

The clinical development pathway of Pafuramidine

The clear advantage of an orally available analog of pentamidine (pafuramidine) stimulated preclinical and Phase 1 clinical trials. Pafuramidine began clinical development in 2000 for treatment of first stage HAT by the CPDD and Immtech Pharmaceuticals, Inc. Pafuramidine underwent preclinical microbiology, pharmacology, and toxicokinetic evaluation and demonstrated good efficacy with an acceptable safety profile [49-52]. Reversible liver toxicity in rodents and monkeys was observed, which was anticipated based on known toxicity of pentamidine.

Phase I safety and pharmacokinetic evaluations in healthy volunteers indicated that pafuramidine was absorbed and converted to the active metabolite furamidine, yielding plasma concentrations appropriate for treatment of HAT. The compound was well tolerated [53]. Phase II testing with pafuramidine (100 mg BID for 5 days) was initiated in 2001 by the Pharmaceutical Medicine Unit of the Swiss Tropical Institute and Immtech Pharmaceuticals, Inc., the first time a new chemical entity had been studied in controlled

trials for HAT. The trials, conducted in the Democratic Republic of Congo (DRC) and Angola with patients affected by first stage *T. b. gambiense* HAT, were promising in terms of drug safety. Increased treatment duration of 10 days was needed for acceptable efficacy and resulted in a cure rate of 93% at 3 months post treatment [54].

A Phase III trial was conducted between August 2005 and March 2007 in the DRC, Angola and South Sudan and enrolled 273 patients, including pregnant and lactating women and adolescents [55]. Patients were randomized in an open-label design to treatment with pafuramidine (100 mg BID orally for 10 days) or pentamidine (4 mg/kg QD intramuscularly for 7 days) and followed for two years. Both drugs were well tolerated, liver toxicity during treatment was significantly less in the pafuramidine group, and the 12-month post treatment efficacy (primary endpoint) for pafuramidine was 89% compared to 95% for pentamidine ($p=0.067$) [56]. The 24-month post treatment efficacy was 85% and 94%, respectively.

In October 2007, a Phase I study was initiated to expand the safety database needed for pafuramidine registration for trypanosomiasis and pneumocystis pneumonia. The development program was placed on clinical hold when approximately 25% of subjects in this study developed elevated transaminases approximately 5 days after the last dose; all subjects returned to baseline without sequelae. When acute renal insufficiency was observed in five subjects approximately 8 weeks after dosing, the pafuramidine program was discontinued [56]. Subjects were treated with corticosteroids and other supportive care, and BUN and creatinine significantly improved in the following months. The affected subjects continue to be followed by specialists.

The Phase III HAT study was in follow-up at the time of the clinical hold. Three subjects were subsequently identified with glomerulonephritis or nephropathy post

pafuramidine treatment; two of these cases may retrospectively be considered possibly related to pafuramidine [56]. These three subjects recovered without sequelae following treatment with corticosteroids. The cause for these unforeseen adverse drug reactions is unclear and is being investigated. No new drug-related adverse events were observed in any other pafuramidine study. Whether the adverse events are a class effect or specific to pafuramidine is not yet clear, but it is of significance that CPD-0801 is accumulated significantly less into host tissue, including liver and especially kidney, than furamidine, as discussed above.

The discontinuation of the pafuramidine program has represented a major setback in drug development for HAT. However, many positive outcomes resulted from this project. For example, the program delivered many infrastructure improvements and investigator training at the clinical sites. Over 250,000 patients were screened, and 416 patients were treated in the Phase II and III clinical trials. The rate of participation in the 24 month follow-up visits for the Phase III study was a remarkable 97%. Patients who were actively screened for study participation, but who were ineligible due to the presence of late stage HAT, also received appropriate treatment and follow up.

It is notable that the incidence of HAT has shown a significant and sustained reduction over the time frame of the pafuramidine clinical trials. This suggests that the conduct of the trials, along with other initiatives such as the WHO-sponsored surveillance and drug distribution campaigns and enhanced engagement of various non-governmental organisations (MSF, Malteser International and Merlin), has contributed to the decrease in HAT witnessed over the past decade [57,58].

Conclusions

The extraordinary efficacy of diamidines against trypanosomal infection indicates that this class of compounds continues to advance drug development campaigns for HAT. New scientific knowledge of current diamidines regarding mechanism(s) of action, distribution to the brain and accumulation in tissue can be utilized to design improved compounds for evaluation in animal models of efficacy and safety.

Enhanced awareness of HAT has brought a number of groups forward to develop new drugs and, in addition to the diamidines, several new classes of compounds e.g. the nitroheterocycle fexinidazole, are now entering preclinical and clinical development for late stage disease through DNDi. The clinical trials to test the efficacy and safety of pafuramidine in HAT coincided with a sustained and significant reduction in the incidence of the disease, which can be attributed partially to the trials themselves. The CPDD continues to evaluate diamidines in preclinical trials and anticipates selecting a clinical candidate for late stage disease in the near future, with DB829 (figure 1 and described above) the most likely candidate). It is anticipated that this renewed interest in HAT, coupled with the experiences gained from the first large scale clinical trials for a new chemical entity for HAT, will in time lead to a sustainable pipeline of medications to control the disease, or even fulfil the WHO mission of eliminating HAT [58,59].

References

1. Barrett MP, Burchmore RJ, Stich A, Lazzari JO, Frasch AC, Cazzulo JJ, Krishna S: The trypanosomiases. *Lancet* (2003) 362:1469-1480.

2. McCulloch R: Antigenic variation in African trypanosomes: monitoring progress. *Trends Parasitol* (2004) 20:117-121.

3. Barrett MP, Boykin DW, Brun R, Tidwell RR. Human African trypanosomiasis: pharmacological re-engagement with a neglected disease. *Br J Pharmacol* (2007) 152:1155-1171.

A comprehensive review setting out much of what is known about current drugs and the current renewed efforts to dvelop drugs for HAT

4. Guilbride DL, Votýpka J, Zíková A, Benne R, Englund PT, Lukes J: Kinetoplast DNA network: evolution of an improbable structure. *Eukaryot Cell* (2002) 1:495-502.

5. Liu Y, Englund PT: The rotational dynamics of kinetoplast DNA replication. Mol Microbiol (2007) 64:676-690.

6. Mathis AM, Bridges AS, Ismail MA, Kumar A, Francesconi I, Anbazhagan M, Hu Q, Tanious FA, Wenzler T, Saulter J, Wilson WD, Brun R, Boykin DW, Tidwell RR, Hall JE: Diphenyl furans and aza analogs: effects of structural modification on in vitro activity, DNA binding, and accumulation and distribution in trypanosomes. *Antimicrob Agents Chemother* (2007) 51:2801-2810.

7. Ntambi JM, Marini JC, Bangs JD, Hajduk SL, Jimenez HE, Kitchin PA, Klein VA, Ryan KA, Englund PT: Presence of a bent helix in fragments of kinetoplast DNA minicircles from several trypanosomatid species. *Mol Biochem Parasitol* (1984) 12:273-286.

8. Marini JC, Effron PN, Goodman TC, Singleton CK, Wells RD, Wartell RM, Englund PT: Physical characterization of a kinetoplast DNA fragment with unusual properties. *J Biol Chem* (1984) 259:8974-8979.

9. Tevis DS, Kumar A, Stephens CE, Boykin DW, Wilson WD: Large, sequence-dependent effects on DNA conformation by minor groove binding compounds. *Nucleic Acids Res* (2009) Jul 3. [Epub ahead of print].

10. Stuart K: RNA editing in mitochondrial mRNA of trypanosomatids. *Trends Biochem Sci* (1991) 16:68-72.

11. Ochsenreiter T, Anderson S, Wood ZA, Hajduk SL: Alternative RNA editing produces a novel protein involved in mitochondrial DNA maintenance in trypanosomes. *Mol Cell Biol* (2008) 28:5595-5604.

12. Wilson WD, Tanious FA, Mathis A, Tevis D, Hall JE, Boykin DW: Antiparasitic compounds that target DNA. *Biochimie* (2008) 90:999-1014.

13. Wilson WD, Nguyen B, Tanious FA, Mathis A, Hall JE, Stephens CE, Boykin DW: Dications that target the DNA minor groove: compound design and preparation, DNA interactions, cellular distribution and biological activity. *Curr Med Chem Anticancer Agents* (2005) 5:389-408.

A recent review summarising DNA binding of diamidines

14. Wang Z, Englund PT: RNA interference of a trypanosome topoisomerase II causes progressive loss of mitochondrial DNA. *EMBO J* (2001) 20:4674-4683.

15. Schnaufer A, Clark-Walker GD, Steinberg AG, Stuart K: The F1-ATP synthase complex in bloodstream stage trypanosomes has an unusual and essential function. *EMBO J*. (2005) 24:4029-4040.

16. Mathis AM, Holman JL, Sturk LM, Ismail MA, Boykin DW, Tidwell RR, Hall JE Accumulation and distribution of antitrypanosomal diamidine compounds DB75 and DB820 in African trypanosomes. *Antimicrob Agents Chemother* (2006) 50:2185-2191.

17. Damper D, Patton CL: Pentamidine transport and sensitivity in brucei-group trypanosomes. *J. Protozool* (1976) 23:349-356

18. Ollivier G, Legros D : Trypanosomiase humaine africaine: historique de la therapeutique et de ses échecs. *Trop Med Int Health* (2001) 6:855-863.

19. Carter NS, Fairlamb AH: Arsenical-resistant trypanosomes lack an unusual adenosine transporter. *Nature* (1993) 361: 173-176.

●● The original demonstration of the crucial P2 aminopurine transporter in drug uptake and resistance

20. Carter NS, Berger BJ, Fairlamb AH: Uptake of diamidine drugs by the P2 nucleoside transporter in melarsen-sensitive and -resistant *Trypanosoma brucei brucei*. *J Biol Chem* (1995) 270:28153-28157.

● The original demonstration of the crucial P2 aminopurine transporter in diamidine uptake and resistance

21. Carter NS, Barrett MP, De Koning HP: A drug resistance determinant from *Trypanosoma brucei*. *Trends Microbiol* (1999) 7:469-471.

22. Barrett MP, Zhang ZQ, Denise H, Giroud C, Baltz T: A diamidine-resistant *Trypanosoma equiperdum* clone contains a P2 purine transporter with reduced substrate affinity. *Mol Biochem Parasitol* (1995) 73:223-229.

23. De Koning HP, Jarvis SM: Adenosine transporters in bloodstream forms of *T. b. brucei*: Substrate recognition motifs and affinity for trypanocidal drugs. *Mol Pharmacol* (1999) 56:1162-1170.

24. Barrett MP, Fairlamb AH: The biochemical basis of arsenical-diamidine crossresistance in African trypanosomes. *Parasitol Today* (1999) 15:136-140.

25. Collar CJ, Al-Salabi MI, Stewart ML, Barrett MP, Wilson WD, De Koning HP: Predictive computational models of substrate binding by a nucleoside transporter. *J. Biol. Chem*. (2009) in press, doi/10.1074/jbc.M109.049726

● A recent detailed account of the substrate recognition pattern of the P2 transporter explaining why diamidines, melamine-based arsenicals and aminopurines can all share this permease.

26. De Koning HP, Stewart M, Anderson L, Burchmore R, Wallace LJM, Barrett MP The trypanocide diminazene aceturate is accumulated predominantly through the TbAT1 purine transporter; additional insights in diamidine resistance in African trypanosomes. *Antimicrob Agents Chemother* (2004) 48:1515-1519

27. Lanteri CA, Stewart ML. Brock JM, Alibu VP, Meshnick SR, Tidwell RR, Barrett MP: Roles for the *Trypanosoma brucei* P2 transporter in DB75 uptake and resistance. *Mol Pharmacol* (2006) 70:1585-1592.

● An important description of the reliance of DB75 (furamidine on the P2 transporter, but also revealing important roles for other carriers in uptake of this compound).

28. Witola WH, Inoue N, Ohashi K, Onuma M: RNA-interference silencing of the adenosine transporter-1 gene in *Trypanosoma evansi confers resistance to diminazene aceturate. Exp Parasitol* (2004) 107:47-57.

29. Matovu E, Stewart M, Geiser F, Brun R, Mäser P, Wallace LJM, Burchmore RJ, Enyaru JCK, Barrett MP, Kaminsky R, Seebeck T, De Koning HP The mechanisms of arsenical and diamidine uptake and resistance in *Trypanosoma brucei*. *Eukaryot Cell* (2003) 2:1003-1008.

●● The knockout of the TbAT1 gene that encodes the P2 transporter proved its central role in uptake of melaminophenylarsenicals and diamidines but also pointed to key roles of other transporters in their accumulation.

30. Bridges D, Gould MK, Nerima B, Mäser P, Burchmore RJS, De Koning, HP: Loss of the High Affinity Pentamidine Transporter is responsible for high levels of cross-resistance between arsenical and diamidine drugs in African trypanosomes. *Mol Pharmacol* (2007) 71:1098-1108.

31. Bernhard SC, Nerima B, Mäser P, Brun R: Melarsoprol- and pentamidine-resistant Trypanosoma brucei rhodesiense populations and their cross-resistance. *Int J Parasitol.* (2007) 37:1443-1448.

32. Bray PG, Barrett MP, Ward SA, De Koning HP: Pentamidine uptake and resistance in pathogenic protozoa. *Trends Parasitol* (2003) 19:232-239.

33. Wallace LJM, Candlish D, De Koning HP Different substrate recognition motifs of human and trypanosome nucleobase transporters: selective uptake of purine antimetabolites. *J Biol Chem* (2002) 277:26149-26156.

34. Al-Salabi MI, Wallace LJM, Lüscher A, Mäser P, Candlish D, Rodenko B, Gould MK, Jabeen I, Ajith SN, De Koning HP: Molecular interactions underlying the unusually high affinity of a novel *Trypanosoma brucei* nucleoside transporter. *Mol. Pharmacol* (2007) 71:921-929.

35. Boykin DW, Kumar A, Spychala J, Zhou M, Lombardy RJ, Wilson WD, Dykstra CC, Jones SK, Hall JE, Tidwell RR: Dicationic diarylfurans as anti-pneumocystis carinii agents. *J Med Chem* (1995) 38:912-916.

36. Ettmayer P, Amidon GL, Clement B Testa B: Lessons learned from marketed and investigational prodrugs. *J Med Chem* (2004) 47:2393-2404.

37. Ismail MA, Brun R, Easterbrook JD, Tanious FA, Wilson WD, Boykin DW:, Synthesis and antiprotozoal activity of aza-analogues of furamidine. *J Med Chem* (2003) 46:4761-4769

● The original report of the aza analogues of furamidine which have gone on to show brain permeation

38. Zhou L, Lee K, Thakker DR, Boykin DW, Tidwell RR and Hall JE: Enhanced permeability of the antimicrobial agent 2,5-bis(4-amidinophenyl)furan across Caco-2 cell monolayers via its methylamidoidme prodrug. *Pharm Res* (2002) 19:1689-1695.

39. Saulter JY Permeability and metabolism of potential prodrugs for the antimicrobial agent 2,5 BIS(4-amidinophenyl)furan (DB75). University of North Carolina School of Pharmacy, Chapel Hill, NC. (2005)

40. Midgley I, Fitzpatrick K, Taylor LM, Houchen TL, Henderson SJ, Wright SJ, Cybulski ZR, John BA, McBurney A, Boykin DW, Trendler KL: Pharmacokinetics and metabolism of the prodrug DB289 (2,5-bis[4-(N-methoxyamidino)phenyl]furan monomaleate) in rat and monkey and its conversion to the antiprotozoal/antifungal drug DB75 (2,5-bis(4-guanylphenyl)furan dihydrochloride). *Drug Metab Dispos* (2007) 35:955-967.

● A key description of the metabolic conversion and PK of the methoxy prodrug DB289 (pafuramidine).

41. Boykin DW, Kumar A, Bender BC, Hall JE, Tidwell RR: Anti-*Pneumocystis* activity of bis-amidoximes and bis-*O*-alkylamidoximes. *Bioorganic Med Chem Lett* (1996) 6:3017-3020.

42. Saulter J, Kurian J, Trepanier L, Tidwell R, Bridges A, Boykin D, Stephens C, Anbazhagan M, Hall JE: Unusual dehydroxylation of antimicrobial amidoxime prodrugs by cytochrome b5 and NADH cytochrome b5 reductase. *Drug Metab Dispos* (2005) 33:1886-1893.

43. Wang MZ, Saulter JY, Usuki E, Cheung YL, Hall M, Bridges AS, Loewen G, Parkinson OT, Stephens CE, Allen JL, Zeldin DC, Boykin DW, Tidwell RR, Parkinson A, Paine MF, Hall JE: CYP4F enzymes are the major enzymes in human liver microsomes that catalyze the O-demethylation of the antiparasitic prodrug DB289 [2,5-bis(4-amidinophenyl)furan-bis-O-methylamidoxime]. *Drug Metab Dispos* (2006) 34:1985-1994.

44.Wenzler T, Boykin DW, Ismail MA, Hall JE, Tidwell RR, Brun R: (2009) New treatment option for second-stage African sleeping sickness: in vitro and in vivo efficacy of aza analogs of DB289. *Antimicrob Agents Chemother* (2009) 53:4185-4192.

●● The original demonstration of activity of the aza analogues of furamidine against second stage trypanosomiasis in a mouse model.

45. Mdachi RE, Thuita JK, Kagira JM, Ngotho JM, Murilla GA, Ndung'u JM, Tidwell RR, Hall JE, Brun R: Efficacy of the novel diamidine compound 2,5-Bis(4-amidinophenyl)-furan-bis-O-Methlylamidoxime (Pafuramidine, DB289) against Trypanosoma brucei rhodesiense infection in vervet monkeys after oral administration. *Antimicrob Agents Chemother* (2009) 53:953-957.

46.Ming X, Ju W, Wu H, Tidwell RR, Hall JE, Thakker DR Transport of dicationic drugs pentamidine and furamidine by human organic cation transporters. *Drug Metab Dispos* (2009) 37:424-430.

47. Zhang L, Dresser MJ, Gray AT, Yost SC, Terashita S and Giacomini KM Cloning and functional expression of a human liver organic cation transporter. *Mol Pharmacol* (1997) 51:913-921.

48. Kusuhara H, Sugiyama Y Active efflux across the blood-brain barrier: role of the solute carrier family. *NeuroRx* (2005) 2:73-85.

49. Ismail MA, Brun R, Wenzler T, Tanious FA, Wilson WD, Boykin DW*:* Dicationic biphenyl benzimidazole derivatives as antiprotozoal agents. *Bioorg Med Chem* (2004) 12:5405-5413.

50. Brun R, Balmer O: New developments in human African trypanosomiasis. *Curr Opin Infect Dis* (2006) 19: 415-20.

51. Allen JL, Bottomley AM, Fulcher SM, Ruckman SA, Boykin DW, Tidwell RR: Lack of embryo-fetal toxicity with the anti-infective DB289 and its active metabolite DB75, a diamidine with DNA minor groove binding activity.

52. Bak PM, Allen JL, Erexson GL, Mecchi MM, Murli H, Tidwell RR, Boykin DW: Lack of genotoxicity with the novel anti-infective prodrug DB289 and its active metabolite DB75, a 2,4-diphenyl furan diamidine with DNA minor groove binding activities. *Society of Toxicology*, 2003.

53. Yeramian P, Kruse M, Kecskes A, Allen J, McChesney-Harris L, Trendler K, Hall JE, Tidwell R. Safety and Clinical Pharmacokinetics of DB289, a New Orally Bioavailable

Dication. *Abstr Intersci Conf Antimicrob Agents Chemother*. 2001 Dec 16-19; 41: abstract no. F-2163.

54. Blum J, Pizzagalli f, Thompson M, Kande Beta Ku Mesu V, Mpoo Mpoto A, Miaka Mia Bilenge C, Fina Lubaki JP, Mpanya Kabeya A, Allen JL, Yeramian PD, Pohlig G, Tidwell RR, Burri C. Efficacy and safety of DB289, a new oral drug for treatment of first stage sleeping sickness: preliminary results from Phase II Trials. Medicine and Health in the Tropics, Marseilles, France, 11-15 Sep 2005, Abst O-101.

55. Burri C, Pohlig G, Bernhard S, Kabeya AM, Lubaki J-PF, Mpoto AM, Gratias KM, Kuikumbi FM, Mintwo AF, Mununngi AK, Bage JT, Macharia S, Bilenge CM, Mesu VK, Franco JR, Situvanga ND, Olson CA. Phase III trial of pafuramidine maleate (DB289), a novel oral drug, for treatment of first stage sleeping sickness. 56th American Society for Tropical Medicine and Hygiene, Philadelphia, Nov 2007.

56. Pohlig G, Bernhard S, Blum J, Burri C, Kabeya AM, Lubaki J-P F, Mpoto AM, Mununngu BF, Deo GKM, Mutantu PN, Kuikumbi FM, Mintwo AF, Mununngi AK, Dala A, Macharia S, Bilenge CMM, MesuVKBK, J Franco JR, Dituvanga ND, Olson CA. Phase 3 trial of pafuramidine maleate (DB289), a novel, oral drug, for treatment of first stage sleeping sickness: safety and efficacy. 57th American Society for Tropical Medicine and Hygiene, New Orleans, LA. Dec 2008.

57. Barrett MP: The rise and fall of sleeping sickness. *Lancet*. (2006) 367:1377-1378.

58. Anon: Human African trypanosomiasis (sleeping sickness): epidemiological update .*Weekly Epidem. Rec*. (2006) 81:69–80.

59. Brun R, Blum J, Chappuis F, Burri C: Human African trypanosomiasis. *Lancet.* (2009) Oct 13. [Epub ahead of print]

Websites

MarvinSketch 5.1.3-2, 2008, ChemAxon http://www.chemaxon.com